


7-2003

Characterization of Environmentally Friendly Polymers: Amylopectin and Its Blends

Mohammad Osman Melibari
Columbus State University

Follow this and additional works at: https://csuepress.columbusstate.edu/theses_dissertations

 Part of the [Earth Sciences Commons](#), and the [Environmental Sciences Commons](#)


Recommended Citation

Melibari, Mohammad Osman, "Characterization of Environmentally Friendly Polymers: Amylopectin and Its Blends" (2003). *Theses and Dissertations*. 21.
https://csuepress.columbusstate.edu/theses_dissertations/21

This Thesis is brought to you for free and open access by the Student Publications at CSU ePress. It has been accepted for inclusion in Theses and Dissertations by an authorized administrator of CSU ePress.

CHARACTERIZATION OF ENVIRONMENTALLY FRIENDLY POLYMERS:
AMYLOPECTIN AND ITS BLENDS

Mohammad Osman Melibari



Digitized by the Internet Archive
in 2012 with funding from
LYRISIS Members and Sloan Foundation

<http://archive.org/details/characterization00meli>

Columbus State University
The College of Science
The Graduate Program in Environmental Science

Characterization of Environmentally Friendly Polymers: Amylopectin and its Blends

A Thesis in
Environmental Science
By
Mohammad Osman Melibari

Submitted in Partial Fulfillment
of the Requirements
for the Degree of
Master of Science

July 2003

© 2003 by Mohammad Osman Melibari

6/11 9.22.03

I have submitted this thesis in partial fulfillment of the requirements for the degree of Master of Science.

July 23, 2003

Date



Mohammad Osman Melibari

We approve the thesis of Mohammad Osman Melibari as presented here.

7/23/03

Date



Floyd R. Jackson, Associate
Professor of Chemistry, Thesis
Advisor

07-28-03

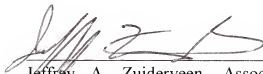
Date



Zeki Y. Al-Saigh, Professor of
Chemistry, Buffalo State College,
SUNY

8/6/03

Date



Jeffrey A. Zuiderveen, Associate
Professor of Biology

ABSTRACT

Biodegradable polymers are desirable for a variety of applications, such as in packaging, agriculture, and medicine. Its biological degradation by microorganisms accelerated the interest in biodegradable polymers during the last decades. Within this group of innovative environmentally friendly biodegradable polymers, starch or Amylopectin plays a predominant role, due to their potential biodegradability. This research was attempted to characterize Amylopectin to obtain its physico-chemical properties. In addition, characterizations were extended to include blends of Amylopectin and biodegradable diluents. Blends of Amylopectin with biodegradable diluents including Polycaprolactone, Poly(DL-lactide-co-glycolide), and Poly(3-hydroxybutyric acid) were prepared. The physical properties and the thermodynamic characteristics of these blends were investigated using the Inverse Gas Chromatography (IGC) method. This was conducted over a range of temperatures until a complete set of data was obtained. Nineteen solutes with different chemical natures were selected in this study. Solute, including a series of alkanes, acetates, alcohols, diethylamine, formic acid, and water, were injected into Amylopectin and its blends chromatographic columns. The retention times of solutes were measured for each solute. Slopes and heats of mixing of solutes with pure Amylopectin and its blends were calculated. All columns except the 50-50 Amylopectin-Polycaprolactone column showed a minimum of two regions in the retention diagram. These regions were identified as crystalline and amorphous regions. A third region was identified above 200°C as the polymer started to decompose. However, for 50-50 Amylopectin-Polycaprolactone column, a straight line was observed in most solutes due to the lack of data at higher temperatures. All columns except for some solutes of 50-50 Amylopectin-Polycaprolactone column showed a glass transition temperature (T_g) that has a range from 90°C to 140°C. The T_g is the first minimum temperature in the curvature that can be identified. In addition, all columns except for some solutes of 50-50 Amylopectin-Polycaprolactone column showed maxima of the curvature. These maxima were identified as the melting point (T_m) of the polymers, which ranged from 100°C to 170°C. By blending Amylopectin with other polymers, the T_m was decreased or a depression phenomenon was formed and this is due to less melting amorphous. The dispersive surface energy value of the 100% Amylopectin column was 0.07 mJ/m² at 200°C. The dispersive surface energy values of the 75-25 Amylopectin-Polycaprolactone column were ranged from 18.59 mJ/m² at 170°C to 10.27 mJ/m² at 260°C. In addition, the dispersive surface energy values of the 50-50 Amylopectin-Poly(DL-lactide-co-glycolide) column were ranged from 46.30 mJ/m² at 160°C to 39.03 mJ/m² at 180°C, while, the dispersive surface energy values of the 50-50 Amylopectin-Poly(3-hydroxybutyric acid) column were ranged from 55.46 mJ/m² at 160°C to 1.31 mJ/m² at 200°C. Therefore, blending Amylopectin with other polymer will increase its mechanical properties and thus, the surface energy.

TABLE OF CONTENTS

ABSTRACT	iii
TABLE OF CONTENTS	iv
LIST OF FIGURES	v
LIST OF TABLES	xii
INTRODUCTION	1
Background	1
Biodegradable Polymers	5
Amylopectin and Other Biodegradable Polymers	7
Inverse Gas Chromatography	11
Objectives	13
MATERIALS AND METHODS	16
Amylopectin and its Blends	16
Columns Preparation	16
Data Analysis	21
RESULTS	23
DISCUSSION AND CONCLUSIONS	65
REFERENCES	72
APPENDIX A - Thermodynamic Calculations	74
APPENDIX B – Specific Retention Volumes Tables	76
APPENDIX C – Retention Diagrams Figures	87

LIST OF FIGURES

Figure		Page
1-1	Structure of Amylopectin.	8
1-2	Structure of Polycaprolactone.	9
1-3	Structure of Poly(DL-lactide-co-glycolide).	10
1-4	Structure of Poly(3-hydroxybutyric acid).	11
1-5	Diagram of Inverse Gas Chromatography (IGC).	12
3-1	Degree of crystallinity for 100% Poly(DL-lactide-co-glycolide)-Decane.	35
3-2	Degree of crystallinity for 100% Poly(3-hydroxybutyric acid)-Decane.	36
3-3	Degree of crystallinity for 75-25 Amylopectin-Polycaprolactone-PropylAcetate.	37
3-4	Degree of crystallinity for 50-50 Amylopectin-Poly(DL-lactide-co-glycolide)-Nonane.	38
3-5	Degree of crystallinity for 50-50 Amylopectin-Poly(3-hydroxybutyric acid)-Nonane.	39
3-6	Surface energy for 100% Amylopectin-200°C.	40
3-7	Surface energy for 100% Poly(DL-lactide-co-glycolide)-170°C.	41
3-8	Surface energy for 100% Poly(3-hydroxybutyric acid)-160°C.	42
3-9	Surface energy for 100% Poly(3-hydroxybutyric acid)-170°C.	43
3-10	Surface energy for 100% Poly(3-hydroxybutyric acid)-180°C.	44
3-11	Surface energy for 100% Poly(3-hydroxybutyric acid)-190°C.	45
3-12	Surface energy for 100% Poly(3-hydroxybutyric acid)-200°C.	46
3-13	Surface energy for 75-25 Amylopectin-Polycaprolactone--170°C.	47

Figure		Page
3-14	Surface energy for 75-25 Amylopectin-Polycaprolactone--180°C.	48
3-15	Surface energy for 75-25 Amylopectin-Polycaprolactone--190°C.	49
3-16	Surface energy for 75-25 Amylopectin-Polycaprolactone--200°C.	50
3-17	Surface energy for 75-25 Amylopectin-Polycaprolactone-210°C.	51
3-18	Surface energy for 75-25 Amylopectin-Polycaprolactone-220°C.	52
3-19	Surface energy for 75-25 Amylopectin-Polycaprolactone-230°C.	53
3-20	Surface energy for 75-25 Amylopectin-Polycaprolactone-240°C.	54
3-21	Surface energy for 75-25 Amylopectin-Polycaprolactone-250°C.	55
3-22	Surface energy for 75-25 Amylopectin-Polycaprolactone-260°C.	56
3-23	Surface energy for 50-50 Amylopectin-Poly(DL-lactide-co-glycolide)-160°C.	57
3-24	Surface energy for 50-50 Amylopectin-Poly(DL-lactide-co-glycolide)-170°C.	58
3-25	Surface energy for 50-50 Amylopectin-Poly(DL-lactide-co-glycolide)-180°C.	59
3-26	Surface energy for 50-50 Amylopectin-Poly(3-hydroxybutyric acid)-160°C.	60
3-27	Surface energy for 50-50 Amylopectin-Poly(3-hydroxybutyric acid)-170°C.	61
3-28	Surface energy for 50-50 Amylopectin-Poly(3-hydroxybutyric acid)-180°C.	62
3-29	Surface energy for 50-50 Amylopectin-Poly(3-hydroxybutyric acid)-190°C.	63
3-30	Surface energy for 50-50 Amylopectin-Poly(3-hydroxybutyric acid)-200°C.	64
C-1	Retention diagram for 100% Amylopectin-Pentane.	88

Figure		Page
C-2	Retention diagram for 100% Amylopectin-Hexane.	89
C-3	Retention diagram for 100% Amylopectin-Heptane.	90
C-4	Retention diagram for 100% Amylopectin-Methanol.	91
C-5	Retention diagram for 100% Amylopectin-Ethanol.	92
C-6	Retention diagram for 100% Amylopectin-Propanol.	93
C-7	Retention diagram for 100% Amylopectin-Butanol.	94
C-8	Retention diagram for 100% Amylopectin-Diethylamine.	95
C-9	Retention diagram for 100% Poly(DL-lactide-co-glycolide)-Heptane.	96
C-10	Retention diagram for 100% Poly(DL-lactide-co-glycolide)-Octane.	97
C-11	Retention diagram for 100% Poly(DL-lactide-co-glycolide)-Nonane.	98
C-12	Retention diagram for 100% Poly(DL-lactide-co-glycolide)-Decane.	99
C-13	Retention diagram for 100% Poly(DL-lactide-co-glycolide)-Undecane.	100
C-14	Retention diagram for 100% Poly(DL-lactide-co-glycolide)-Dodecane.	101
C-15	Retention diagram for 100% Poly(DL-lactide-co-glycolide)-EthylAcetate.	102
C-16	Retention diagram for 100% Poly(DL-lactide-co-glycolide)-PropylAcetate.	103
C-17	Retention diagram for 100% Poly(DL-lactide-co-glycolide)-Water.	104
C-18	Retention diagram for 100% Poly(3-hydroxybutyric acid)-Heptane.	105

Figure		Page
C-19	Retention diagram for 100% Poly(3-hydroxybutyric acid)-Octane.	106
C-20	Retention diagram for 100% Poly(3-hydroxybutyric acid)-Nonane.	107
C-21	Retention diagram for 100% Poly(3-hydroxybutyric acid)-Decane.	108
C-22	Retention diagram for 100% Poly(3-hydroxybutyric acid)-Undecane.	109
C-23	Retention diagram for 100% Poly(3-hydroxybutyric acid)-Dodecane.	110
C-24	Retention diagram for 100% Poly(3-hydroxybutyric acid)-MethylAcetate.	111
C-25	Retention diagram for 100% Poly(3-hydroxybutyric acid)-EthylAcetate.	112
C-26	Retention diagram for 100% Poly(3-hydroxybutyric acid)-PropylAcetate.	113
C-27	Retention diagram for 100% Poly(3-hydroxybutyric acid)-ButylAcetate.	114
C-28	Retention diagram for 50-50 Amylopectin-Polycaprolactone-Pentane.	115
C-29	Retention diagram for 50-50 Amylopectin-Polycaprolactone-Hexane.	116
C-30	Retention diagram for 50-50 Amylopectin-Polycaprolactone-Heptane.	117
C-31	Retention diagram for 50-50 Amylopectin-Polycaprolactone-Octane.	118
C-32	Retention diagram for 50-50 Amylopectin-Polycaprolactone-MethylAcetate.	119
C-33	Retention diagram for 50-50 Amylopectin-Polycaprolactone-EthylAcetate.	120

Figure		Page
C-34	Retention diagram for 50-50 Amylopectin-Polycaprolactone-PropylAcetate.	121
C-35	Retention diagram for 50-50 Amylopectin-Polycaprolactone-Methanol.	122
C-36	Retention diagram for 50-50 Amylopectin-Polycaprolactone-Ethanol.	123
C-37	Retention diagram for 50-50 Amylopectin-Polycaprolactone-Propanol.	124
C-38	Retention diagram for 50-50 Amylopectin-Polycaprolactone-Butanol.	125
C-39	Retention diagram for 50-50 Amylopectin-Polycaprolactone-Diethylamine.	126
C-40	Retention diagram for 50-50 Amylopectin-Polycaprolactone-Formic acid.	127
C-41	Retention diagram for 50-50 Amylopectin-Polycaprolactone-Water.	128
C-42	Retention diagram for 75-25 Amylopectin-Polycaprolactone-Hexane.	129
C-43	Retention diagram for 75-25 Amylopectin-Polycaprolactone-Heptane.	130
C-44	Retention diagram for 75-25 Amylopectin-Polycaprolactone-Octane.	131
C-45	Retention diagram for 75-25 Amylopectin-Polycaprolactone-Nonane.	132
C-46	Retention diagram for 75-25 Amylopectin-Polycaprolactone-Decane.	133
C-47	Retention diagram for 75-25 Amylopectin-Polycaprolactone-Undecane.	134
C-48	Retention diagram for 75-25 Amylopectin-Polycaprolactone-Dodecane.	135

Figure		Page ^x
C-49	Retention diagram for 75-25 Amylopectin-Polycaprolactone-MethylAcetate.	136
C-50	Retention diagram for 75-25 Amylopectin-Polycaprolactone-EthylAcetate.	137
C-51	Retention diagram for 75-25 Amylopectin-Polycaprolactone-PropylAcetate.	138
C-52	Retention diagram for 75-25 Amylopectin-Polycaprolactone-ButylAcetate.	139
C-53	Retention diagram for 50-50 Amylopectin-Poly(DL-lactide-co-glycolide)-Heptane.	140
C-54	Retention diagram for 50-50 Amylopectin-Poly(DL-lactide-co-glycolide)-Octane.	141
C-55	Retention diagram for 50-50 Amylopectin-Poly(DL-lactide-co-glycolide)-Nonane.	142
C-56	Retention diagram for 50-50 Amylopectin-Poly(DL-lactide-co-glycolide)-Decane.	143
C-57	Retention diagram for 50-50 Amylopectin-Poly(DL-lactide-co-glycolide)-Undecane.	144
C-58	Retention diagram for 50-50 Amylopectin-Poly(DL-lactide-co-glycolide)-Dodecane.	145
C-59	Retention diagram for 50-50 Amylopectin-Poly(DL-lactide-co-glycolide)-MethylAcetate.	146
C-60	Retention diagram for 50-50 Amylopectin-Poly(DL-lactide-co-glycolide)-EthylAcetate.	147
C-61	Retention diagram for 50-50 Amylopectin-Poly(DL-lactide-co-glycolide)-PropylAcetate.	148
C-62	Retention diagram for 50-50 Amylopectin-Poly(DL-lactide-co-glycolide)-ButylAcetate.	149
C-63	Retention diagram for 50-50 Amylopectin-Poly(3-hydroxybutyric acid)-Heptane.	150

Figure		Page
C-64	Retention diagram for 50-50 Amylopectin-Poly(3-hydroxybutyric acid)-Octane.	151
C-65	Retention diagram for 50-50 Amylopectin-Poly(3-hydroxybutyric acid)-Nonane.	152
C-66	Retention diagram for 50-50 Amylopectin-Poly(3-hydroxybutyric acid)-Decane.	153
C-67	Retention diagram for 50-50 Amylopectin-Poly(3-hydroxybutyric acid)-Undecane.	154
C-68	Retention diagram for 50-50 Amylopectin-Poly(3-hydroxybutyric acid)-Dodecane.	155
C-69	Retention diagram for 50-50 Amylopectin-Poly(3-hydroxybutyric acid)-MethylAcetate.	156
C-70	Retention diagram for 50-50 Amylopectin-Poly(3-hydroxybutyric acid)-EthylAcetate.	157
C-71	Retention diagram for 50-50 Amylopectin-Poly(3-hydroxybutyric acid)-PropylAcetate.	158
C-72	Retention diagram for 50-50 Amylopectin-Poly(3-hydroxybutyric acid)-ButylAcetate.	159
C-73	Retention diagram for 50-50 Amylopectin-Poly(3-hydroxybutyric acid)-Butanol.	160

LIST OF TABLES

Table		Page
3-1	100% Amylopectin thermodynamic parameters.	26
3-2	100% Poly(DL-lactide-co-glycolide) thermodynamic parameters.	27
3-3	100% Poly(3-hydroxybutyric acid) thermodynamic parameters.	28
3-4	50-50 Amylopectin-Polycaprolactone thermodynamic parameters.	29
3-5	75-25 Amylopectin-Polycaprolactone thermodynamic parameters.	30
3-6	50-50 Amylopectin- Poly(DL-lactide-co-glycolide) thermodynamic parameters.	31
3-7	50-50 Amylopectin- Poly(3-hydroxybutyric acid) thermodynamic parameters.	32
3-8	Dispersive surface energies (γ_s^d) of Amylopectin and its blends.	33
B-1	Specific retention volumes (V_g) of solutes at a temperature range 80°C to 200°C for 100% Amylopectin column.	77
B-2	Specific retention volumes (V_g) of solutes at a temperature range 80°C to 170°C for 100% Poly(DL-lactide-co-glycolide) column.	78
B-3	Specific retention volumes (V_g) of solutes at a temperature range 80°C to 200°C for 100% Poly(3-hydroxybutyric acid) column.	79
B-4	Specific retention volumes (V_g) of solutes at a temperature range 80°C to 160°C for 50-50 Amylopectin-Polycaprolactone column.	81
B-5	Specific retention volumes (V_g) of solutes at a temperature range 80°C to 260°C for 75-25 Amylopectin-Polycaprolactone column.	82
B-6	Specific retention volumes (V_g) of solutes at a temperature range 80°C to 180°C for 50-50 Amylopectin-Poly(DL-lactide-co-glycolide) column.	84
B-7	Specific retention volumes (V_g) of solutes at a temperature range 80°C to 200°C for 50-50 Amylopectin-Poly(3-hydroxybutyric acid) column.	85

ACKNOWLEDGMENTS

In the name of Allah, the most beneficent, the most merciful. Praise be to almighty Allah, Lord of the whole universe, whom we worship and to whom we offer supplication for aid.

A heartfelt word of appreciation goes to my dear parents and my faithful wife for their support. They maintained and made the climate suitable for me to work out this research thesis, and patiently tolerated the disruption made thereby to their lives. In addition, the same thanks go to my father-in-law and my mother-in-law.

Next, I would like to thank my thesis committee for their assistance in conducting and reviewing this research thesis. My special gratitude and thanks go to Professor Zeki Y. Al-Saigh for his directions, guidance, continuous help, and his close supervision during the work conducted in this research thesis. My gratitude and thanks also, go to both Associate Professor Floyd R. Jackson, and Associate Professor Jeffrey A. Zuiderveen for their invaluable support and help during the work conducted.

Moreover, I would like to thank both Professor James A. Gore and Mrs. Catherine J. Anderson for their invaluable support.

Last but not least, great thanks and appreciations go to my employer, Saudi Arabian Oil Company (Saudi ARAMCO), Kingdom of Saudi Arabia, for the invaluable support during my graduate study.

INTRODUCTION

Background.

At the beginning of the 21st century, six billion people lived on earth, and it is anticipated that the population will surpass ten billion in the middle of this century (Okada, 2002). Because of this explosive increase in population, we are confronting several serious problems such as deficiencies in food, resources and energy, and global environmental pollution. Sciences and technologies in the last century, have made astonishing progress, particularly after World War II, and made our daily life more comfortable and convenient (Josephson, 1993). As for polymeric materials, a variety of synthetic polymers have been developed and used as synthetic fibers, plastics, and synthetic rubbers in place of traditionally used natural fibers, woods, and natural rubbers (Okada, 2002). Synthetic polymers are utilized in a wide variety of fields including transportation, construction, packaging, electronic devices, medical appliances, etc. Nowadays, about 150 million tons of plastics are produced annually all over the world, and the production and consumption continue to increase (Okada, 2002). Most of these plastics are of petroleum origin, and the increase in the production of plastics, as a consequence, results in the increase of oil consumption.

In the 1970s, it became evident that the very technical advantages, which made polymers so useful, were disadvantages when polymer-based products were discarded at the end of their useful life and in particular when they appeared as litter in the environment (Scott, 2000). Packaging is one industry that has been revolutionized by oil-based polymers such as polyethylene, polypropylene, polystyrene, and poly(vinyl

chloride) (Amass et al., 1998). Despite the major advances in the synthesis, manufacturing and processing of these materials, one of the major problems still confront the industry is the use of non-renewable oil-based chemicals for the ultimate fate of the waste materials (Nere and Jagtap, 2001). The effects of some items of plastics packaging was found to be very damaging to wild-life and this led to calls from the green movement to return to biologically based renewable polymers (Nayak, 1999).

The management of solid waste disposal, with regard to the decreasing availability of landfills, the litter problem, and the pollution of marine environment, is becoming very urgent in the industrialized countries. Hence, the need for solutions extends very quickly to the developing countries (Bastioli, 1998). The fundamental solid waste issues today comprise the areas of increasing municipal solid waste particularly when non-biodegradable materials are present. In addition, municipal solid waste is becoming increasingly difficult with the accumulations of thousands of tons of non-biodegradable plastics in the landfills. Plastic waste is often especially newsworthy because of reported wildlife deaths by entanglement and ingestion of discarded plastic articles (Van Volkenburgh and White, 1993).

In the last 30 years, the United States of America (USA) has increased their yearly output of trash from 176 billion pounds to over 360 billion pounds (Van Volkenburgh and White, 1993). This is an average of nearly 1500 pounds of trash per year for every man, woman, and child in the USA. The bill for handling this much garbage is currently about 15 billion dollars per year. Consequently, a 73% majority of this waste goes into landfills, 14% undergoes incineration, and 13% is recycled (Bastioli, 1998). Landfills, especially in urban areas, are therefore filling at an alarming rate. It is

difficult to site new landfills because of stricter Environmental Protection Agency (EPA) rules, the high cost to construct new, safe landfills, and the dislike of the general public for a landfill situated nearby (Van Volkenburgh and White, 1993).

Over the last years, there have been a number of proposed solutions concerning the best ways to deal with the solid-waste crisis. These generally fall into the categories such as, source reduction, recycling, waste to energy incineration, landfilling, education, composting, and degradable plastics (Van Volkenburgh and White, 1993).

Because plastics are a high profile item in garbage, there is apparently a public perception that plastic is the major contributor to the landfill congestion problem. In 1991, domestic manufacturers produced over 50 billion pounds of plastics, yet plastics represent about 20% by volume of the solid waste of an average city (Van Volkenburgh and White, 1993). The essential idea is to minimize land filling by better using source reduction, recycling, and incineration.

The plastic component is resistant to microbial attack and, hence, accumulates. The plastic waste can neither add to the fertility of the soil nor improve its firmness in landfill operations. Disposal of polymer waste is a serious problem, which can be solved either by recycling, incineration, or land filling. Recycling is a part-time solution to a long-term reduction process in plastic waste. However, incineration has the advantage that the plastics have high calorific value, but incineration plants have to be modified for efficient combustion of the polymers and regulation of the gas emissions to ensure that no toxic gases are released into the atmosphere (Dempsy and Oppelt, 1993). The problems associated with incineration are evolution of air pollutants such as NO_2 , SO_2 , NH_3 , etc (Corbitt, 1990). And, landfilling is a way of disposal of plastic but it affects the

environment. The plastic waste material remains there for several years, causing aesthetic problems; hence, there is need for search of polymers, which are completely biodegradable (Bastioli, 1998).

The use of degradable plastics is, as yet, a minor factor in this overall strategy, but development of biodegradable polymers has considerable implications for medical, food and agricultural packaging. The main factors that are needed for development of biodegradable polymers are as follows (Amass et al., 1998):

- Non-toxic materials with non-toxic degradation products that would not affect the drainage water from landfill sites.
- Polymers with suitable mechanical properties for specific uses.
- Economic viability.

Current EPA mandates require layering and sealing of the typical landfill in such a manner that very little air or moisture is present. This significantly retards biodegradation. For most biodegradation additives or biodegradable plastics to degrade at a rapid rate, it is necessary that air and moisture are present. In addition, the pro-oxidant system requires certain levels of oxygen to function effectively. If there is insufficient air and moisture present in the typical landfill to biodegrade common food waste rapidly, one would generally not expect a given plastic biodegradation system to degrade very effectively either (Swift, 1993).

While biodegradable materials are not expected to replace completely all of the plastic currently used in these markets, it represents an exciting, huge business opportunity to be seized. There are two major areas for small business involvement. The first, obviously, is one to design and engineer fully biodegradable plastics that have the

required functional requirements for marketing. The other very profitable and promising area for existing and new small businesses is in the downstream processing of biodegradable polymers currently being produced (Nayak, 1999). One of the easiest options is to discard the use of plastics in packaging applications and think of using non-plastic packaging materials, but it will not be a viable option as there would be a drastic increase in terms of weight and volume; also the additional energy consumption would be prohibitive (Nere and Jagtap, 2001). Hence, use of friendly polymer is becoming a need for making clean environment. One of the most suited options is "Biodegradable Polymers".

Biodegradable Polymers.

Biodegradable polymers are defined as, polymers which undergo chemical degradation, caused by biochemical reaction, especially those catalyzed by enzymes produced by microorganism under aerobic or anaerobic conditions (Nere and Jagtap, 2001). Since 1990, the prospective markets for the biodegradable polymers includes wrappers for various consumer goods, such as medicines, agriculture, forestry, and fishery products. The latest example was at the Sydney Olympics, about 40 million articles made from biodegradable polymer used for packaging and food serving purposes (Nere and Jagtap, 2001). In addition, biodegradable polymeric materials are targeted toward single-use disposable short-life packaging materials.

Although the term "biodegradable polymers" is becoming more popular, it has different meanings. The definitions are not always clear and they are open to a large diversity of interpretations. On the one hand, in the biomedical area, "biodegradation"

refers to hydrolyses and oxidations that are the primary polymer degradation processes. On the other hand, for materials exposed to a natural environment, this term means fragmentation, loss of mechanical properties or chemical modifications through the action of microorganisms (Chandra and Rustgi, 1998).

Degradation can be defined as "a change in the chemical structure of a plastic involving a deleterious change in properties." (Scott, 2000). The material is degraded under environmental conditions such as, microorganisms, temperature, light, and water and in a reasonable period of time in one or more steps. It has been suggested that the degradation of plastics could be divided into "deterioration" and "decomposition". Deterioration corresponds to physical and chemical degradation with a permanent change in the physical and chemical properties, which results in a decrease in weight (Calmon-Decriaud et al., 1998).

Biodegradation is a natural process by which organic chemicals in the environment are converted to simpler compounds, mineralized and redistributed through elemental cycles such as the carbon, nitrogen and sulfur cycles (Satyanarayana and Chatterji, 1993). Thus, biodegradation can only occur within the biosphere as microorganisms play a central role in the biodegradation process (Chandra and Rustgi, 1998). For most biodegradation, additives or biodegradable plastics to degrade at a rapid rate, it is necessary that air and moisture are present. If there is insufficient air and moisture present in the typical landfill to biodegrade common food waste rapidly, one would generally not expect a given plastic biodegradation system to degrade very effectively, either (Demirgoz et al., 2000). The applications of biodegradable polymers have been the focus of three major areas: medical, agricultural, and consumer goods

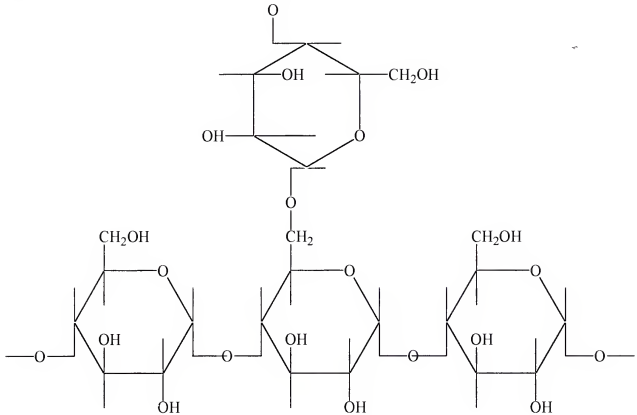
packaging. Some of these have resulted in commercial products. Because of their specialized nature and greater unit value, medical device applications have developed faster than the other two.

Amylopectin and Other Biodegradable Polymers.

Starch is one of the main natural materials that have been extensively investigated for use as packaging material and it has the added advantage of being a renewable source of polymeric material. The main sources for the commercial production of starch are potatoes, wheat, corn and rice. Starch comprises two polymeric components, amylose and amylopectin; they are built of α -D-glucopyranose residues but differ in both structure and function (Suvorva et al., 2000). Amylopectin (Figure 1-1), constitutes the greater part (70%) of the starch molecule. The molecular mass of amylopectin is approximately 10^5 kg/mol. (Suvorva et al., 2000). It is totally biodegradable in a wide variety of environments and permits the development of totally degradable products for specific market demands. Starch is a potentially useful polymer for thermoplastic biodegradable materials because of its low cost, availability, and production from annually renewable resources (Blanshard, 1987). Degradation or incineration of starch products recycles atmospheric CO₂ trapped by starch-producing plants and does not contribute to potential global warming (Bastioli, 1998). Starch and its blends have attracted much attention as an environmentally biodegradable polymer. Like polymer blends wide applications, starch-based blends have potential to be used in the environmental and biomedical fields, as they are easily obtained in a large quantity by an inexpensive route and totally biodegradable (Demirgoz et al., 2000). Most of these applications require accurate

control of polymer water up-take ability, degradation rate and mechanical performance in various media (Nere and Jagtap, 2001).

Figure 1-1. Structure of Amylopectin (Nayak, 1999).



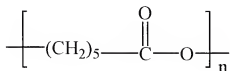
Recently, there has been increasing interest in developing starch-based polymers and its blend to produce biodegradable plastics to be used in many applications. Starch is a good candidate for such a development due to the fact that starch is abundant and is mechanically weak because of its poor physical, mechanical, and low dimensional stability (Nere and Jagtap, 2001).

The blending of biodegradable polymers is a method of both reducing the overall cost of material and increasing the degradation rates. The rate of biodegradation is

correlated with the type of morphology, crystallinity, surface area, and additives. The main disadvantages of biodegradable polymers are their dominant hydrophilic character, fast degradation rate, and in some cases unsatisfactory mechanical properties particularly under wet conditions (Amass et al., 1998). Blending Amylpectin with other biodegradable polymers may offer opportunities to modify the physical properties of Amylopectin, improve the processability, reduce the water-uptake ability and possibly enhance the mechanical properties.

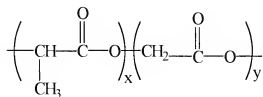
Polycaprolactone (Figure 1-2), is sold under the trade name of Tone Polymer by Union Carbide. Grades of Polycaprolactone have been commercially available since 1975 and are used in coatings (Jun, 2000). Polycaprolactone is obtained by the ring opening polymerization of ϵ -caprolactone (Amass et al., 1998). The low melting temperature of Polycaprolactone is an advantage in accelerating degradation in composting environments in which temperatures often reach 60°C. However, problems may arise in applications in which elevated storage or use temperatures may be experienced that could compromise mechanical integrity and thus performance (Jun, 2000). Blending starch with Polycaprolactone, a non-toxic polymer, may enhance the mechanical properties of starch (Karlsson and Albertsson, 1998). It should be noted, however, that Polycaprolactone degradation rate is slow due to its high crystallinity and low melting temperature (Chandar and Rustgi, 1998).

Figure 1-2. Structure of Polycaprolactone (Nayak, 1999).



Poly(DL-lactide-c-glycolide) (Figure 1-3), is a polyester synthesized by the condensation polymerization of lactides and glycolides and has molecular weight averaging between 75,000 to 120,000 g/mol. Condensation polymerization of lactic acid produces low molecular weight, which is then spliced together using coupling agents to produce the higher molecular weights essential for good mechanical properties, significantly more amorphous, and a lower melting point (Park et al., 2000). Poly(DL-lactide-c-glycolide) is a biodegradable material and used for biomedical applications. In recent years, environmental concerns have led to an escalated interest in Poly(DL-lactide-c-glycolide), as well as other biodegradable polymers, as an alternative to traditional commodity plastics (Arvanitoyannis, 1999). Poly(DL-lactide-c-glycolide) has the advantage of being not only biodegradable but also renewable since the raw material, lactic acid, may be produced by microbial fermentation of biomass. Also, it has low glass transition temperature, and slow crystallization rate (Bastioli, 1998).

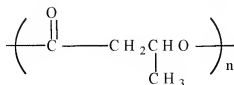
Figure 1-3. Structure of Poly(DL-lactide-c-glycolide) (Sigma-Aldrich Co., 2003).



Poly(3-hydroxybutyric acid) (Figure 1-4), is produced commercially by Monsanto and sold as Biopol. Poly(3-hydroxybutyric acid) has molecular weight of 437,000 g/mol. Poly(3-hydroxybutyric acid) is representative of a useful range of potential biodegradable polymers (Zhang et al., 1997). Poly(3-hydroxybutyric acid) can be degraded to water and

carbon dioxide under environmental conditions by a variety of bacteria, and has much potential for applications of environmentally degradable plastics (Vasnev, 1997).

Figure 1-4. Structure of Poly(3-hydroxybutyric acid) (Sigma-Aldrich Co., 2003).



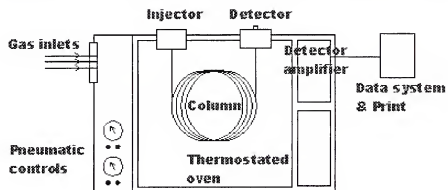
Physical characteristics of packaging polymers are greatly influenced by the chemical structure, molecular weight, crystallinity and processing conditions of the polymers used. The physical characteristics required in packaging depend on what item will be packaged as well as the environment in which the package will be stored. The challenge in the development of biodegradable packaging will be to combine polymers which are truly biodegradable into a laminate film or a film blend which has properties as good as those found in synthetic laminates (Chandar and Rustgi, 1998).

Inverse Gas Chromatography

Chromatography can separate complex mixtures with great precision. In fact, chromatography can purify basically any soluble or volatile substance if the right adsorbent material, carrier fluid, and operating conditions are employed (Gutierrez et al., 1999). Gas Chromatography (GC) like any other chromatographic technique, is based on the distribution of probe molecule between two phases. In gas solid chromatography, the phases are gas and solid as the injected compound is carried by the gas phase through a column filled with solid phase. Separation of two or more components injected

simultaneously is due to their differing affinities for the stationary phase. In gas liquid chromatography, the stationary phase is a liquid coated onto a solid support (Gutierrez et al., 1999). The Inverse Gas chromatography (IGC) (Figure 1-2) is a gas phase technique for characterizing surface and bulk properties of solid materials. It is the reverse of a conventional GC experiment.

Figure 1-5. Diagram of Inverse Gas Chromatography (IGC) (Gutierrez, et al. 1999).



A cylindrical column is uniformly packed with the solid material of interest, typically a powder, fiber or film. A pulse or constant concentration of gas is then injected down the column at a fixed carrier gas flow rate. The time taken for pulse or concentration front to elute down the column are measurements with different gas phase probe molecules that allow access to a wide range of physicochemical properties of the solid sample. The term inverse refers to the polymer that can be studied in the solid phase as the stationary phase, either as a finely divided powder or coating, dispersed on a suitable inert support and packed into a chromatographic column unlike the conventional GC where the separation of solvents (solutes) is the prime interest (Gutierrez et al., 1999). The most typical IGC applications are as follows:

- Natural and Artificial Fibers.
- Coatings and Thin-Films.
- Polymers, Composites and Fillers.

Recently, IGC has emerged as a promising method for polymers and polymer blends characterization. It has shown that the IGC method can be useful in obtaining thermodynamic data on polymeric systems even when the morphology is complex (Amass et al., 1998). It can also be used to measure surface energies, glass transitions in polymers, and degrees of crystalline in polymeric materials. The attraction of the IGC method lies in its ability to generate a fast and accurate physicochemical data on polymeric systems. It is a relatively rapid, convenient method and has the flexibility of selecting the desired temperature ranges. IGC can also be applied over a wide range of temperatures. Solutes may be changed more easily. The combination of these advantages makes it possible to characterize, quickly and accurately, the interactions of polymer blends with a wide variety of solutes over a wide range of temperatures and concentrations (Gutierrez et al., 1999). For the characterization of polymers, the most informative IGC data is obtained from the retention diagrams. The value of V_g is determined over a range of temperatures and $\ln V_g$ is plotted as a function of $1/T$.

Objectives.

As mentioned earlier, the challenge in the development of biodegradable packaging is to blend two biodegradable polymers into a laminate film or a film blend which has properties as good as those found in synthetic laminates. This could significantly contribute to the solution to the problem of solid waste management.

To accomplish this goal, the physical properties of the blends need to be investigated with certain precision. Such properties will provide information as to whether the blends are compatible over a range of temperatures and composition. In this research thesis, the objective was to study the characterization of selective biodegradable polymers using the IGC method which are considered to be environmentally friendly polymers. Starch or Amylopectin is totally biodegradable in a wide variety of environments and it is a potentially useful polymer for thermoplastic biodegradable materials (Blanshard, 1987). IGC was used to obtain information on Amylopectin and its blends such as, Polycaprolactone, Poly(DL-lactide-co-glycolide), and Poly(3-hydroxybutyric acid).

A variety of chemically different solutes with different chemical natures were used in this research thesis, including a series of alkanes, acetates, alcohols, diethylamine, formic acid, and water. Vanishing amounts of these solutes were injected into the chromatographic columns.

All chromatographic columns were measured using the IGC method, as mentioned, with increasing the oven temperature until a complete set of data was obtained. The retention time of solutes was measured on a completely automated data handling system. This allowed for precise measurements of the retention times of the solutes injected into the chromatographic columns.

The changes in the morphology of the blend systems will reveal the melting temperature, the glass transition temperature, the degree of crystallinity, and the amorphous nature of these blends. Thus, the thermodynamics were also established for

the amorphous region. Slopes, and heats of mixing of the pure Amylopectin and its blends were also calculated.

Since Amylopectin is a semi-crystalline polymer and the degree of crystallinity is expected to change when it is blended with another biodegradable polymer, IGC is considered to be a versatile technique by which the degree of crystallinity can be obtained at each individual temperature (Holmes, 1988). In addition, surface energy, which is considered to be one of the methods, reported for characterization of polymers was also obtained from the IGC experiments for the Amylopectin and its blends. Therefore, by finding and calculating the results obtained on the pure Amylopectin and Amylopectin blends, the characterization of the physio-chemical properties of the pure Amylopectin and Amylopectin blends could be drawn of each one.

MATERIALS AND METHODS

Amylopectin and its Blends.

In this research thesis, we utilized the chemicals and instrumentation available in the Chemistry and Geology Department, College of Sciences, Columbus State University. All Amylopectin, Polycaprolactone, Poly(DL-lactide-co-glycolide), and Poly(3-hydroxybutyric acid) polymers were purchased from Sigma.

Columns Preparation.

Many techniques were used in this research thesis in order to prepare the subject columns. Each sample was weighed carefully and dissolved in the appropriate solvent. The polymer solution was used to coat the solid support using the pile method. The loading of the polymer sample was calculated relative to the weight of the solid support (% wt/wt). Chromosorb W (AW-DMCS treated, 60/80 mesh), was obtained from Analabs. The chromatographic columns were prepared using five-foot-long, 1/4 inch ID copper tubing, which were purchased from Lowe's hardware store, Columbus, GA. Seven (7) chromatographic columns were prepared and used in this research thesis. Preparation of these columns is described as follows:

100% Amylopectin Column:

- Dissolved 0.40 g from Amylopectin in 25 mL of hot water. Stirred it and left it for overnight (between 12-24 hours).
- Placed 7.90 g of Chromosorb-W in a porcelain-evaporating dish. Then, added drops, gently, of the dissolved solution in order to coat the solid support (so as not

to touch the surface of the dish). Then, mixed the whole mixture together while adding the drops of the dissolved solution.

- Dried the coated mixture in an oven at 80°C for 24 hours by covering it with aluminum foil.
- Prepared 5 ft column of 0.25-inch ID copper tubing by washing it with methyl alcohol and dried it in the oven at 80°C for 2 hours. Packed the coated solid support in the copper tubing using silanized glass wool for plugging both ends. So, the stationary phase studied.

100% Poly(DL-lactide-co-glycolide) Column:

- Dissolved 0.40 g from Poly(DL-lactide-co-glycolide) in 50 mL of Acetonitrile (Methyl Cyanide, CH_3CN). Stirred the solution and left it for overnight (between 12-24 hours).
- Placed 7.90 g of Chromosorb-W in a porcelain-evaporating dish. Then, added drops, gently, of the dissolved solution in order to coat the solid support (so as not to touch the surface of the dish). Then, mixed the whole mixture together while adding the drops of the dissolved solution.
- Dried the mixture in an oven at 80°C for 24 hours by covering it with aluminum foil.
- Prepared 5 ft column of 0.25-inch ID copper tubing by washing it with methyl alcohol and dried it in the oven at 80°C for 2 hours. Packed the coated solid support in the copper tubing using silanized glass wool for plugging both ends. So, the stationary phase studied.

100% Poly(3-hydroxybutyric acid) Column:

- Dissolved 0.40 g from Poly(3-hydroxybutyric acid) and dissolved it in 100 mL of a heated Chloroform (CHCl_3). Stirred it and left it for overnight (between 12-24 hours).
- Placed 7.90 g of Chromosorb-W in a porcelain-evaporating dish. Then, added drops, gently, of the dissolved solution in order to coat the solid support (so as not to touch the surface of the dish). Then, mixed the whole mixture together while adding the drops of the dissolved solution.
- Dried the coated mixture in an oven at 80°C for 24 hours by covering it with aluminum foil.
- Prepared 5 ft column of 0.25-inch ID copper tubing by washing it with methyl alcohol and dried it in the oven at 80°C for 2 hours. Packed the coated solid support in the copper tubing using silanized glass wool for plugging both ends. So, the stationary phase studied.

50-50 Amylopectin-Polycaprolactone Column:

- Dissolved 0.20 g from Amylopectin and dissolve it in 25 mL of hot water. Then, 0.20 g from Polycaprolactone and dissolved it in it in 25 mL of hot water. Then, mixed the two solutions together. Stirred it and left it for overnight (between 12-24 hours).
- Placed 7.90 g of Chromosorb-W in a porcelain-evaporating dish. Then, added drops, gently, of the dissolved solution in order to coat the solid support (so as not to touch the surface of the dish). Then, mixed the whole mixture together while adding the drops of the dissolved solution.

- Dried the coated mixture in an oven at 80°C for 24 hours by covering it with aluminum foil.
- Prepared 5 ft column of 0.25-inch ID copper tubing by washing it with methyl alcohol and dried it in the oven at 80°C for 2 hours. Packed the coated solid support in the copper tubing using silanized glass wool for plugging both ends. So, the stationary phase studied.

75-25 Amylopectin-Polycaprolactone Column:

- Dissolved 0.30 g from Amylopectin and dissolved it in 25 mL of hot water. Then, 0.10 g from Polycaprolactone and dissolved it in it in 25 mL of hot water. Then, mixed the two solutions together. Stirred it and left it for overnight (between 12-24 hours).
- Placed 7.90 g of Chromosorb-W in a porcelain-evaporating dish. Then, added drops, gently, of the dissolved solution in order to coat the solid support (so as not to touch the surface of the dish). Then, mixed the whole mixture together while adding the drops of the dissolved solution.
- Dried the coated mixture in an oven at 80°C for 24 hours by covering it with aluminum foil.
- Prepared 5 ft column of 0.25-inch ID copper tubing by washing it with methyl alcohol and dried it in the oven at 80°C for 2 hours. Packed the coated solid support in the copper tubing using silanized glass wool for plugging both ends. So, the stationary phase studied.

50-50 Amylopectin-Poly(DL-lactide-co-glycolide) Column:

- Dissolved 0.20 g from Amylopectin and dissolved it in 35 mL of water. Then, 0.20 g from Poly(DL-lactide-co-glycolide) and dissolved it in 50 mL of Acetonitrile (Methyl Cyanide, CH_3CN). Then, mixed the two solutions together. Stirred it and left it for overnight (between 12-24 hours).
- Placed 7.90 g of Chromosorb-W in a porcelain-evaporating dish. Then, added drops, gently, of the dissolved solution in order to coat the solid support (so as not to touch the surface of the dish). Then, mixed the whole mixture together while adding the drops of the dissolved solution. so as
- Dried the coated mixture in an oven at 80°C for 24 hours by covering it with aluminum foil.
- Prepared 5 ft column of 0.25-inch ID copper tubing by washing it with methyl alcohol and dried it in the oven at 80°C for 2 hours. Packed the coated solid support in the copper tubing using silanized glass wool for plugging both ends. So, the stationary phase studied.

50-50 Amylopectin-Poly(3-hydroxybutyric acid) Column:

- Dissolved 0.20 g from Amylopectin and 0.20 g from Poly(3-hydroxybutyric acid) in 100 mL of Chloroform (CHCl_3). Stirred it and left it for overnight (between 12-24 hours).
- Placed 7.90 g of Chromosorb-W in a porcelain-evaporating dish. Then, added drops, gently, of the dissolved solution in order to coat the solid support (so as not to touch the surface of the dish). Then, mixed the whole mixture together while adding the drops of the dissolved solution.

- Dried the coated mixture in an oven at 80°C for 24 hours by covering it with aluminum foil.
- Prepared 5 ft column of 0.25-inch ID copper tubing by washing it with methyl alcohol and dried it in the oven at 80°C for 2 hours. Packed the coated solid support in the copper tubing using silanized glass wool for plugging both ends. So, the stationary phase studied.

A total of nineteen (19) solutes with different chemical nature, chromatographic grade, were purchased from Aldrich Chemical Co and Fisher Scientific Co in a pure form. These includes, Pentane, Hexane, Heptane, Octane, Nonane, Decane, Undecane, Dodecane, MethylAcetate, EthylAcetate, PropylAcetate, ButylAcetate, Methanol, Ethanol, Propanol, Butanol, Diethylamine, Formic acid, and Water were injected into the chromatographic columns.

Data Analysis.

The chromatographic measurements were performed using a modified conventional Hewlett Packard 5730A GC equipped with a thermal conductivity detector. The GC was modified to allow continuous monitoring of the carrier gas flow rate, the inlet and outlet pressure, and the column temperature. To avoid change in the morphology of Amylopectin and its blends, such as recrystallization, the GC was kept operational at all times. During the course of the experiments, the oven temperature was increased from 80°C to 200°C until a complete set of data was obtained. The flow rate was monitored throughout this research thesis.

The retention time of solutes were measured on a completely automated data handling system, Shimadzu, C-R3A, Chromatopac. This was allowed for precise measurements of the retention times of the solutes injected into the chromatographic columns. The chromatographic signal was analyzed as a function of time and recorded in a log sheet for further thermodynamic calculations.

All data was computed and presented as retention diagrams. Retention diagrams of all solutes were analyzed to reveal the changes in the morphology of the systems. Slopes were calculated only for the straight line of the graphs where the polymer is completely amorphous. In addition, detailed calculations were carried out using the data collected such as, specific retention volume (V_g) which is commonly used to describe the elution behavior of solutes (Gutierrez et al., 1999), heat of mixing (ΔH), melting point (T_m), glass transition temperature (T_g), degree of crystallinity (χ), and dispersive surface energy (γ_s^d).

RESULTS

Nineteen (19) solutes were injected into seven (7) separate chromatographic columns containing pure Amylpectin and Amylopectin and its blends. From chromatographic retention times of solutes, the specific retention volumes (V_g) of all solutes were calculated as shown in Appendix A and are computed in table B-1 to table B-7, Appendix B. From V_g values, plots of $\ln V_g$ versus $1/T$ are generated as retention diagrams for all solutes. These plots are presented in figure C-1 to figure C-73, Appendix C.

For 100% Amylopectin column, retention diagrams are presented in figure C-1 to figure C-8. For 100% Poly(DL-lactide-co-glycolide) column, retention diagrams are presented in figure C-9 to figure C-17. For 100% Poly(3-hydroxybutyric acid) column, retention diagrams are presented in figure C-18 to figure C-27. For 50-50 Amylopectin-Polycaprolactone column, retention diagrams are presented in figure C-28 to figure C-41. For 75-25 Amylopectin-Polycaprolactone column, retention diagrams are presented in figure C-42 to figure C-52. For 50-50 Amylopectin-Poly(DL-lactide-co-glycolide) column, retention diagrams are presented in figure C-53 to figure C-62. For 50-50 Amylopectin-Poly(3-hydroxybutyric acid) column, retention diagrams are presented in figure C-63 to figure C-73.

Slopes were calculated only for the straight line of the retention diagrams where the polymer is completely amorphous and are computed in table 3-1 to table 3-7. In addition, heats of mixing (ΔH), melting point (T_m), and glass transition temperature (T_g) were calculated as shown in Appendix A and are computed in table 3-1 to table 3-7.

The degree of crystallinity (α) of the polymers was calculated as shown in Appendix A and are computed in table 3-1 to table 3-7. For 100% Poly(DL-lactide-co-glycolide) column, Decane was selected to show the relationship of the crystallinity and is presented in figure 3-1. For 100% Poly(3-hydroxybutyric acid) column, Decane was selected to show the relationship of the crystallinity and is presented in figure 3-2. For 75-25 Amylopectin-Polycaprolactone column, PropylAcetate was selected to show the relationship of the crystallinity and is presented in figure 3-3. For 50-50 Amylopectin-Poly(DL-lactide-co-glycolide) column, Nonane was selected to show the relationship of the crystallinity and is presented in figure 3-4. For 50-50 Amylopectin-Poly(3-hydroxybutyric acid) column, Nonane was selected to show the relationship of the crystallinity and is presented in figure 3-5.

Plots of $RT \ln V_g$ versus the number of carbons in the alkane series were generated for each temperature. A linear relationship was obtained in all of these plots and the slopes of the straight lines were computed as the free energy of desorption of a CH_2 group, and used in the calculation of the surface energy (γ_s^d). A complete theoretical calculation of the dispersive component of the γ_s^d of Amylopectin and its blends were calculated as shown in Appendix A and computed in table 3-8.

For 100% Amylopectin column, the surface energy diagram is presented in figure 3-6. For 100% Poly(DL-lactide-co-glycolide) column, the surface energy diagram is presented in figure 3-7. For 100% Poly(3-hydroxybutyric acid) column, the surface energy diagrams are presented in figure 3-8 to figure 3-12. For 75-25 Amylopectin-Polycaprolactone column, the surface energy diagrams are presented in figure 3-13 to figure 3-22. For 50-50 Amylopectin-Poly(DL-lactide-co-glycolide) column, the surface

energy diagrams are presented in figure 3-23 to figure 3-25. For 50-50 Amylopectin-Poly(3-hydroxybutyric acid) column, the surface energy diagrams are presented in figure 3-26 to figure 3-30.

Table 3-1. 100% Amylopectin thermodynamic parameters.

SOLUTE	SLOPE	ΔH (KJ)	T_m ($^{\circ}C$)	T_g ($^{\circ}C$)	α	TEMP. ($^{\circ}C$)
Pentane	4092.70	-34.03	160.00	N/D	N/A	N/A
Hexane	2852.40	-23.71	160.00	N/D	N/A	N/A
Heptane	1569.90	-13.05	160.00	120.00	N/A	N/A
Methanol	4652.50	-38.68	N/D	N/D	N/A	N/A
Ethanol	4299.90	-35.75	160.00	N/D	N/A	N/A
Propanol	3810.10	-31.68	160.00	N/D	N/A	N/A
Butanol	4915.50	-40.87	160.00	120.00	N/A	N/A
Diethylamine	3374.00	-28.05	160.00	120.00	N/A	N/A

N/A: Not Applicable.

N/D: Not Detectable.

Table 3-2. 100% Poly(DL-lactide-co-glycolide) thermodynamic parameters

SOLUTE	SLOPE	ΔH (KJ)	T_m (°C)	T_g (°C)	α	TEMP. (°C)
Heptane	15251.00	-126.80	130.00	110.00	N/A	N/A
Octane	6846.30	-56.92	130.00	110.00	N/A	N/A
Nonane	7702.90	-64.04	130.00	110.00	N/A	N/A
Decane	16601.0	-138.0	130.00	110.00	99.84%, 99.66%, and 98.09%	80.00, 90.00, and 100.00
Undecane	6025.90	-50.10	130.00	110.00	69.88%, 64.30%, and 58.94%	90.00, 100.00, and 110.00
Dodecane	7772.30	-64.62	130.00	N/D	N/A	N/A
EthylAcetate	5681.00	-47.23	130.00	110.00	N/A	N/A
PropylAcetate	2701.20	-22.46	130.00	110.00	N/A	N/A
Water	2774.60	-23.07	N/D	N/D	N/A	N/A

N/A: Not Applicable.

N/D: Not Detectable.

Table 3-3. 100% Poly(3-hydroxybutyric acid) thermodynamic parameters

SOLUTE	SLOPE	ΔH (KJ)	T_m (°C)	T_g (°C)	α	TEMP. (°C)
Heptane	8792.10	-73.10	140.00	130.00	98.64%, 98.50%, 97.61%, and 95.09%	80.00, 90.00, 100.00, and 120.00
Octane	5910.30	-49.14	140.00	130.00	87.13%, 82.44%, 77.22%, and 70.85%	80.00, 90.00, 100.00, and 120.00
Nonane	4722.50	-39.26	140.00	130.00	69.58%, 58.51%, 52.31%, and 50.83%	80.00, 90.00, 100.00, and 120.00
Decane	6036.70	-50.19	140.00	130.00	72.19%, 58.10%, 57.67%, 45.13%, and 47.28%	80.00, 90.00, 100.00, 110.00, and 120.00
Undecane	6723.10	-55.90	140.00	130.00	40.54%, 33.64%, and 32.28%	100.00, 110.00, and 120.00
Dodecane	10525.0	-87.50	N/D	N/D	N/A	N/A
Methyl/acetate	5379.60	-44.73	N/D	N/D	N/A	N/A
Ethyl/acetate	10896.0	-90.59	140.00	130.00	98.44%, 96.27%, 93.36%, and 84.45%	80.00, 90.00, 100.00, and 120.00
Propyl/acetate	7168.00	-59.59	140.00	130.00	94.21%, 87.88%, 86.74, and 75.07%	80.00, 90.00, 100.00, and 120.00
Butyl/acetate	19018.0	-158.10	N/D	N/D	N/A	N/A

N/A: Not Applicable.

N/D: Not Detectable.

Table 3-4. 50-50 Amylopectin-Polycaprolactone thermodynamic parameters.

SOLUTE	SLOPE	ΔH (KJ)	T_m (°C)	T_g (°C)	α	TEMP. (°C)
Pentane	336.46	-2.80	N/D	N/D	N/A	N/A
Hexane	680.63	-5.66	N/D	N/D	N/A	N/A
Heptane	1577.70	-13.12	100.00	90.00	N/A	N/A
Octane	1613.70	-13.42	100.00	90.00	N/A	N/A
Methyl/acetate	1442.90	-12.00	N/D	N/D	N/A	N/A
Ethyl/acetate	1856.00	-15.43	N/D	N/D	N/A	N/A
Propyl/acetate	2654.40	-22.07	N/D	N/D	N/A	N/A
Methanol	1045.60	-8.69	110.00	100.00	N/A	N/A
Ethanol	1074.70	-8.94	N/D	N/D	N/A	N/A
Propanol	1364.10	-11.34	N/D	N/D	N/A	N/A
Butanol	2410.10	-20.04	N/D	N/D	N/A	N/A
Diethylamine	300.47	-2.50	110.00	90.00	N/A	N/A
Formic acid	N/A	N/A	N/D	N/D	N/A	N/A
Water	2520.10	-20.95	N/D	N/D	N/A	N/A

N/A: Not Applicable.

N/D: Not Detectable.

Table 3-5. 75-25 Amylopectin-Polycaprolactone thermodynamic parameters.

SOLUTE	SLOPE	ΔH (KJ)	T_m (°C)	T_g (°C)	χ	TEMP. (°C)
Hexane	2569.00	-21.36	160.00	120.00	N/A	N/A
Heptane	2466.10	-20.50	160.00	130.00	77.68%	84.14
Octane	2395.70	-19.92	170.00	130.00	N/A	N/A
Nonane	2973.30	-24.72	170.00	130.00	N/A	N/A
Decane	3979.60	-33.09	170.00	N/D	N/A	N/A
Undecane	4236.90	-35.23	170.00	N/D	N/A	N/A
Dodecane	4014.80	-33.38	170.00	N/D	N/A	N/A
MethylAcetate	1486.70	-12.36	170.00	130.00	N/A	N/A
EthylAcetate	2149.50	-17.87	170.00	120.00	N/A	N/A
PropylAcetate	2565.80	-21.33	170.00	130.00	80.60%, 80.80%, 75.34%, 77.68%, and 76.77%	80.00, 90.00, 100.00, 110.00, and 120.00
ButylAcetate	3136.70	-26.08	170.00	N/D	N/A	N/A

N/A: Not Applicable.

N/D: Not Detectable.

Table 3-6. 50-50 Amylopectin- Poly(DL-lactide-co-glycolide) thermodynamic parameters

SOLUTE	SLOPE	ΔH (KJ)	T_m (°C)	T_g (°C)	α	TEMP. (°C)
Heptane	8936.00	-74.29	N/D	N/D	N/A	N/A
Octane	9021.70	-75.01	150.00	140.00	94.27%, 84.12%, and 86.94%	90.00, 110.00, and 130.00
Nonane	10234.0	-85.09	150.00	140.00	91.11%, 89.68%, and 75.78%	90.00, 100.00, and 130.00
Decane	4060.20	-33.76	150.00	140.00	54.62%, 57.68%, and 50.82%	90.00, 100.00, and 130.00
Undecane	2833.40	-23.56	N/D	N/D	N/A	N/A
Dodecane	3713.50	-30.87	N/D	N/D	N/A	N/A
MethylAcetate	26451.0	-219.9	150.00	140.00	N/A	N/A
EthylAcetate	5676.20	-47.19	N/D	N/D	N/A	N/A
PropylAcetate	6216.40	-51.68	150.00	140.00	N/A	N/A
ButylAcetate	4532.60	-37.68	N/D	N/D	N/A	N/A

N/A: Not Applicable.

N/D: Not Detectable.

Table 3-7. 50-50 Amylopectin- Poly(3-hydroxybutyric acid) thermodynamic parameters.

SOLUTE	SLOPE	ΔH (KJ)	T_m (°C)	T_g (°C)	α	TEMP. (°C)
Heptane	9761.80	-81.16	130.00	120.00	99.15%, and 98.73%	100.00, and 110.00
Octane	10027.0	-83.36	130.00	120.00	96.31%, and 90.39%	100.00, and 110.00
Nonane	7203.30	-59.89	130.00	120.00	84.74%, 81.90%, and 79.17%	90.00, 100.00, and 110.00
Decane	5036.40	-41.87	130.00	120.00	61.32%, 61.31%, and 46.77%	90.00, 100.00, and 110.00
Undecane	5624.40	-46.76	N/D	N/D	N/A	N/A
Dodecane	5153.10	-42.84	N/D	N/D	N/A	N/A
Methyl/Acetate	7892.70	-65.62	130.00	120.00	95.35%, and 98.25%	90.00, and 110.00
Ethyl/Acetate	7799.20	-64.84	130.00	N/D	N/A	N/A
Propyl/Acetate	9887.70	-82.21	130.00	120.00	N/A	N/A
Butyl/Acetate	8820.50	-73.33	130.00	120.00	80.98%, and 73.77%	90.00, and 110.00
Butanol	2331.50	-19.38	130.00	120.00	82.80%, and 62.79	80.00, and 110.00

N/A: Not Applicable.

N/D: Not Detectable.

Table 3-8. Despersive surface energies (γ_s^d) of Amylopectin and its blends.

TEMP. (°C)	100% Amylopectin, γ_s^d (mJ/m ²)	100% Poly(DL-lactide-co-glycolide), γ_s^d (mJ/m ²)	100% Poly(3-hydroxybutyric acid), γ_s^d (mJ/m ²)
160.00	N/A	N/A	48.90
170.00	N/A	3.90	53.74
180.00	N/A	N/A	33.54
190.00	N/A	N/A	28.91
200.00	0.07	N/A	20.58
210.00	N/A	N/A	N/A
220.00	N/A	N/A	N/A
230.00	N/A	N/A	N/A
240.00	N/A	N/A	N/A
250.00	N/A	N/A	N/A
260.00	N/A	N/A	N/A

N/A: Not Applicable.

Table 3-8 (Continued). Dispersive surface energies (γ_s^d) of Amylopectin and its blends.

TEMP. (°C)	75-25 Amylopectin- Polycaprolactone, γ_s^d (mJ/m ²)	50-50 Amylopectin- Poly(DL- lactide-co-glycolide), γ_s^d (mJ/m ²)	50-50 Amylopectin- Poly(3- hydroxybutyric acid), γ_s^d (mJ/m ²)
160.00	N/A	46.30	55.46
170.00	18.59	35.41	33.92
180.00	24.67	39.03	22.84
190.00	19.85	N/A	0.71
200.00	18.46	N/A	1.31
210.00	13.65	N/A	N/A
220.00	8.36	N/A	N/A
230.00	14.72	N/A	N/A
240.00	13.80	N/A	N/A
250.00	12.99	N/A	N/A
260.00	10.27	N/A	N/A

N/A: Not Applicable.

Figure 3-1. Degree of crystallinity for 100% Poly(DL-lactide-co-glycolide)-Decane.

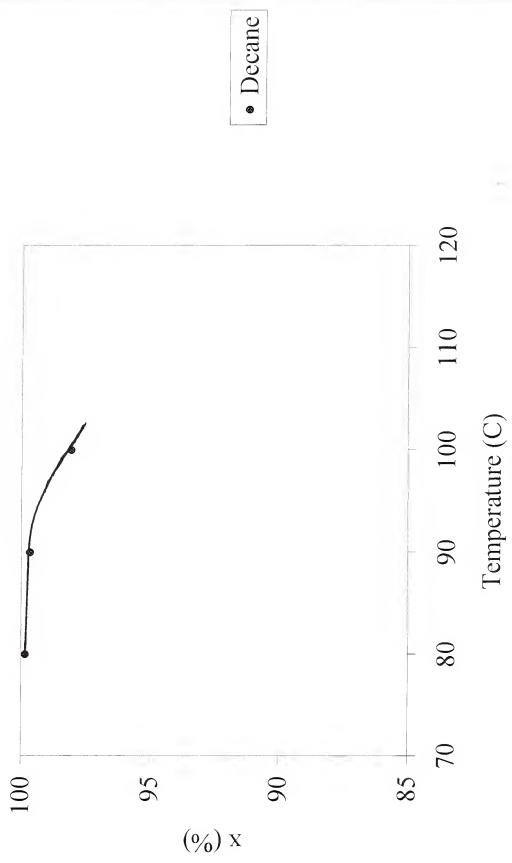


Figure 3-2. Degree of crystallinity for 100% Poly(3-hydroxybutyric acid)-Decane.

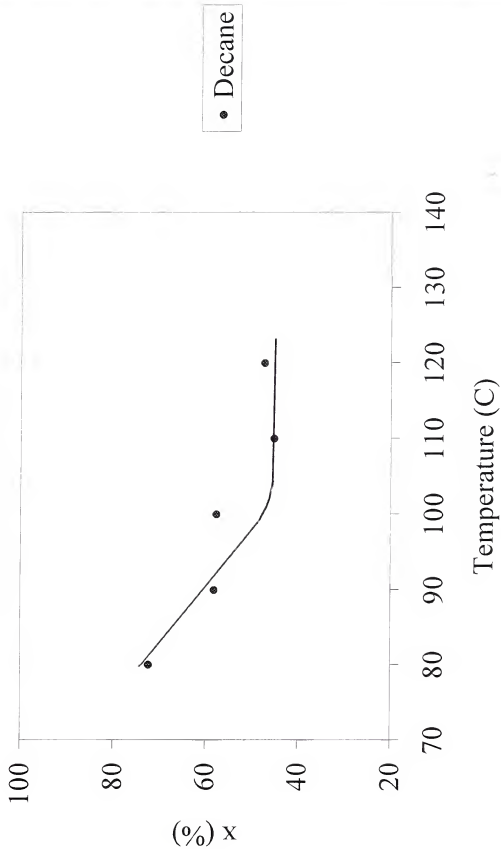


Figure 3-3. Degree of crystallinity for 75-25 Amylopectin-Polycaprolactone-PropylAcetate.

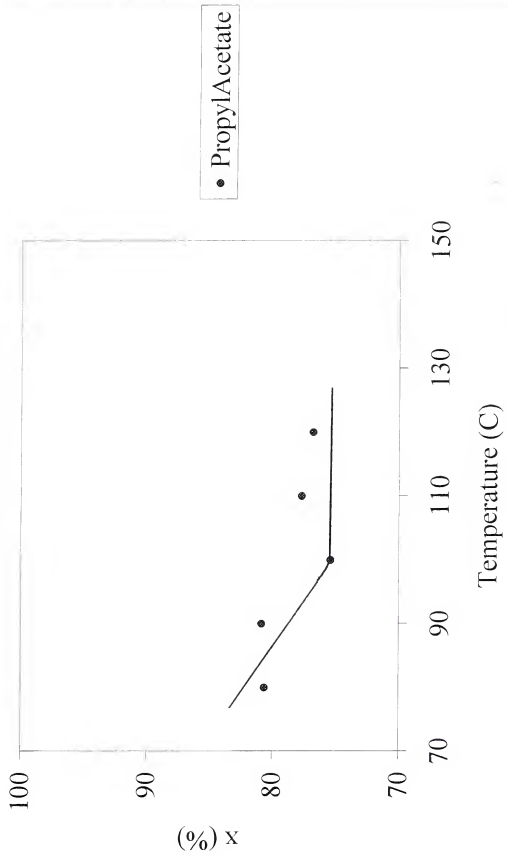


Figure 3-4. Degree of crystallinity for 50-50 Amylopectin-Poly(DL-lactide-co-glycolide)-Nonane.

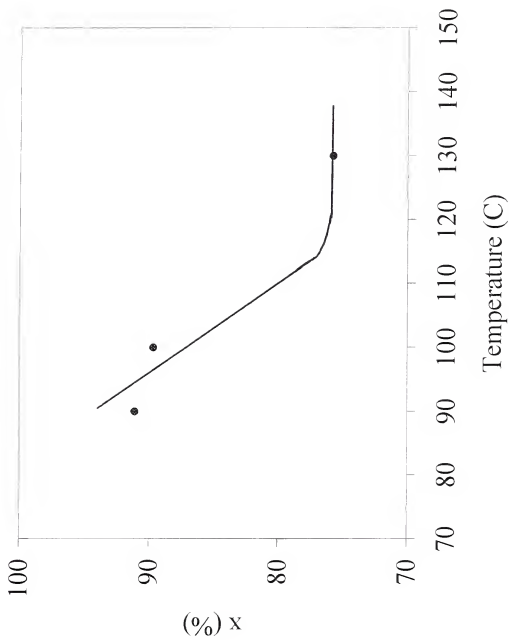


Figure 3-6. Surface energy for 100% Amylopectin-
200 C.

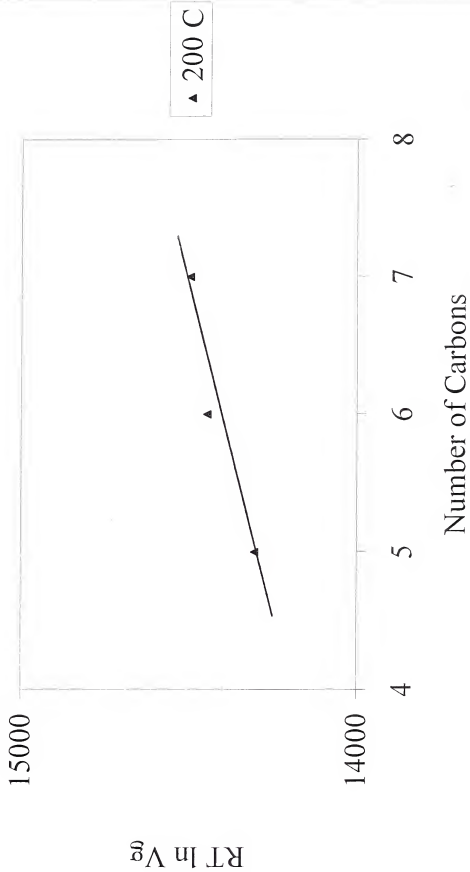


Figure 3-7. Surface energy for 100% Poly(DL-lactide-co-glycolide)-170 C.

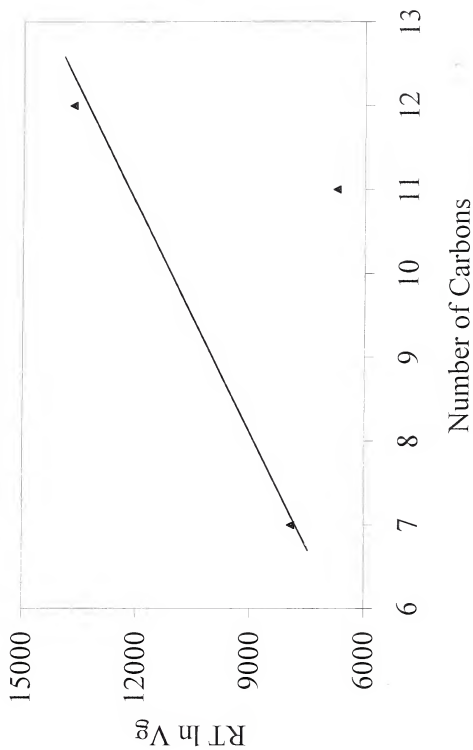


Figure 3-8. Surface energy for 100% Poly(3-hydroxybutyric acid)-160 C.

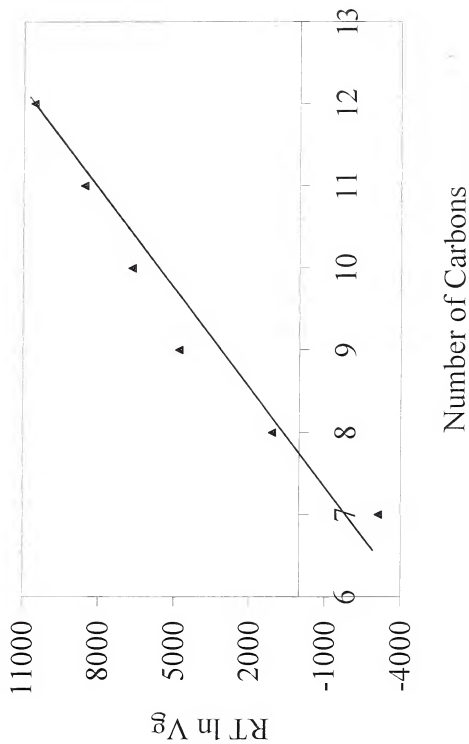


Figure 3-9. Surface energy for 100% Poly(3-hydroxybutyric acid)-170C.

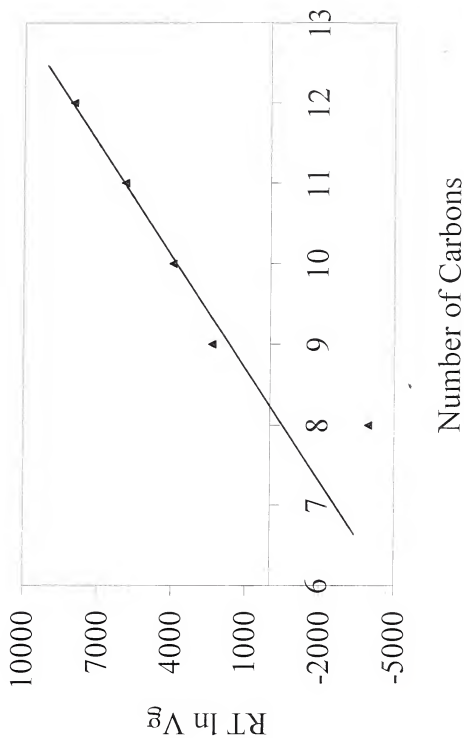


Figure 3-10. Surface energy for 100% Poly(3-hydroxybutyric acid)-180 C.

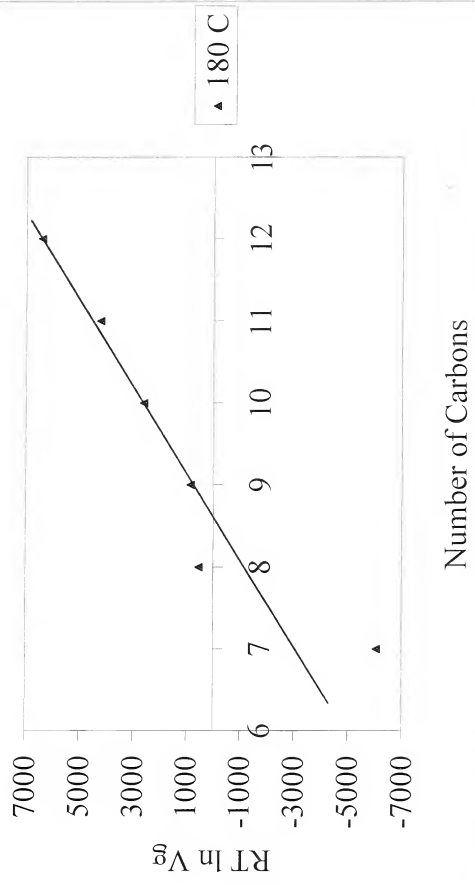


Figure 3-11. Surface energy for 100% Poly(3-hydroxybutyric acid)-190 C.

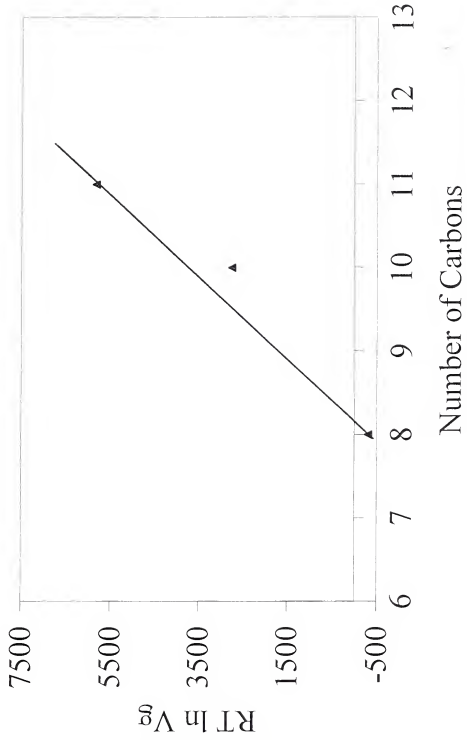


Figure 3-12. Surface energy for 100% Poly(3-hydroxybutyric acid)-200 C.

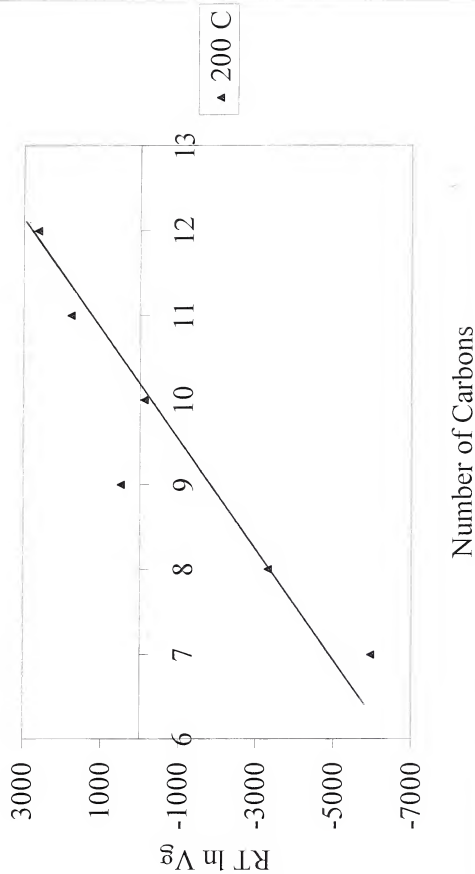


Figure 3-13. Surface energy for 75-25 Amylopectin-Polycaprolactone-170 C.

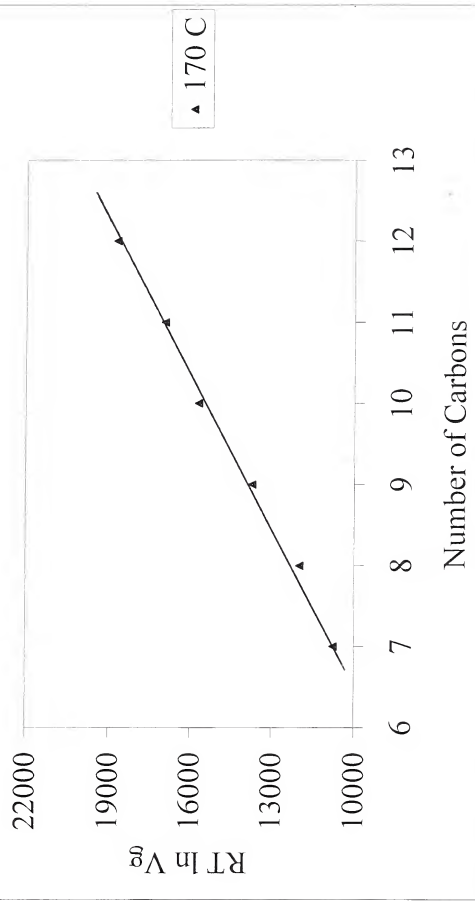


Figure 3-14. Surface energy for 75-25 Amylopectin-Polycaprolactone-180 C.

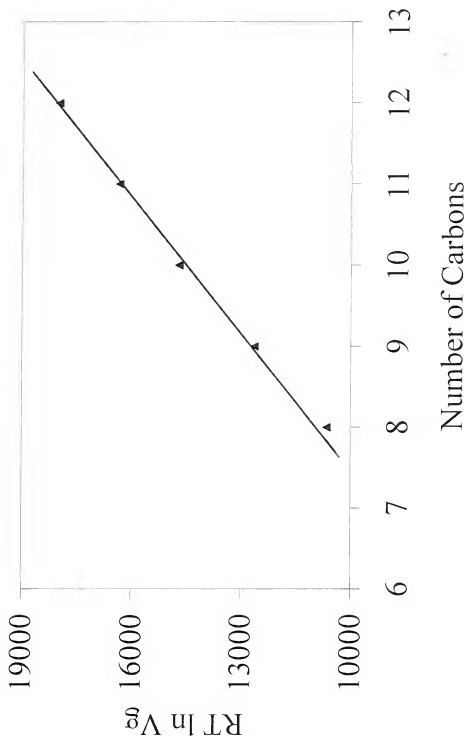


Figure 3-15. Surface energy for 75-25 Amylopectin-Polycaprolactone-190 C.

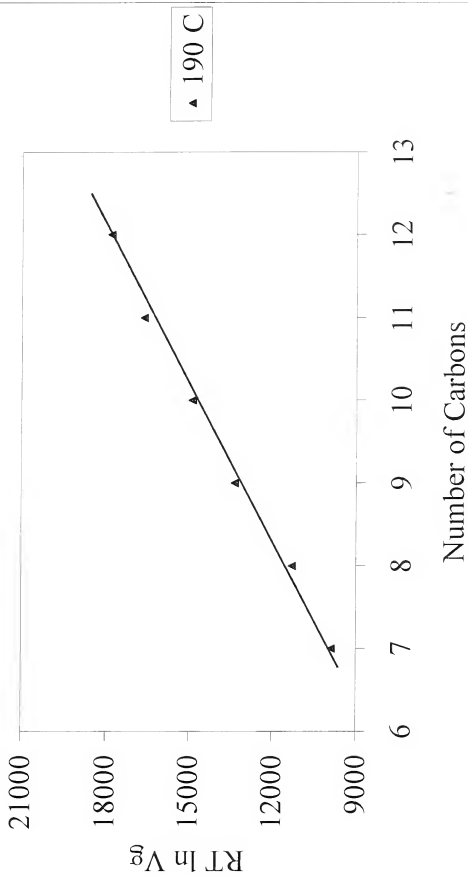


Figure 3-16. Surface energy for 75-25 Amylopectin-Polycaprolactone-200 C.

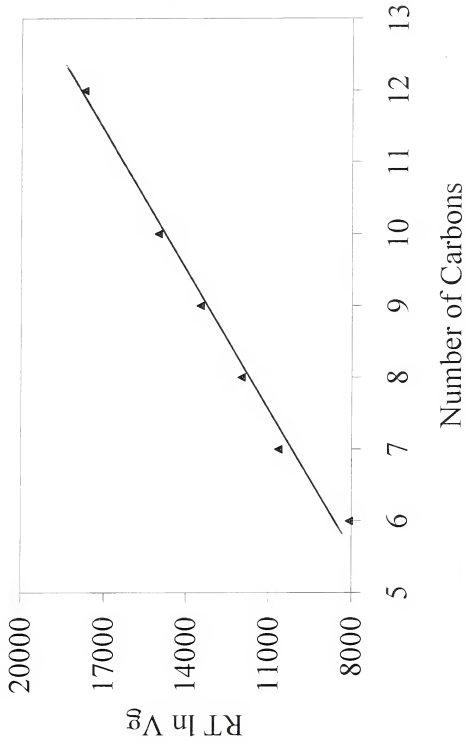


Figure 3-17. Surface energy for 75-25 Amylopectin-Polycaprolactone-210 C.

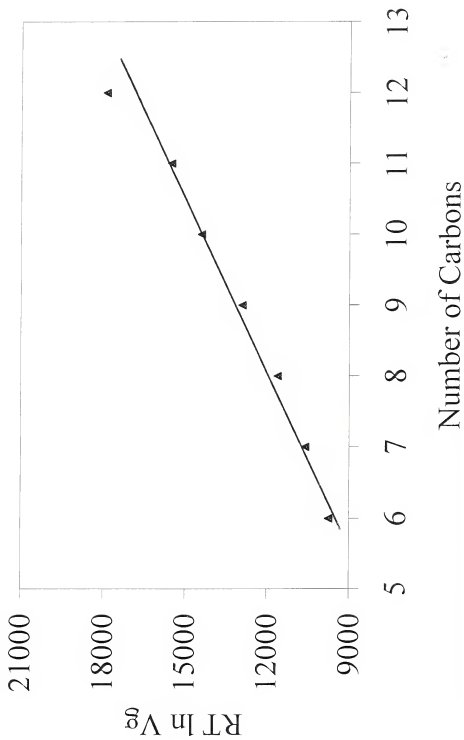


Figure 3-18. Surface energy for 75-25 Amylopectin-Polycaprolactone-220 C.

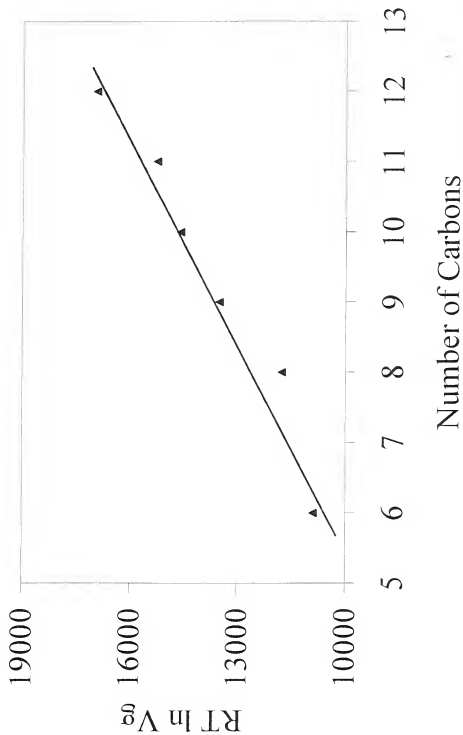


Figure 3-19. Surface energy for 75-25 Amylopectin-Polycaprolactone-230 C.

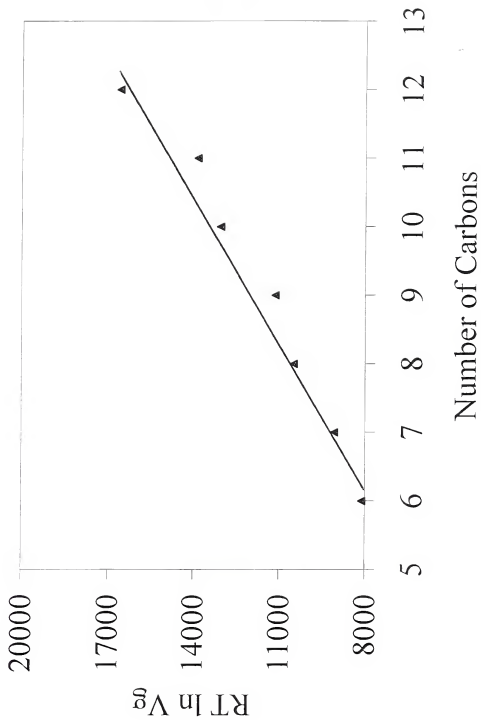


Figure 3-20. Surface energy for 75-25 Amylopectin-Polycaprolactone-240 C.

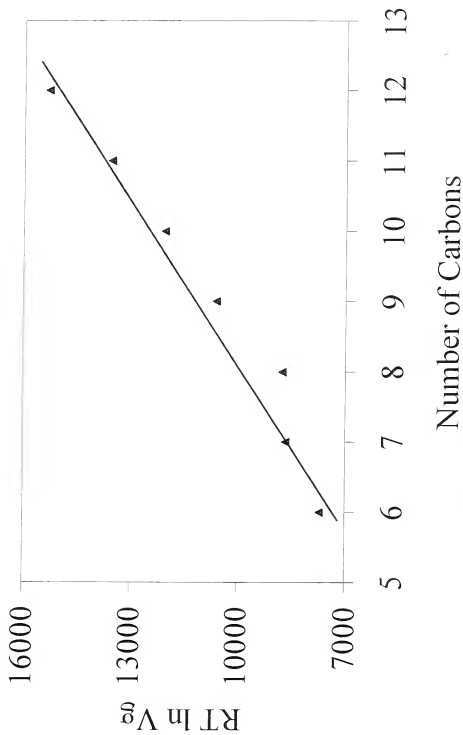


Figure 3-21. Surface energy for 75-25 Amylopectin-Polycaprolactone-250 C.

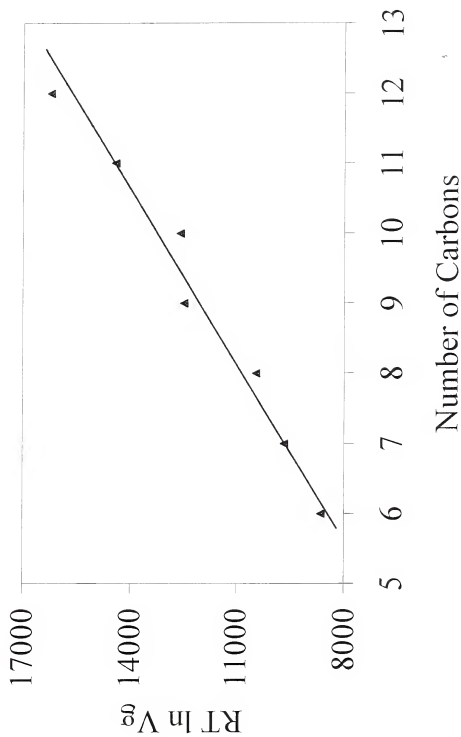


Figure 3-22. Surface energy for 75-25 Amylopectin-Polycaprolactone-260 C.

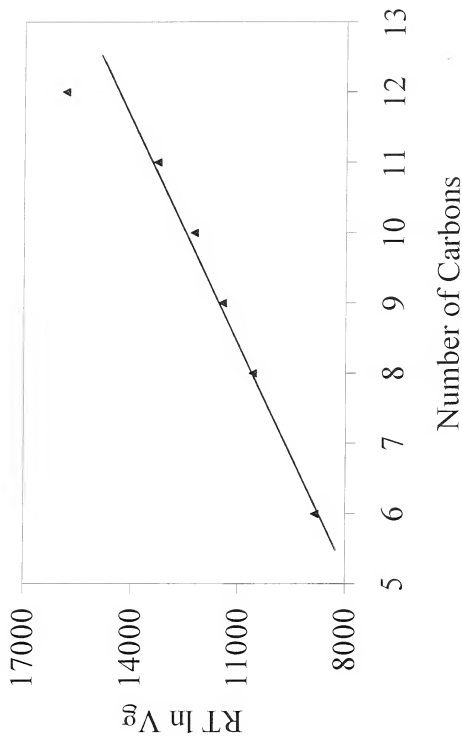


Figure 3-23. Surface energy for 50-50 Amylopectin-Poly(DL-lactide-co-glycolide)-160 C.

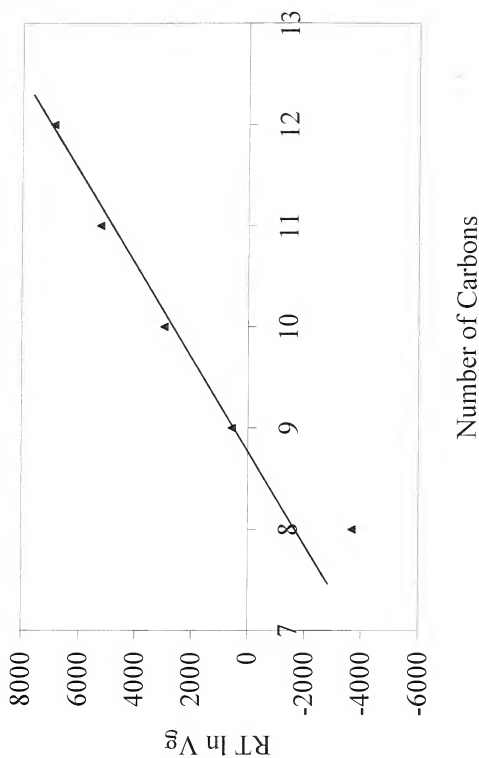


Figure 3-24. Surface energy for 50-50 Amylopectin-Poly(DL-lactide-co-glycolide)-170 C.

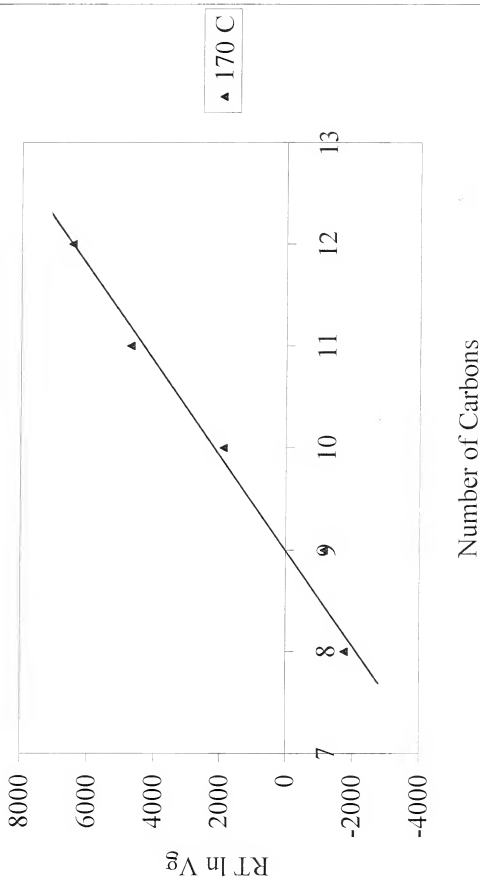


Figure 3-25. Surface energy for 50-50 Amylopectin-Poly(DL-lactide-co-glycolide)-180 C.

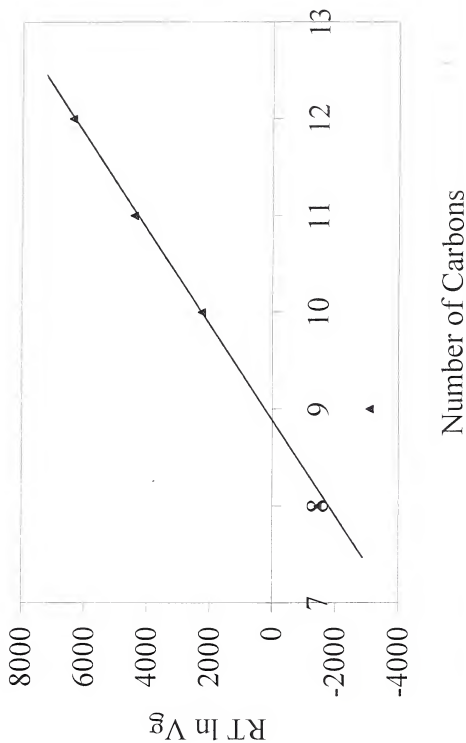


Figure 3-26. Surface energy for 50-50 Amylopectin-Poly(3-hydroxybutyric acid)-160 C.

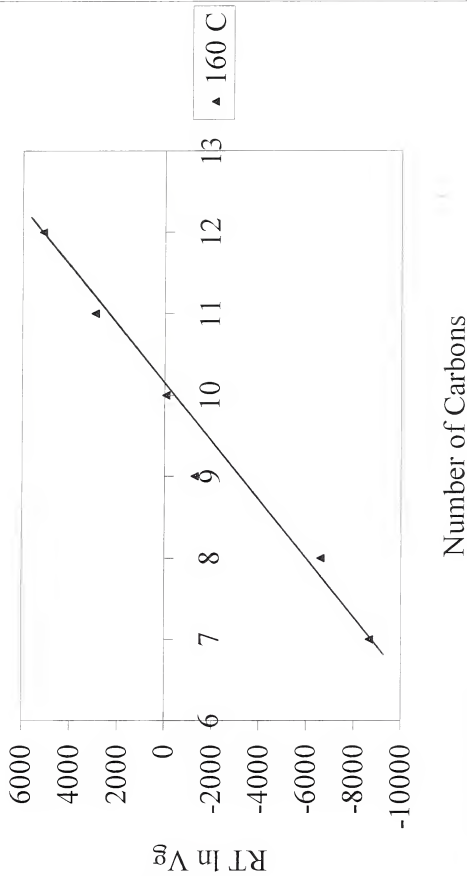


Figure 3-27. Surface energy for 50-50 Amylopectin-Poly(3-hydroxybutyric acid)-170 C.

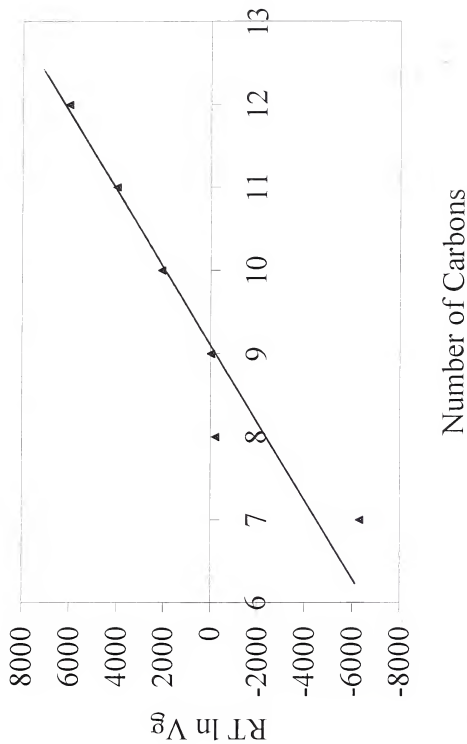
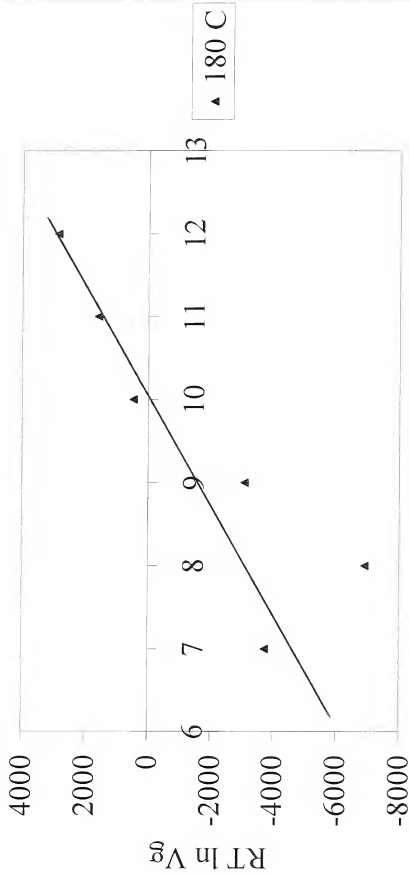


Figure 3-28. Surface energy for 50-50 Amylopectin-Poly(3-hydroxybutyric acid)-180 C.



Number of Carbons

Figure 3-29. Surface energy for 50-50 Amylopectin-Poly(3-hydroxybutyric acid)-190 C.

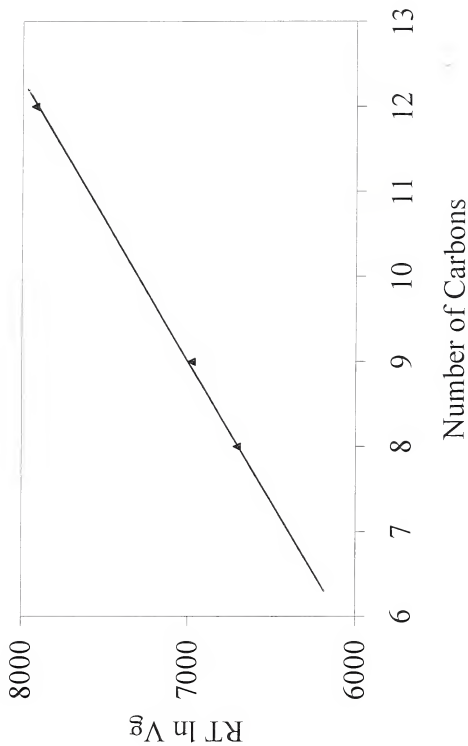
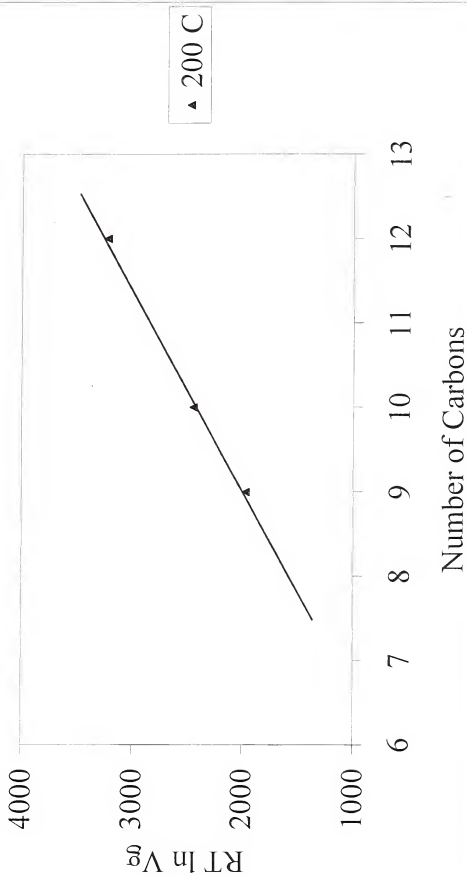


Figure 3-30. Surface energy for 50-50 Amylopectin-Poly(3-hydroxybutyric acid)-200 C.



DISCUSSION AND CONCLUSIONS

A series of three (3) families of nineteen (19) solutes were selected with an increasing number of carbons in the solutes backbone. Thus, alkanes will reveal the effect of the dispersive forces on the solubility of alkanes with Amylopectin and its blends and on the dispersive surface energy of all columns. Acetates and alcohols will reveal the effect of dipole-dipole and H-bonding of solutes with the polymers backbone. Their interaction with the stationary phase will reveal the effect of the chemical nature of the injected solutes on their miscibility with the columns. In addition, Diethylamine and Formic acid will reveal the acid-base characteristics of the columns (Swift, 1993). Several solutes did not show retention times due to either volatility or high boiling points of these solutes. Retention volumes of these solutes were recorded as Not Detectable (N/D) values. Some solutes behaviors are non-ideal, particularly for volatile solutes, such as Pentane, Hexane, and Methanol. At lower temperatures, high boiling solutes would not record retention times, such as Undecane, and Dodecane. In addition, at higher temperature, the low boiling solutes behave non-ideal. Therefore, their retention volumes were recorded as N/D.

To ensure that the thermodynamics are valid in these ranges of temperature, a linear relationship of $\ln V_g$ versus $1/T$ plots are an indication of the establishment of equilibrium between the mobile gaseous phase and the stationary phase (Ratajska and Boryniec, 1998). However, this was not the case for all columns used. Curvatures in phase diagram were observed indicating the change in the morphology of the polymers used as a function of temperature. As temperature increases the morphology of the

polymer changed. The equilibrium between the mobile and stationary phase is usually established which allows for the calculations of the thermodynamic parameters. The determination is based on the assumption that the solute molecules interact only with the amorphous polymer (Arvanitoyannis, 1999). In some cases, the change of both T_g and T_m were very close. Thus, several N/D values were recorded for different solutes for both glass transition temperature (T_g) and melting point (T_m). This is related to the slow action of the thermal change. Both T_g and T_m will shift in positions when a blend is used. This is a phenomenon called melting point depression (Ratajska and Boryniec, 1998). In addition, several Not Applicable (N/A) values were recorded for both degree of crystallinity (χ) and surface energy (γ_s^d). This was due to, not enough data to generate and conduct calculations.

For 100% Amylopectin column, figure C-1 to figure C-8, a minimum of two regions were identified in the retention diagram, crystallinity and amorphous. The amorphous region is when the column is completely at melt. A third region was identified above 200°C as the polymer started to decompose. The first minimum in the curvature was identified as the glass transition temperature (T_g) of 120°C. The maximum of the curvature was identified as the melting point (T_m) of 160°C. Following the melting point, a straight line can be observed due to the establishment of the equilibrium between the solute and the polymer and is an indication that the polymer is amorphous. All thermodynamic parameters were calculated using this zone. It is of interest to mention that among alcohols, Methanol neither showed a clear melting point nor a glass transition temperature, this was due to the high volatility of the solute and the non-ideal behavior of Methanol.

For 100% Poly(DL-lactide-co-glycolide) column, figure C-9 to figure C-17, a minimum of two regions were identified, crystallinity and amorphous. A third region was identified above 170°C as the polymer started to decompose. The T_g was 110°C and the T_m was 130°C. It is of interest to mention that, Water neither showed a melting point nor a glass transition temperature. In addition, the degree of crystallinity was calculated for both Decane and Undecane. This is accomplished by extrapolating the linear portion (amorphous) of the retention diagrams to the crystalline region, two retention volumes were measured, V_{g1} is the retention volume of the solute in the amorphous region and V_{g2} is the retention volume of the solute in the crystalline region. The degree of crystallinity for Decane, figure 3-1, was ranged from 99.84% at 80°C to 98.09% at 100°C.

For 100% Poly(3-hydroxybutyric acid) column, figure C-18 to figure C-27, a minimum of two regions were identified, crystallinity and amorphous. A third region was identified above 200°C as the polymer started to decompose. The T_g was 130°C and the T_m was 140°C. It is of interest to mention that, Dodecane, MethylAcetate, and ButylAcetate neither showed a clear melting point nor a glass transition temperature. In addition, the degree of crystallinity was calculated for Heptane, Octane, Nonane, Decane, Undecane, EthylAcetate, and PropylAcetate. The degree of crystallinity for Decane, figure 3-2, was ranged from 72.19% at 80°C to 47.28% at 120°C.

For 50-50 Amylopectin-Polycaprolactone column, figure C-28 to figure C-41, a straight line was observed in most of the figures and this was due to the lack of data at higher temperatures, which was above 160°C. However, Heptane, Octane, Methanol and Diethylamine showed that the T_g was ranged from 90°C to 100°C and the T_m was ranged from 100°C to 110°C.

For 75-25 Amylopectin-Polycaprolactone column, figure C-42 to figure C-52, a minimum of two regions were identified, crystallinity and amorphous. A third region was identified above 260°C as the polymer started to decompose. The T_g was ranged from 120°C to 130°C. The T_m was ranged from 160°C to 170°C. It is of interest to mention that, Decane, Undecane, Dodecane, and ButylAcetate did not show a clear glass transition temperature. In addition, the degree of crystallinity was calculated for Heptane, and PropylAcetate. The degree of crystallinity for PropylAcetate, figure 3-3, was ranged from 80.60% at 80°C to 76.77% at 120°C.

For 50-50 Amylopectin-Poly(DL-lactide-co-glycolide) column, figure C-53 to figure C-62, a minimum of two regions were identified, crystallinity and amorphous. A third region was identified above 180°C as the polymer started to decompose. The T_g was 140°C and the T_m was 150°C. It is of interest to mention that, Heptane, Undecane, Dodecane, EthylAcetate, and ButylAcetate neither showed a clear melting point nor a glass transition temperature. In addition, the degree of crystallinity was calculated for Octane, Nonane, and Decane. The degree of crystallinity for Nonane, figure 3-4, was ranged from 91.11% at 90°C to 75.78% at 130°C.

For 50-50 Amylopectin-Poly(3-hydroxybutyric acid) column, figure C-63 to figure C-73, a minimum of two regions were identified, crystallinity and amorphous. A third region was identified above 200°C as the polymer started to decompose. The T_g was 120°C and the T_m was 130°C. It is of interest to mention that, Undecane, Dodecane, and EthylAcetate neither showed a clear melting point nor a glass transition temperature. In addition, the degree of crystallinity was calculated for Heptane, Octane, Nonane,

Decane, MethylAcetate, ButylAcetate, and Butanol. The degree of crystallinity for Nonane, figure 3-5, was ranged from 84.74% at 90°C to 79.17% at 110°C.

Therefore, all columns except for some solutes of 50-50 Amylopectin-Polycaprolactone column showed maxima of the curvature. These maxima were identified as the T_m of the polymers which ranged from 100°C to 170°C. Therefore, by blending Amylopectin with other polymers, the T_m was decreased or a depression phenomenon was formed and this was due to blending to form a mixture of polymer (Ratajska and Boryniec, 1998). In addition, the degrees of crystallinity were high for all Amylopectin blends at low temperatures. The degree of crystallinity part is much higher than the amorphous (Holmes, 1988). As temperature goes up, the degree of crystallinity decreases and the amorphous part will increase. Therefore, by increasing the temperature, the crystalline part started to melt, then, the degree of crystallinity decreased until reached constant values.

The surface energy (γ_s^d), describes interactions due to dispersive forces or the combination of dispersive forces on the solubility of alkanes with Amylopectin and its blends (Swift, 1993). Table 3-8, showed the dispersive surface energy of all Amylopectin and its blends as a function of temperature. It is clear that, the γ_s^d values were showed different trend with different mixtures of polymers. In general, the γ_s^d for Poly(3-hydroxybutyric acid), 75-25 Amylopectin-Polycaprolactone, 50-50 Amylopectin-Poly(DL-lactide-co-glycolide), and 50-50 Amylopectin-Poly(3-hydroxybutyric acid) decreased as the temperature increased. Thus, the surface of the polymer was expanded as temperature raised, yet, the γ_s^d decreased.

Comparing data values at 180°C, 50-50 Amylopectin-Poly(DL-lactide-co-glycolide) surface energy value showed higher than both 75-25 Amylopectin-Polycaprolactone and 50-50 Amylopectin-Poly(3-hydroxybutyric acid) surface energy values. In addition, comparing data values at 200°C, 100% Amylopectin surface energy value showed less than both 75-25 Amylopectin-Polycaprolactone and 50-50 Amylopectin-Poly(3-hydroxybutyric acid) surface energy values. Therefore, blending Amylopectin with other polymer will increase its mechanical properties and thus, the surface energy. This will slow the biodegradation process, however, it will be less than the regular plastic.

Biodegradable polymers, in general, may never replace the major commodity plastics, but they will offer a viable waste-management option for polymers that are not readily or economically recoverable for recycling and incineration (Chandra and Rustgi, 1998). In essence, this implies that both biodegradable water-soluble polymers and plastics will continue as major targets for research and development efforts in the polymer industry and academia. Success will be measured by balancing properties and biodegradability to meet all demands.

The properties of starch-based polymeric materials including their biodegradability depend on the compatibility of the mixture components and the structure of the system thus prepared. It is these properties of starch mixtures with synthetic polymers that must be the subject of comprehensive analysis in order to establish the general regularities with the ultimate goal to select the components and technologies for the preparation of polymeric materials which are stable in various media and are biodegradable (Blanshard, 1987).

Totally biodegradable polymers have proved to be inferior to non-degradable packaging materials in terms of both functional and cost effectiveness (Nayak, 1999). Their major disadvantage is inadequate mechanical strength. The widening of the range of biodegradable polymeric materials is very important for further and future studies. Therefore, it is hoped that the results described in this research thesis will be useful for further studies based on the use of this environmentally important scientific approach.

REFERENCES

- Amass, W., A. Amass, and B. Tighe. 1998. A review of biodegradable polymers: uses, current developments in the synthesis and characterization of biodegradable polyesters, blends of biodegradable polymers and recent advances in biodegradable studies. *Polymer International* 47: 89-144.
- Arvanitoyannis, I. S. 1999. Totally and partially biodegradable polymer blends based on natural and synthetic macromolecules: preparation, physical properties, and potential as food packaging materials. *Journal of Macromolecular Science* 39: 205-271.
- Bastioli, C. 1998. Biodegradable materials-present situation and future perspectives. *Macromolecular Symposia* 135: 193-204.
- Blanshard, J. M. 1987. *Starch properties and potential*. John Wiley & Sons, New York, NY, USA. 998p.
- Calmon-Decriaud, A., V. Bellon-Maurel, and F. Silvestre. 1998. Standard methods for testing the aerobic biodegradation of polymeric materials: review and perspectives. *Advances in Polymer Science* 135: 207-226.
- Chandra, R. and R. Rustgi. 1998. Biodegradable polymers. *Progress in Polymer Science* 23: 1273-1335.
- Corbitt, R. A. 1990. *Standard handbook of environmental engineering*. McGraw-Hill, New York, NY, USA. 998p.
- Demirgoz, D., C. Elvira, J. F. Mano, A. M. Cunha, E. Piskin, and R. L. Reis. 2000. Chemical modification of starch based biodegradable polymeric blends: effects on water uptake, degradation behavior and mechanical properties. *Polymer Degradation and Stability* 70: 161-170.
- Dempsey, C. R. and E. T. Oppelt. 1993. Incineration of hazardous waste: a critical review update. *Journal of the Air & Waste Management Association* 43: 25-73.
- Gutierrez, M. C., J. Rubio, F. Rubio, and J. L. Oteo. 1999. Inverse gas chromatography: a new approach to the estimation of specific interactions. *Journal of Chromatography A* 845: 53-66.
- Holmes, P. A. 1988. *Developments in crystalline polymers*. Elsevier. 2:1-65
- Josephson, J. 1993. Hazardous waste management: seeking least-cost approaches. *Environmental Science & Technology* 27: 2298-2301.
- Jun, C. L. 2000. Reactive blending of Biodegradable polymers: PLA and starch. *Journal of Polymer and the Environment* 8: 33-37.

- Karlsson, S., and A. Albertsson. 1998. Biodegradable polymers and environmental interaction. *Polymer Engineering and Science* 38: 1251-1253.
- Nayak, P. L. 1999. Biodegradable polymers: opportunities and challenges. *Journal of Macromolecular Science*. 39: 481-505
- Nere, C. K., and R. N. Jagtap. 2001. Biodegradable polymers-latest developments. *Popular Plastics & Packaging* 46: 57-68.
- Okada, M. 2002. Chemical syntheses of biodegradable polymers. *Progress in Polymer Science* 27: 87-133.
- Park, J. W., S. S. Im, S H. Kim and Y. H. Kim. 2000. Biodegradable polymer blends of poly(L-lactic acid) and gelatinized starch. *Polymer Engineering and Science* 40:2539-2550.
- Ratajska, M. and S. Boryniec. 1998. Physical and chemical aspects of biodegradation of natural polymers. *Reactive and Functional Polymers* 38: 35-49.
- Satyanarayana, D. and P. R. Chatterji. 1993. Biodegradable polymers: challenges and strategies. *Journal of Macromolecular Science*. 33: 349-368.
- Scott, G. 2000. Green polymer. *Polymer Degradation and Stability* 68: 1-7.
- Sigma-Aldrich Co. 2003. The sigma-aldrich family. Milwaukee, WI, USA. [accessed July, 2003]. Available from: http://www.sigmaaldrich.com/cgi-bin/hsrun/Distributed/HahtShop/HAHTpage/HS_StructureImage.
- Suvorva, A. I., I. S. Tyukova, and E. I. Trufanova. 2000. Biodegradable starch-based polymeric materials. *Russian Chemical Reviews* 69: 451-459.
- Swift, G. 1993. Directions for environmentally biodegradable polymer research. *Account of Chemical Research* 26: 105-110.
- Van Volkenburgh, W. R. and M. A. White. 1993. Overview of biodegradable polymers and solid-waste issues. *Tappi Journal* 76: 193-197.
- Vasnev, V. A. 1997. Biodegradable polymers. *Polymer Science* 39: 474-485.
- Zhang, L., X. Deng, S. Zhao, and Z. Huang. 1997. Biodegradable polymer blends of poly(3-hydroxybutrate) and starch acetate. *Polymer International* 44: 104-110.

APPENDIX A - Thermodynamic Calculations

Calculation of Specific Retention Volume (V_g):

$$V_g = \Delta t (F/W) (273.15)/(298.15) (3/2) ((P_i/P_o)^2 - 1) / ((P_i/P_o)^3 - 1)$$

Where

$\Delta t = t_{\text{Avg}} - t_{\text{Air}}$

$t_{\text{Avg}} = t_1 + t_2 / 2$

t_1 & t_2 are the retention time recorded for each solute.

t_{Air} = the lowest t_{Avg} .

F = Flow Rate.

W = Weight of the polymer in g.

273.15 = Temperature at 0 °C in K.

298.15 = Temperature at 25 °C in K.

P_i = Inlet Pressure which is 76 + P_o in Cm. Hg.

P_o = Outlet Pressure which is 76 Cm. Hg.

Calculation of heat of mixing (ΔH):

$$\Delta H = \text{Slope} \times 8.314 / 1000$$

Where

Slope is calculated from the straight line in the graph.

Calculation of melting point (T_m):

T_m is the melting point in the graph in °C, which is the maximum of the curvature that can be identified.

Calculation of glass transition temperature (T_g):

T_g is the glass transition temperature in the graph in °C, which is the first minimum in the curvature that can be identified.

Calculation of degree of crystallinity (χ)

$$\chi = 100 (1 - V_{g2} / V_{g1})$$

Where

V_{g1} = Specific Retention Volume of the solute in the amorphous region.

V_{g2} = Specific Retention Volume of the solute in the crystalline region.

TEMP. is the temperature that intersect in X-axis with the value of χ in the graph in °C.

Calculation of Surface Energy (γ_s^d):

$$\gamma_s^d = [1 / (4)(\gamma_{CH2})] [\Delta G_a(CH2) / (N)(a_{CH2})]^2$$

Where

$$\gamma_{CH2} = 36.80 - 0.058 T$$

T is the temperature in °C

ΔG_a is the slope calculated from the straight line in the graph.

N is the Avogadro's number = 6.0221367×10^{23} things/mol.

a_{CH2} is the area of the adsorbed molecules CH_2 group and is estimated to be $6 (A^\circ)^2$. $A^\circ = 1 \times 10^{-10}$ m.

APPENDIX B – Specific Retention Volumes Tables

All specific retention volumes (V_g) tables are presented in the next pages.

Table B-1. Specific retention volumes (V_R) of solutes at a temperature range 80°C to 200°C for 100% Amylopectin column.

SOLUTES	80	90	100	110	120	130	140	150	160	190	200
Pentane	64.86	64.63	65.69	66.11	63.00	67.87	69.53	73.94	77.54	34.63	37.93
Hexane	53.29	49.74	49.95	52.18	50.73	54.17	54.84	58.57	60.57	29.6	39.33
Heptane	53.40	50.37	51.85	50.93	48.57	51.64	53.53	55.08	N/D	35.21	39.84
Methanol	110.92	122.62	N/D	121.72	N/D	122.16	125.38	123.74	121.45	46.01	45.62
Ethanol	68.21	61.67	71.92	71.93	74.24	75.38	74.76	83.92	90.91	37.64	43.54
Propanol	67.89	61.25	68.22	68.29	65.79	70.61	72.85	75.74	78.93	36.75	40.81
Butanol	71.24	71.29	69.17	66.73	59.6	67.06	70.13	70.35	72.35	34.6	N/D
Diethylamine	68.32	68.65	69.6	69.33	62.9	71.83	73.15	77.04	78.63	N/D	40.7

N/D: Not Detectable.

Table B-2. Specific retention volumes (V_R) of solutes at a temperature range 80°C to 170°C for 100% Poly(DL-lactide-co-glycolide) column.

SOLUTES	80	90	100	110	120	130	140	150	160	170
Heptane	2.05	1.21	0.75	0.65	7.67	9.46	6.28	0.25	18.94	8.56
Octane	5.93	3.97	2.91	2.21	11.71	21.24	14.08	1.13	22.93	97.35
Nonane	14.04	10.30	7.28	5.39	13.69	44.12	N/D	1.96	11.75	N/D
Decane	34.70	22.34	14.67	10.86	46.00	49.66	N/D	3.66	1.27	N/D
Undecane	N/D	44.87	32.07	22.42	36.48	N/D	5.05	6.19	10.08	6.22
Dodecane	N/D	N/D	N/D	41.71	51.64	N/D	45.69	10.09	N/D	40.97
EthylAcetate	13.55	9.98	7.38	5.97	N/D	0.84	23.19	2.30	12.68	N/D
PropylAcetate	25.19	18.22	13.92	11.21	N/D	N/D	29.84	3.68	22.06	N/D
Water	38.58	N/D	N/D	N/D	N/D	N/D	N/D	70.05	53.95	52.19

N/D: Not Detectable.

Table B-3. Specific retention volumes (V_R) of solutes at a temperature range 80°C to 200°C for 100% Poly(3-hydroxybutyric acid) column.

SOLUTES	80	90	100	110	120	130	140	150	160	170
Heptane	1.73	1.95	0.80	4.74	0.49	0.55	3.19	0.49	0.42	0.10
Octane	6.36	5.28	4.14	5.94	1.95	1.25	3.63	1.25	1.35	0.34
Nonane	16.65	13.72	9.54	10.29	4.43	3.07	5.06	2.60	3.79	1.89
Decane	37.30	30.97	20.95	16.51	9.61	6.09	7.73	4.91	6.37	2.92
Undecane	N/D	12.46	43.87	29.54	18.33	12.98	12.15	9.20	10.78	4.96
Dodecane	N/D	N/D	84.99	51.99	34.46	25.39	18.95	16.94	18.82	8.76
MethylAcetate	2.49	2.76	1.27	4.91	0.54	0.82	3.46	0.74	1.90	0.05
EthylAcetate	4.21	4.52	2.96	6.40	1.55	1.37	3.36	1.84	2.65	0.54
PropylAcetate	10.45	9.87	6.55	8.68	3.70	2.42	5.45	3.27	3.79	1.03
ButylAcetate	22.93	19.77	14.35	13.65	6.45	4.99	7.04	5.40	7.79	2.73

N/D: Not Detectable.

Table B-3 (Continued). Specific retention volumes (V_R) of solutes at a temperature range 80°C to 200°C for 100% Poly(3-hydroxybutyric acid) column.

SOLUTES	180	190	200
Heptane	0.20	1.81	0.22
Octane	1.15	0.92	0.43
Nonane	1.25	7.28	1.13
Decane	2.00	2.04	0.97
Undecane	3.07	4.53	1.57
Dodecane	5.47	4.78	1.95
MethylAcetate	0.05	4.87	1.23
EthylAcetate	3.50	3.48	0.12
PropylAcetate	0.57	0.98	0.63
ButylAcetate	0.87	6.70	0.19

N/D: Not Detectable.

Table B-4. Specific retention volumes (V_g) of solutes at a temperature range 80°C to 160°C for 50-50 Amylopectin-Polycaprolactone column.

SOLUTES	80	90	100	110	120	130	140	150	160
Pentane	N/D	N/D	21.20	19.12	19.33	18.97	19.13	N/D	N/D
Hexane	19.16	18.42	N/A	15.65	15.54	14.91	14.81	N/D	N/D
Heptane	26.62	23.57	23.53	21.68	18.82	16.33	16.28	N/D	N/D
Octane	46.82	32.94	33.58	28.74	25.36	21.81	19.13	19.07	19.32
MethylAcetate	29.62	24.49	22.42	21.58	19.12	17.55	15.79	14.40	N/D
EthylAcetate	38.64	33.66	29.01	26.79	22.70	19.78	17.76	16.63	N/D
PropylAcetate	68.57	53.42	42.51	36.72	N/D	25.66	21.09	20.33	N/D
Methanol	35.42	36.33	35.61	37.74	35.80	29.62	29.83	30.06	32.90
Ethanol	42.78	37.98	34.29	33.55	31.50	27.29	26.39	26.17	N/D
Propanol	47.44	40.96	36.42	34.88	29.15	27.39	25.61	N/D	N/D
Butanol	108.30	83.68	66.75	59.02	47.56	39.87	36.01	32.59	31.79
Diethylamine	34.28	30.26	29.32	79.32	73.54	71.88	68.83	69.47	73.30
Formic acid	N/D	N/D	N/D	N/D	N/D	78.02	76.34	77.59	81.15
Water	N/D	N/D	N/D	313.30	273.20	245.6	190.80	172.10	N/D

N/D: Not Detectable.

Table B-5. Specific retention volumes (V_R) of solutes at a temperature range 80°C to 260°C for 75-25 Amylopectin-Polycaprolactone column.

SOLUTES	80	90	100	110	120	130	140	150	160	170
Hexane	16.36	16.26	16.36	16.30	15.49	16.20	16.74	20.50	21.63	N/D
Heptane	20.69	21.51	18.32	18.02	18.02	17.31	20.46	21.49	21.83	18.50
Octane	30.26	22.13	26.98	22.48	19.84	19.54	22.12	22.27	22.91	25.80
Nonane	39.52	33.76	37.67	28.86	24.30	25.31	26.73	25.71	25.45	41.22
Decane	92.43	N/D	N/D	N/D	N/D	N/D	N/D	30.51	N/D	70.62
Undecane	N/D	N/D	N/D	N/D	N/D	N/D	N/D	N/D	N/D	99.20
Dodecane	N/D	N/D	N/D	N/D	N/D	N/D	N/D	N/D	N/D	159.95
MethylAcetate	20.58	18.42	17.08	18.22	16.30	16.50	19.48	19.62	19.19	19.12
EthylAcetate	26.04	23.05	24.19	21.36	18.12	18.82	20.46	21.39	21.73	22.61
PropylAcetate	38.91	26.76	26.14	22.07	19.34	18.63	21.54	21.39	N/D	38.03
BurylAcetate	N/D	N/D	N/D	N/D	N/D	N/D	N/D	N/D	N/D	56.74

N/D. Not Detectable.

Table B-5 (Continued). Specific retention volumes (V_R) of solutes at a temperature range 80°C to 260°C for 75-25 Amylopectin-Polycaprolactone column.

SOLUTES	180	190	200	210	220	230	240	250	260
Hexane	N/D	N/D	7.80	11.28	14.19	6.92	6.06	7.28	7.33
Heptane	N/D	12.99	14.88	13.93	N/D	8.72	7.58	9.19	N/D
Octane	16.83	18.71	20.91	17.57	17.95	12.23	7.76	11.02	10.87
Nonane	28.50	31.90	30.74	24.82	26.87	14.24	11.95	17.61	13.17
Decane	49.42	47.51	45.36	36.01	35.05	22.66	16.77	18.04	15.82
Undecane	76.38	74.84	N/D	47.49	41.16	27.38	23.91	27.50	19.98
Dodecane	118.60	101.97	90.58	85.77	62.39	52.56	36.15	41.65	35.64
MethylAcetate	16.27	17.36	16.40	15.50	N/D	9.93	9.82	12.84	10.17
EthylAcetate	N/D	20.48	17.12	19.03	18.70	10.93	10.26	12.76	11.05
PropylAcetate	27.63	27.65	22.76	23.84	21.54	14.95	15.17	16.14	12.91
ButylAcetate	39.11	46.26	37.07	30.42	29.04	20.16	24.54	18.13	15.82

N/D - Not Detectable.

Table B-6. Specific retention volumes (V_g) of solutes at a temperature range 80°C to 180°C for 50-50 Amylopectin- Poly(DL)-lactide-co-glycolide) column.

SOLUTES	80	90	100	110	120	130	140	150	160	170	180
Heptane	1.03	1.83	0.92	1.54	0.69	0.15	0.16	0.93	0.00	0.00	0.00
Octane	3.25	3.83	1.87	2.60	1.74	0.79	0.78	1.61	0.36	0.62	0.68
Nonane	8.32	8.01	5.08	4.72	3.23	1.78	1.71	2.24	1.17	0.73	0.44
Decane	16.38	16.63	10.42	9.01	6.26	3.29	2.97	3.30	2.28	1.67	1.82
Undecane	42.72	36.10	21.50	16.24	12.35	7.12	5.59	4.89	4.28	3.59	3.23
Dodecane	N/D	N/D	43.51	33.89	21.45	14.71	10.86	8.27	6.76	5.78	5.44
Methyl/acetate	2.53	3.58	2.90	3.17	1.89	1.31	0.64	1.31	0.29	0.08	N/D
Ethyl/acetate	4.42	5.20	3.77	3.52	2.34	1.78	1.10	1.17	0.60	0.44	N/D
Propyl/acetate	8.82	9.16	5.62	6.09	4.23	3.07	1.90	2.38	1.01	1.22	N/D
Buryl/acetate	17.65	15.94	10.75	7.92	6.32	4.75	3.59	3.08	2.15	1.69	N/D

N/D: Not Detectable.

Table B-7. Specific retention volumes (V_g) of solutes at a temperature range 80°C to 200°C for 50-50 Amylopectin- Poly(3-hydroxybutyric acid) column

SOLUTES	80	90	100	110	120	130	140	150	160	170
Heptane	3.69	2.46	0.31	0.14	0.09	1.95	0.17	0.07	0.09	0.18
Octane	6.66	4.07	1.65	1.17	1.08	2.60	0.68	0.30	0.16	0.94
Nonane	13.30	8.36	4.44	3.09	2.10	3.59	1.37	0.86	0.70	0.99
Decane	25.80	17.36	10.48	7.90	4.98	5.21	2.55	2.02	0.98	1.75
Undecane	56.58	33.83	20.76	15.67	10.64	8.34	5.43	3.36	2.27	2.96
Dodecane	N/D	74.56	21.19	33.46	21.35	15.16	8.19	6.09	4.14	5.12
Methyl/Acetate	3.38	2.07	0.05	0.26	0.23	1.67	0.12	0.14	0.16	1.06
Ethyl/Acetate	4.39	3.04	0.31	0.75	0.21	1.92	0.64	0.14	0.14	1.10
Propyl/Acetate	6.61	4.18	1.98	2.06	1.50	2.39	0.83	0.30	0.35	1.29
Butyl/Acetate	12.43	8.46	4.46	3.53	2.55	3.57	2.08	1.27	0.75	1.79
Butanol	11.50	N/D	N/D	3.69	2.43	3.99	1.93	2.20	0.82	2.59

N/D: Not Detectable.

Table B-7 (Continued). Specific retention volumes (V_g) of solutes at a temperature range 80°C to 200°C for 50-50 Amylopectin-Poly(3-hydroxybutyric acid) column.

SOLUTES	180	190	200
Heptane	0.37	5.70	1.15
Octane	0.16	5.70	1.31
Nonane	0.44	6.12	1.65
Decane	1.13	5.91	1.86
Undecane	1.52	6.94	2.69
Dodecane	2.14	7.83	2.27
MethylAcetate	0.23	5.96	0.76
EthylAcetate	0.25	5.58	1.88
PropylAcetate	0.14	5.91	1.51
ButylAcetate	0.32	6.26	2.73
Butanol	1.73	5.91	9.82

N/D: Not Detectable.

APPENDIX C – Retention Diagram Figures

All retention diagrams figures are presented in the next pages.

Figure C-1. Retention diagram for 100% Amylopectin-Pentane.

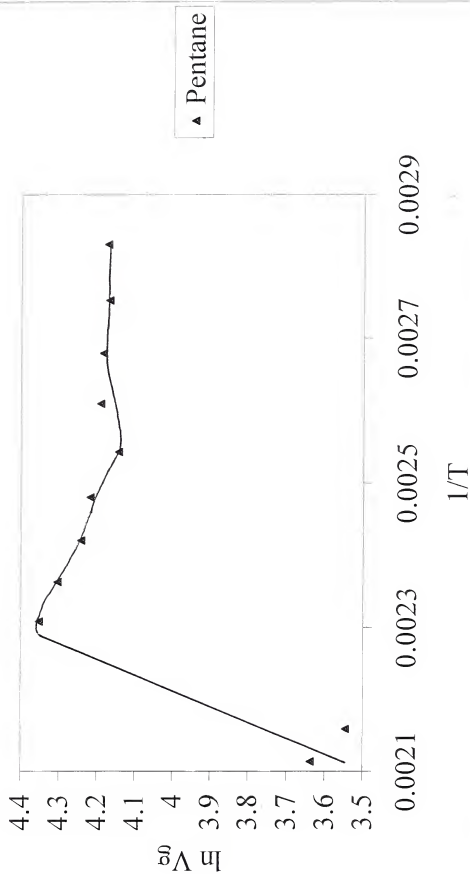


Figure C-2. Retention diagram for 100% Amylopectin-Hexane.

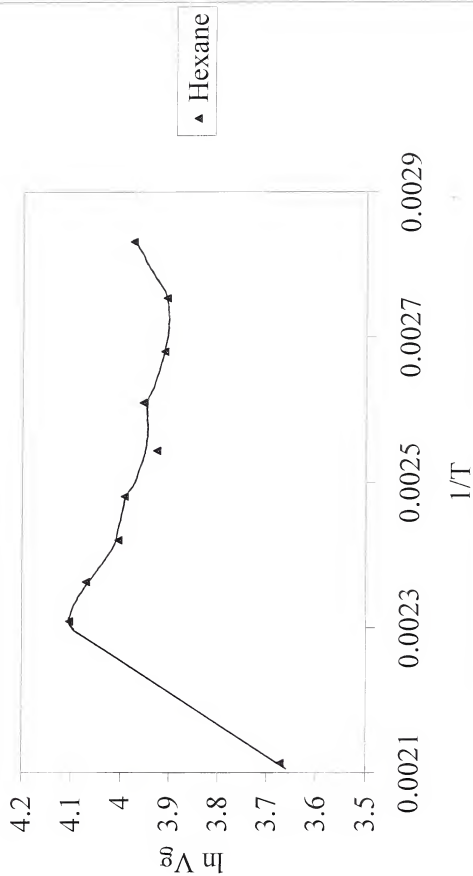
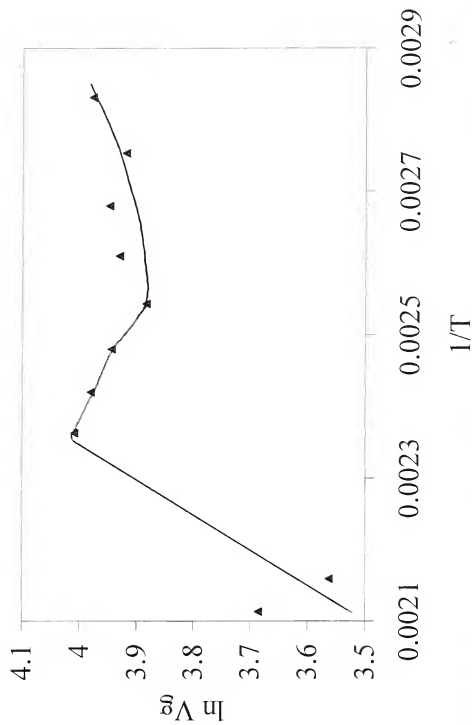


Figure C-3. Retention diagram for 100% Amylopectin-Heptane.



▲ Heptane

Figure C-4. Retention diagram for 100% Amylopectin-Methanol.

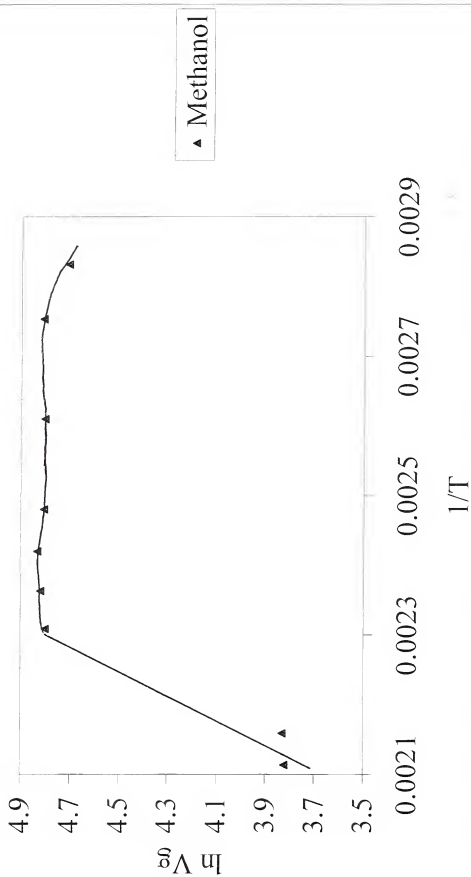


Figure C-5. Retention diagram for 100% Amylopectin-Ethanol.

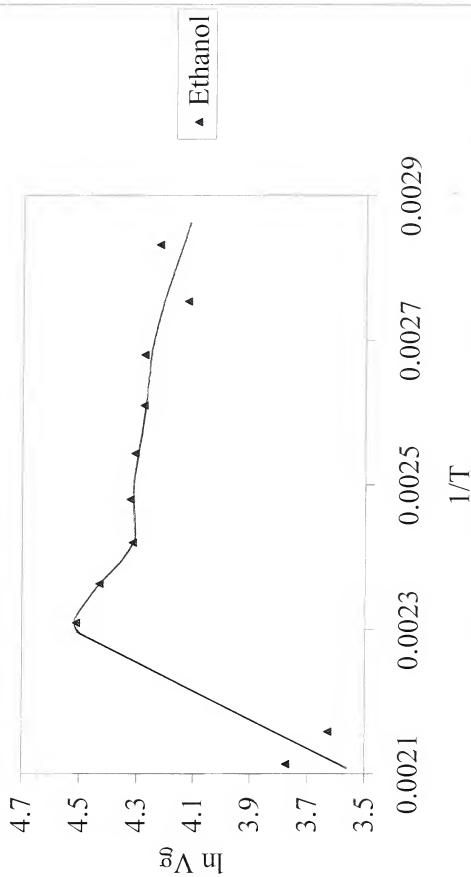
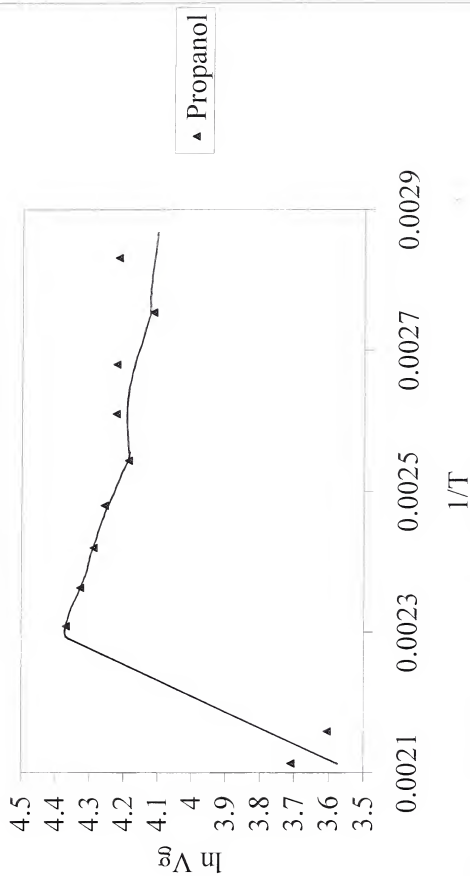
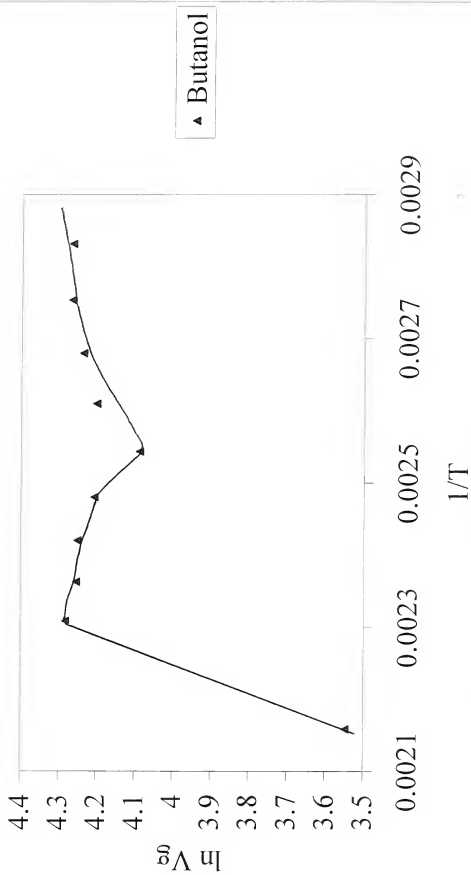


Figure C-6. Retention diagram for 100% Amylopectin-Propanol.



▲ Propanol

Figure C-7. Retention diagram for 100% Amylopectin-
Butanol.



▲ Butanol

Figure C-8. Retention diagram for 100% Amylopectin-Diethylamine.

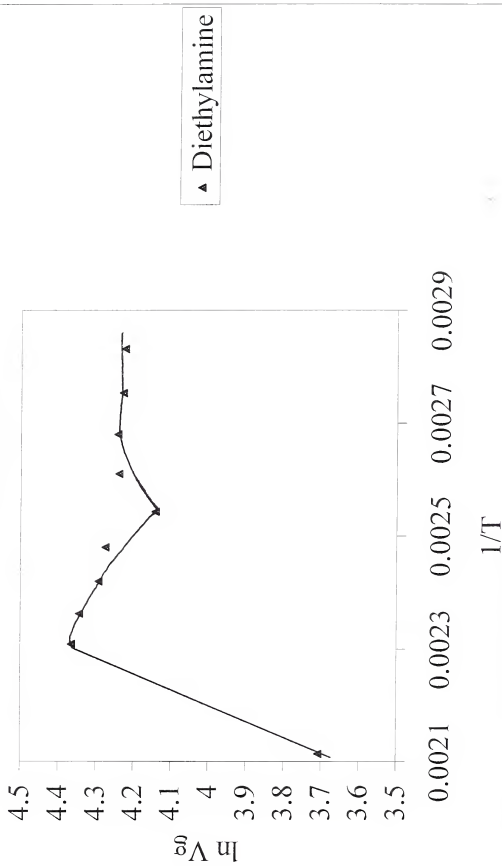


Figure C-9. Retention diagram for 100% Poly(DL-lactide-co-glycolide)-Heptane.

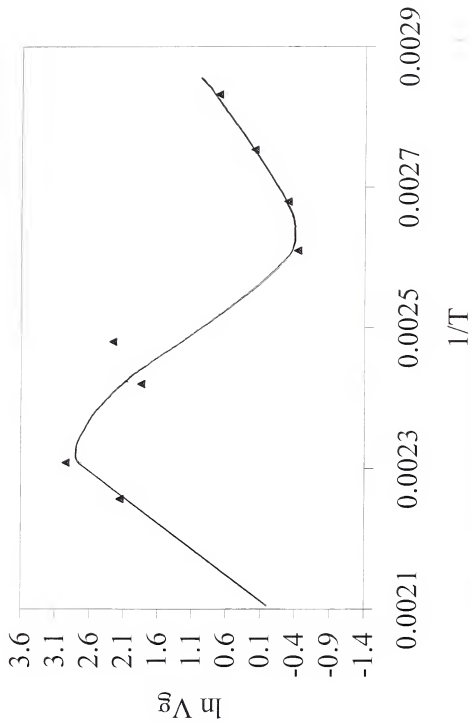


Figure C-10. Retention diagram for 100% Poly(DL-lactide-co-glycolide)-Octane.

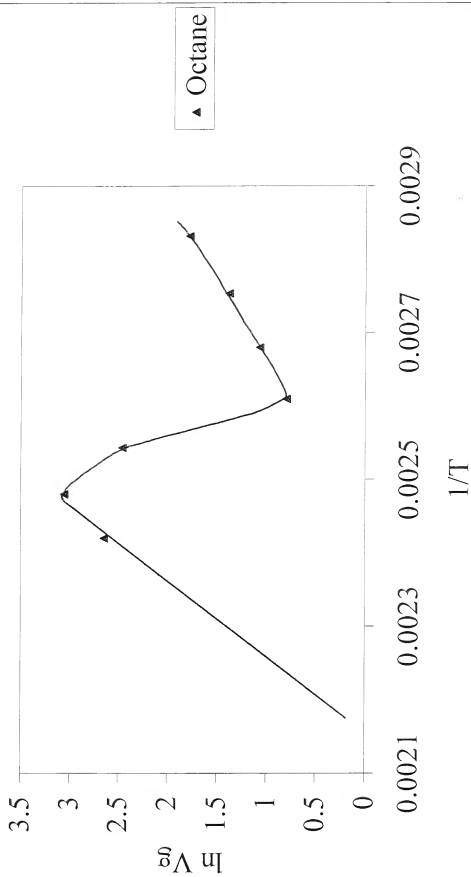


Figure C-11. Retention diagram for 100% Poly(DL-lactide-co-glycolide)-Nonane.

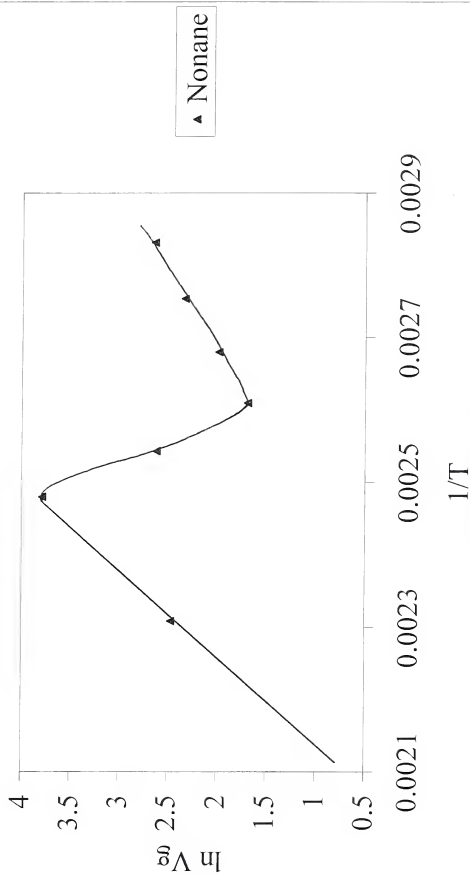


Figure C-12. Retention diagram for 100% Poly(DL-lactide-co-glycolide)-Decane.

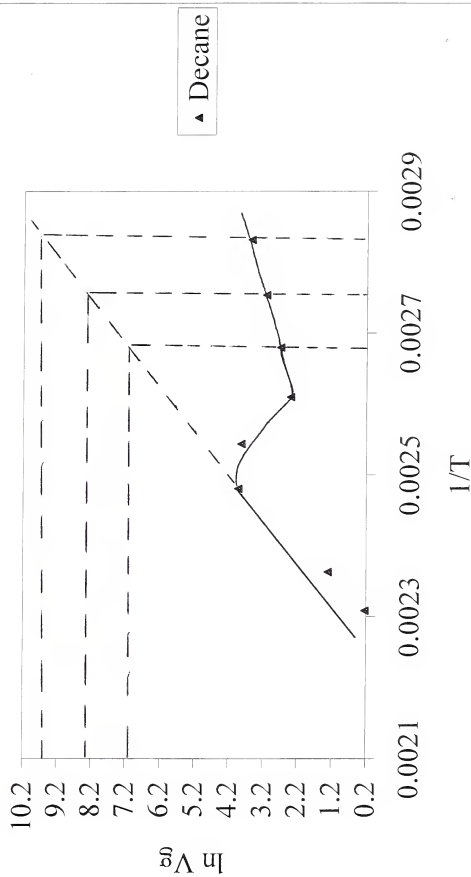


Figure C-13. Retention diagram for 100% Poly(DL-lactide-co-glycolide)-Undecane.

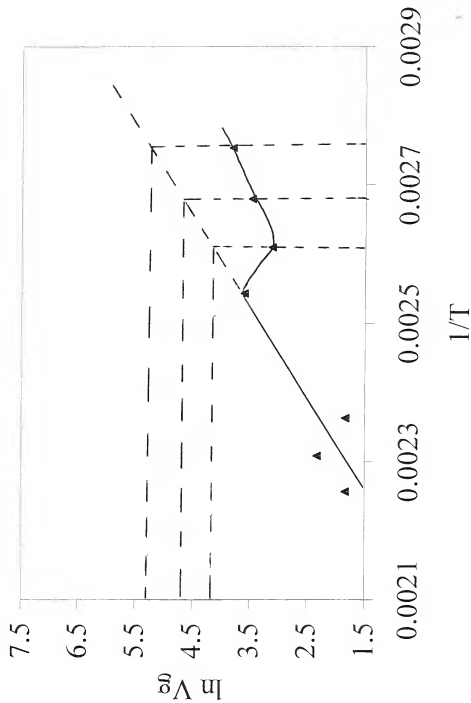


Figure C-14. Retention diagram for 100% Poly(DL-lactide-co-glycolide)-Dodecane.

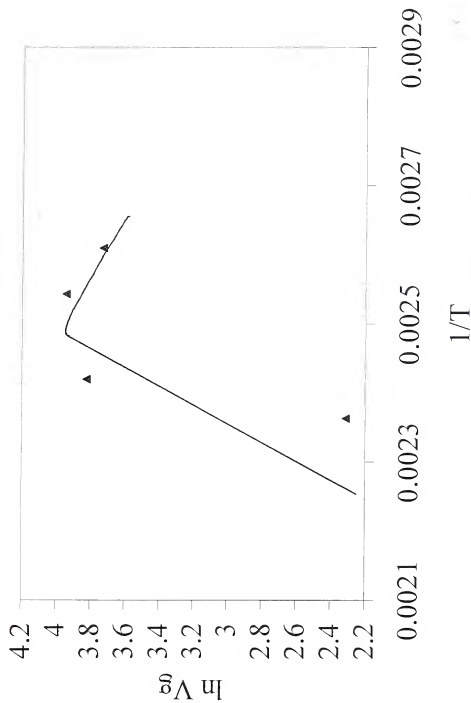


Figure C-15. Retention diagram for 100% Poly(DL-lactide-co-glycolide)-EthylAcetate.

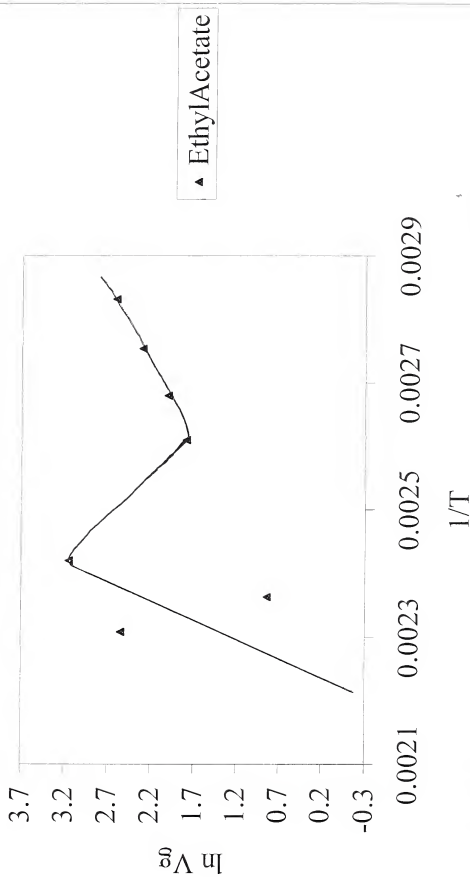


Figure C-16. Retention diagram for 100% Poly(DL-lactide-co-glycolide)-PropylAcetate.

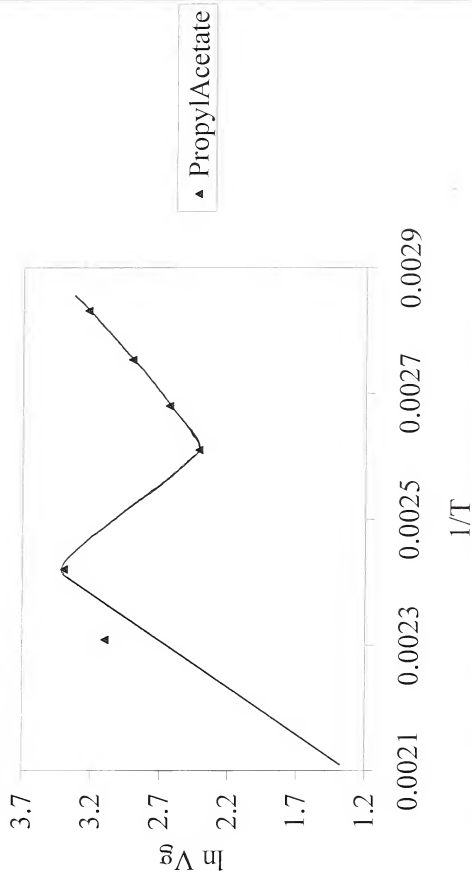


Figure C-17. Retention diagram for 100% Poly(DL-lactide-co-glycolide)-Water.

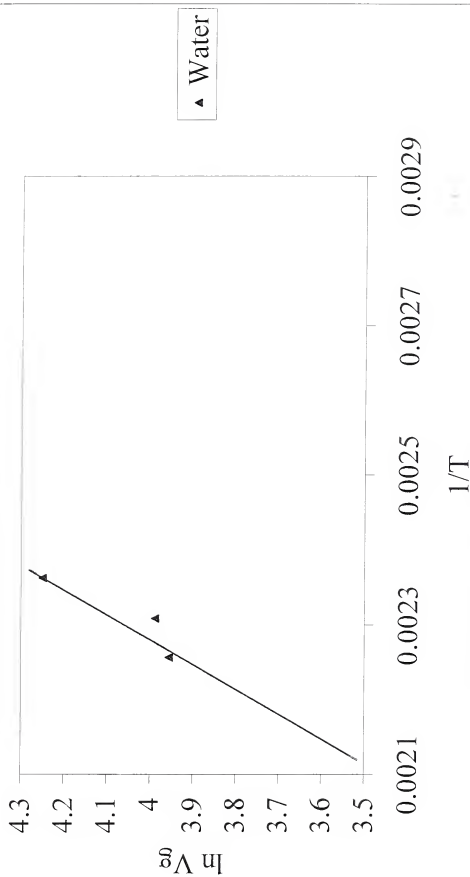


Figure C-18. Retention diagram for 100% Poly(3-hydroxybutyric acid)-Heptane.

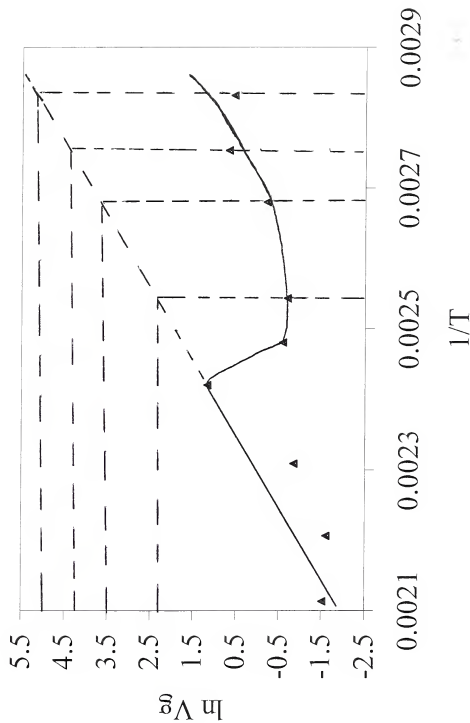


Figure C-19. Retention diagram for 100% Poly(3-hydroxybutyric acid)-Octane.

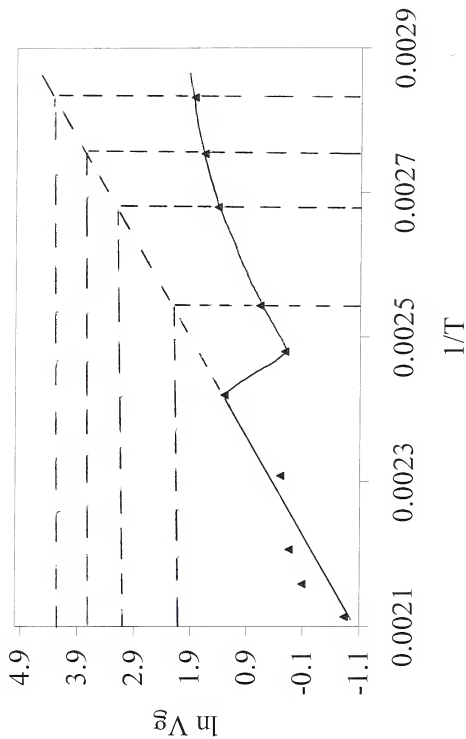


Figure C-20. Retention diagram for 100% Poly(3-hydroxybutyric acid)-Nonane.

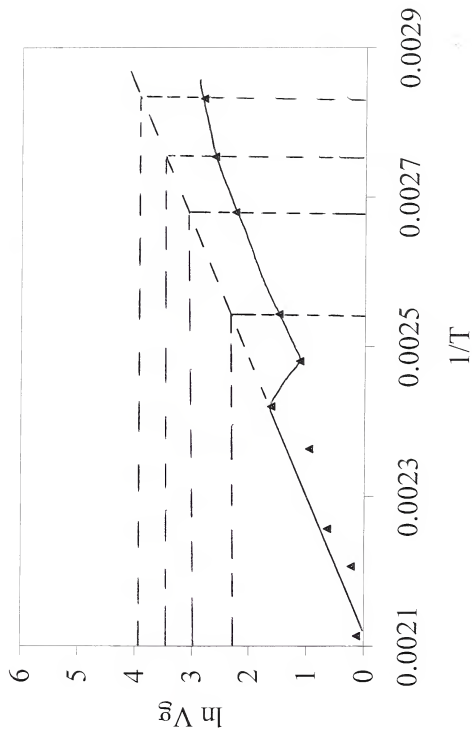


Figure C-21. Retention diagram for 100% Poly(3-hydroxybutyric acid)-Decane.

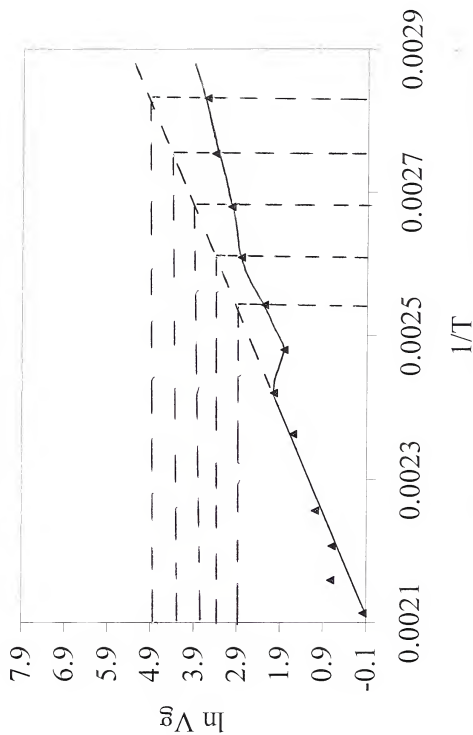
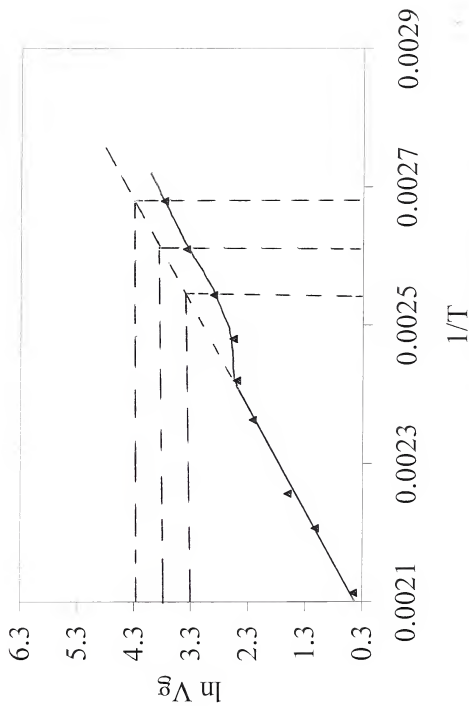


Figure C-22. Retention diagram for 100% Poly(3-hydroxybutyric acid)-Undecane.



▲ Undecane

Figure C-23. Retention diagram for 100% Poly(3-hydroxybutyric acid)-Dodecane.

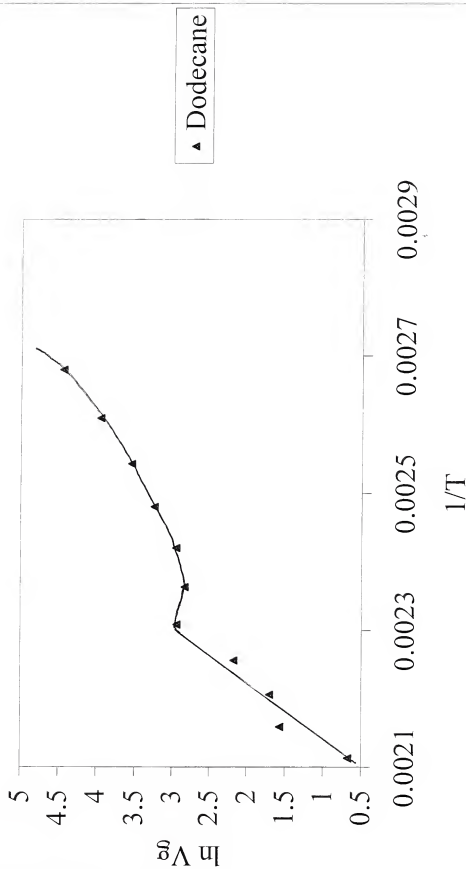


Figure C-24. Retention diagram for 100% Poly(3-hydroxybutyric acid)-MethylAcetate.

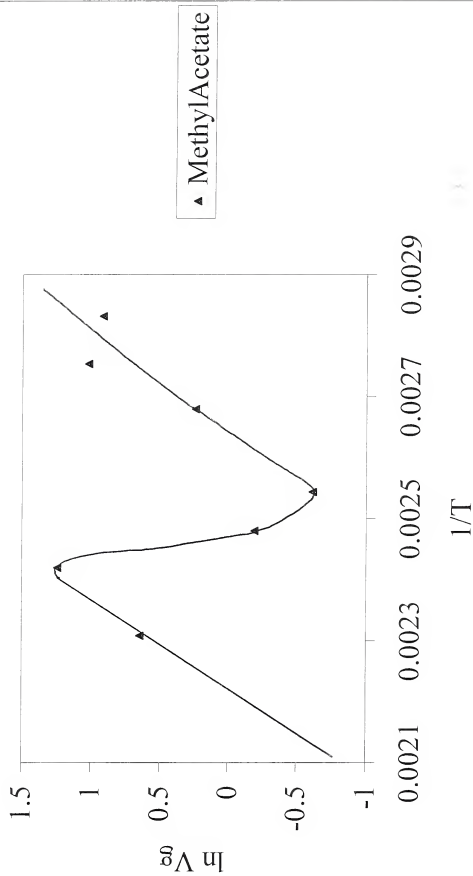


Figure C-25. Retention diagram for 100% Poly(3-hydroxybutyric acid)-EthylAcetate.

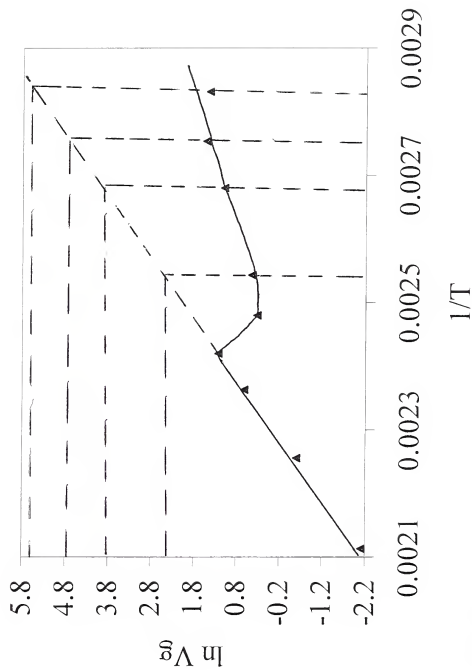


Figure C-26. Retention diagram for 100% Poly(3-hydroxybutyric acid)-PropylAcetate.

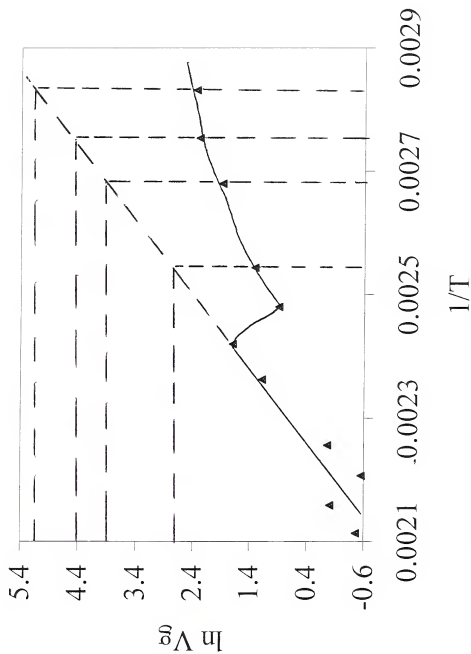


Figure C-27. Retention diagram for 100% Poly(3-hydroxybutyric acid)-ButylAcetate.

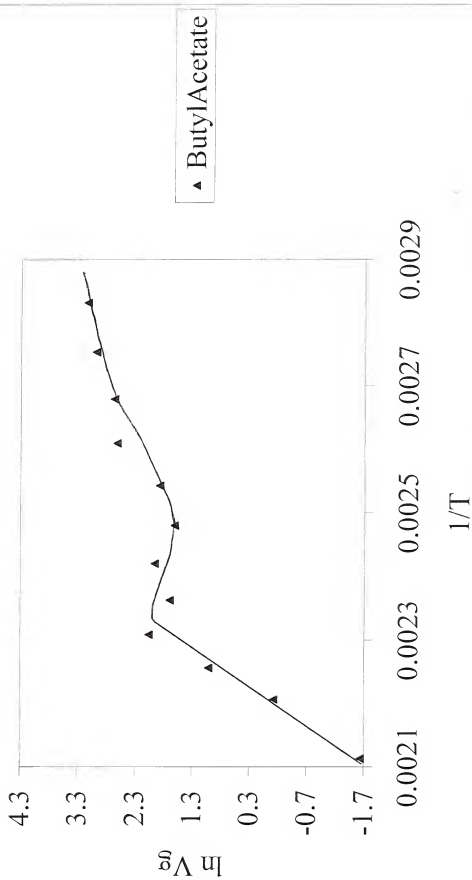


Figure C-28. Retention diagram for 50-50 Amylopectin-Polycaprolactone-Pentane.

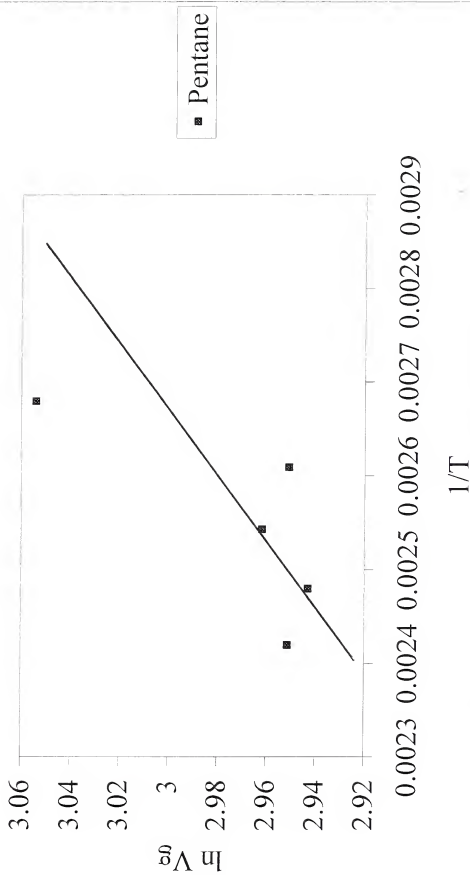


Figure C-29. Retention diagram for 50-50 Amylopectin-Polycaprolactone-Hexane.

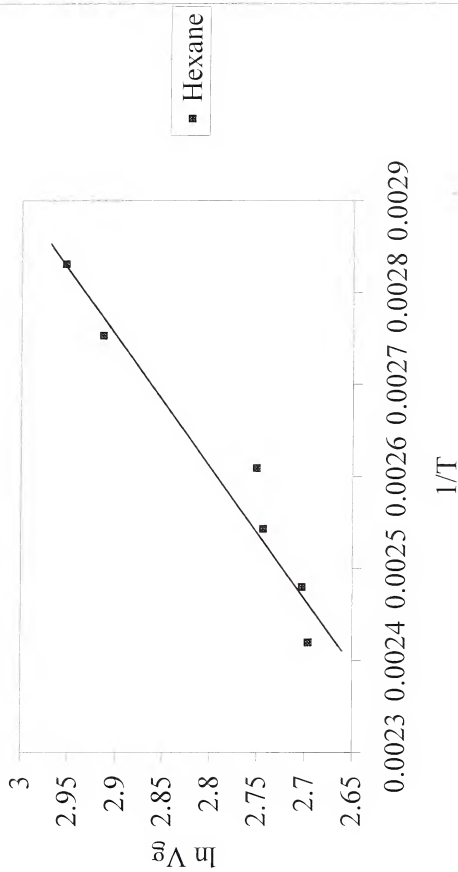


Figure C-30. Retention diagram for 50-50 Amylopectin-Polycaprolactone-Heptane.

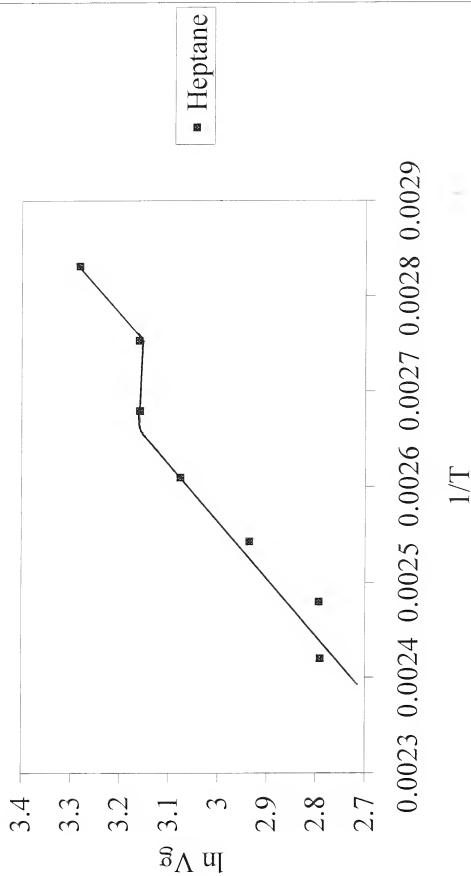


Figure C-31. Retention diagram for 50-50 Amylopectin-Polycaprolactone-Octane.

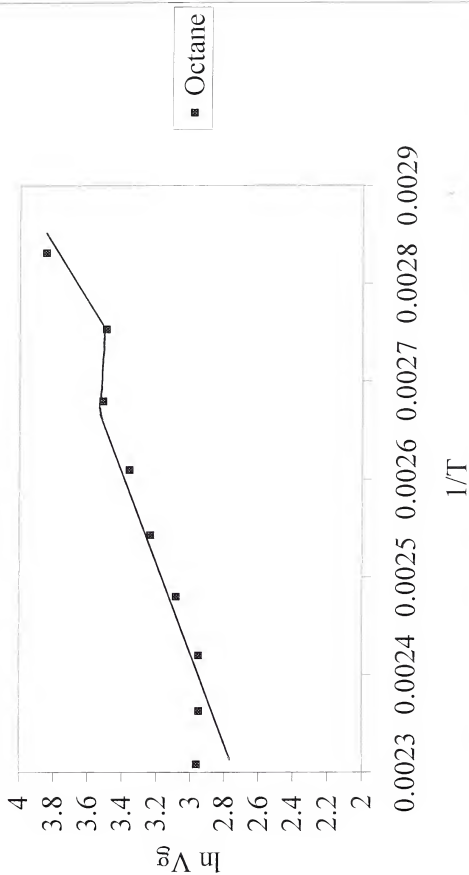


Figure C-32. Retention diagram for 50-50 Amylopectin-Polycaprolactone-MethylAcetate.

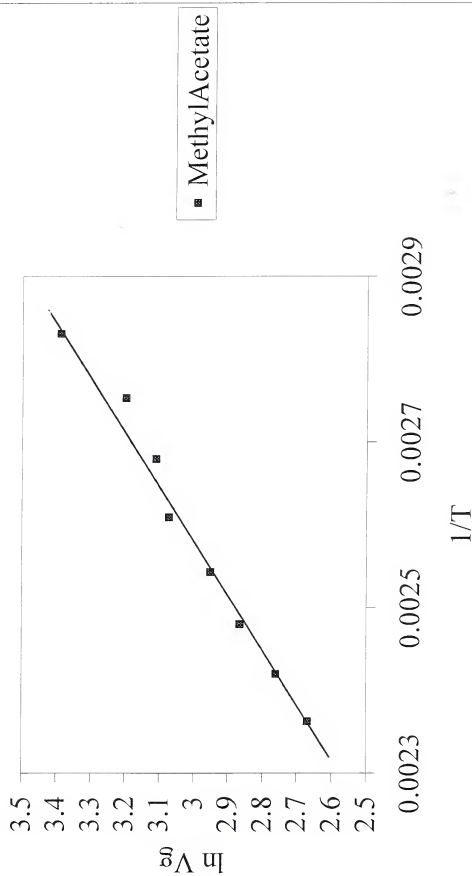


Figure C-33. Retention diagram for 50-50 Amylopectin-Polycaprolactone-EthylAcetate.

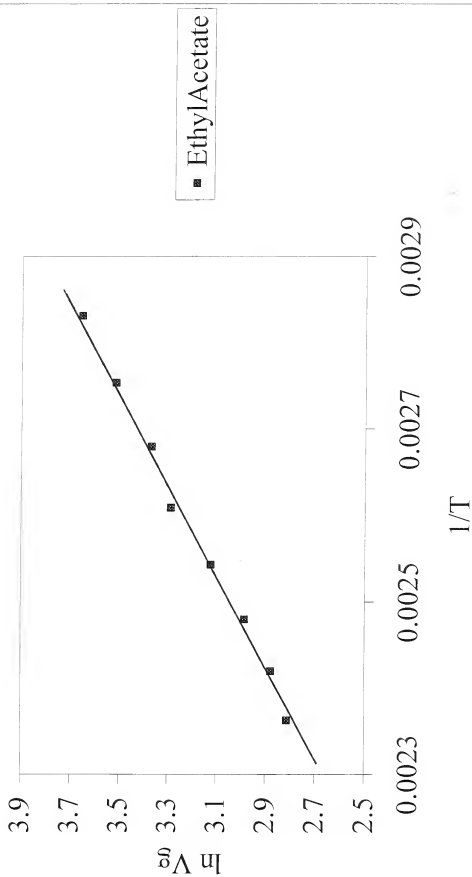


Figure C-34. Retention diagram for 50-50 Amylopectin-Polycaprolactone-PropylAcetate.

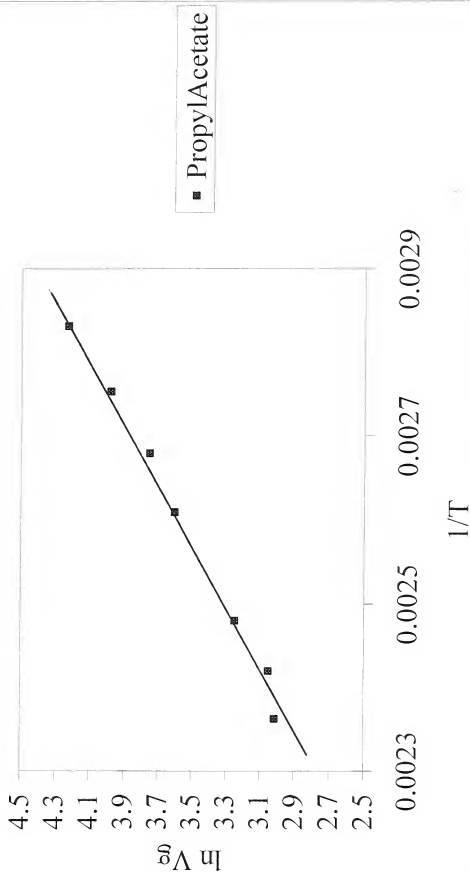


Figure C-35. Retention diagram for 50-50 Amylopectin-Polycaprolactone-Methanol.

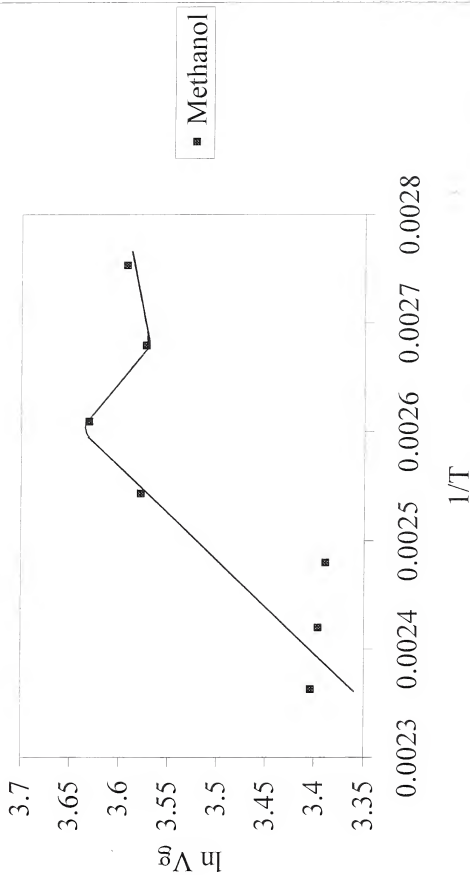


Figure C-36. Retention diagram for 50-50 Amylopectin-Polycaprolactone-Ethanol.

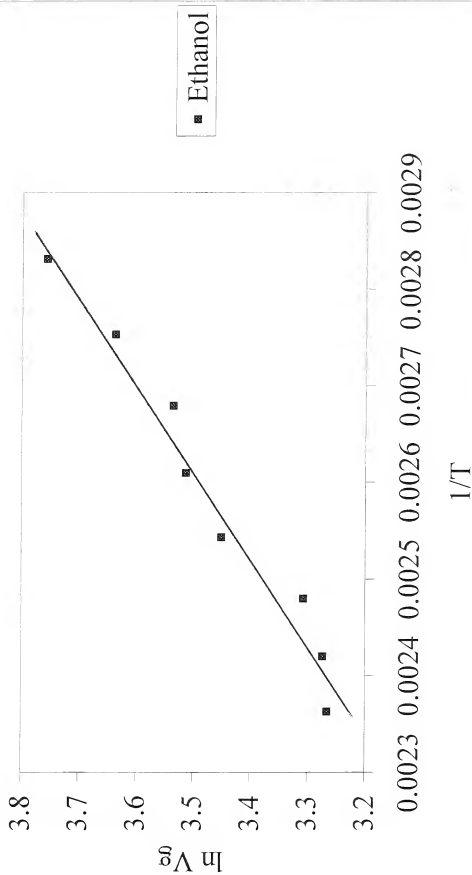


Figure C-37. Retention diagram for 50-50 Amylopectin-Polycaprolactone-Propanol.

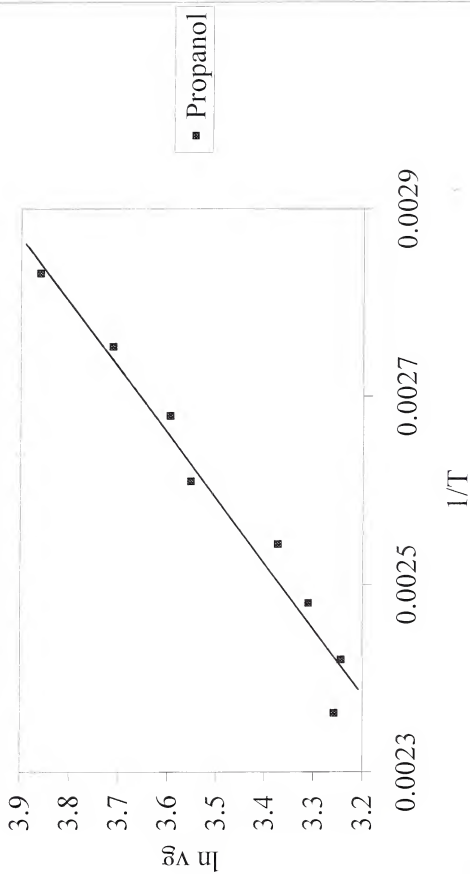


Figure C-38. Retention diagram for 50-50 Amylopectin-Polycaprolactone-Butanol.

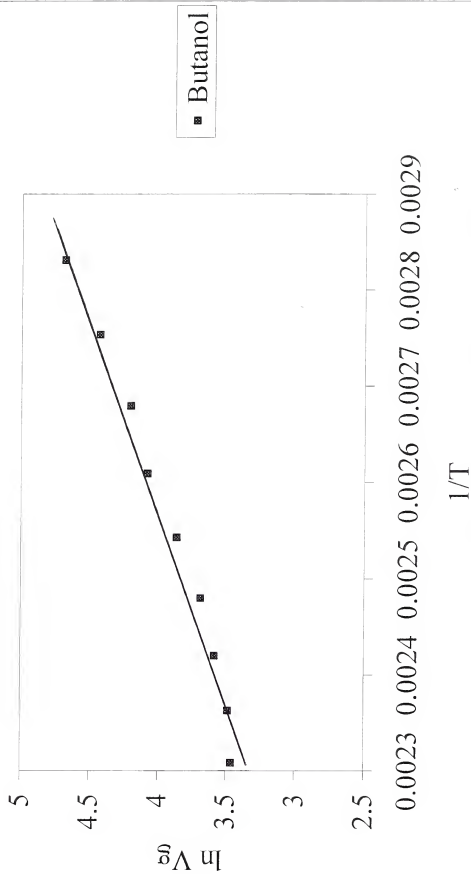


Figure C-39. Retention diagram for 50-50 Amylopectin-Polycaprolactone-Diethylamine.

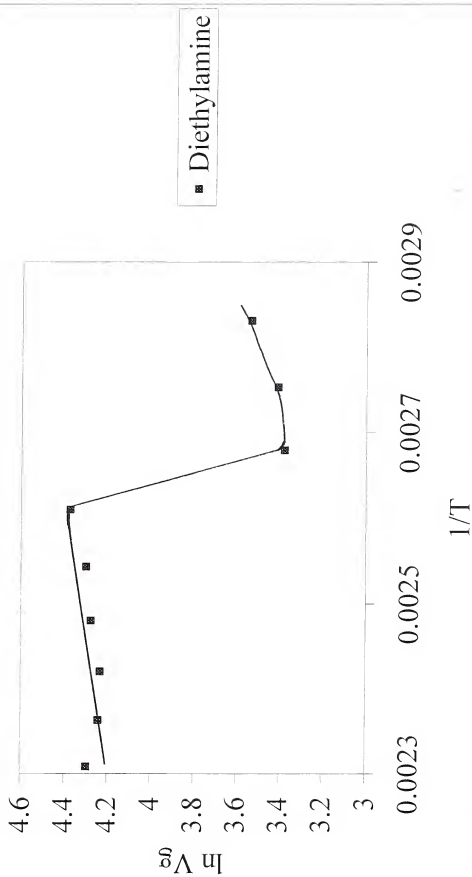


Figure C-40. Retention diagram for 50-50 Amylopectin-Polycaprolactone-Formic acid.

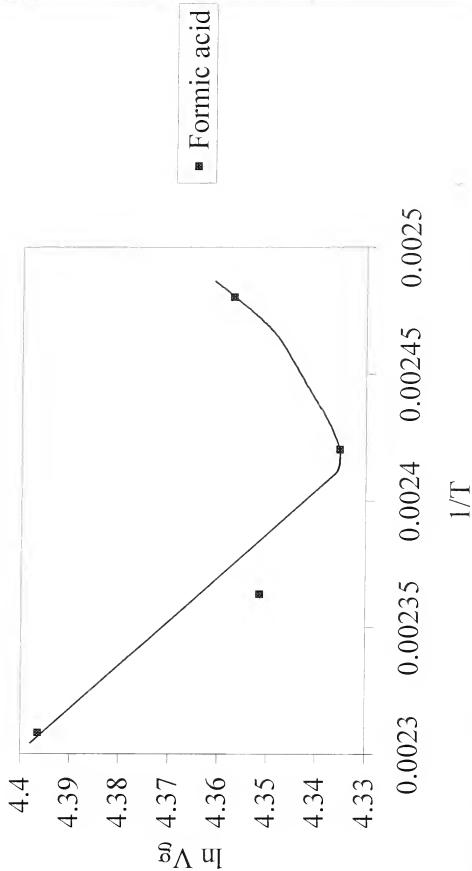


Figure C-41. Retention diagram for 50-50 Amylopectin-Polycaprolactone-Water.

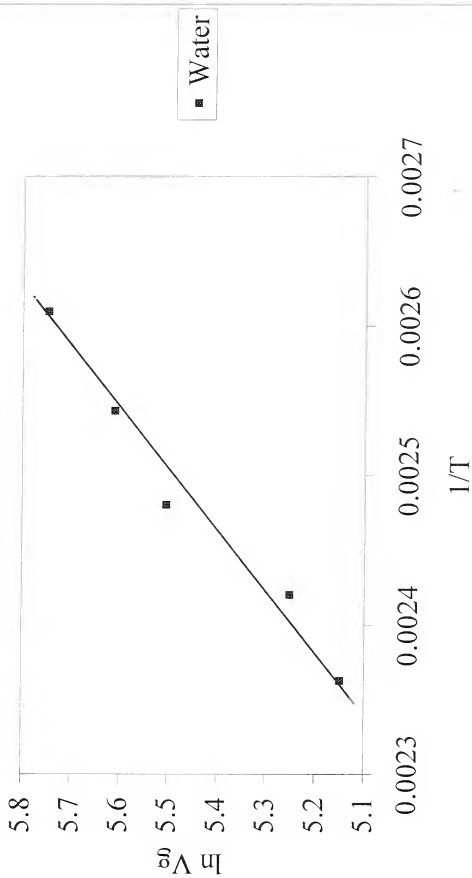


Figure C-42. Retention diagram for 75-25 Amylopectin-Polycaprolactone-Hexane.

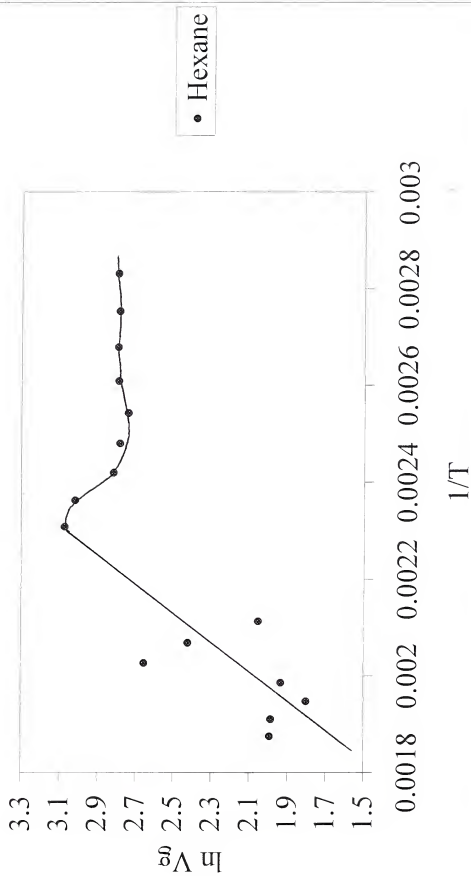


Figure C-43. Retention diagram for 75-25 Amylopectin-Polycaprolactone-Heptane.

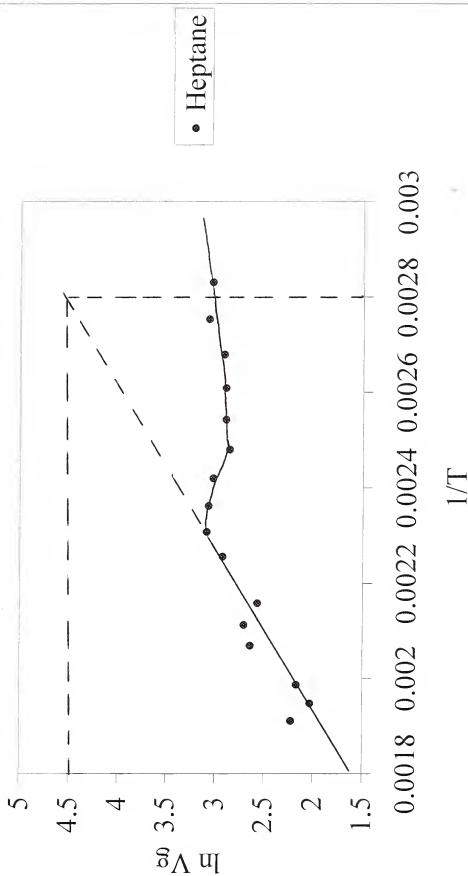


Figure C-44. Retention diagram for 75-25 Amylopectin-Polycaprolactone-Octane.

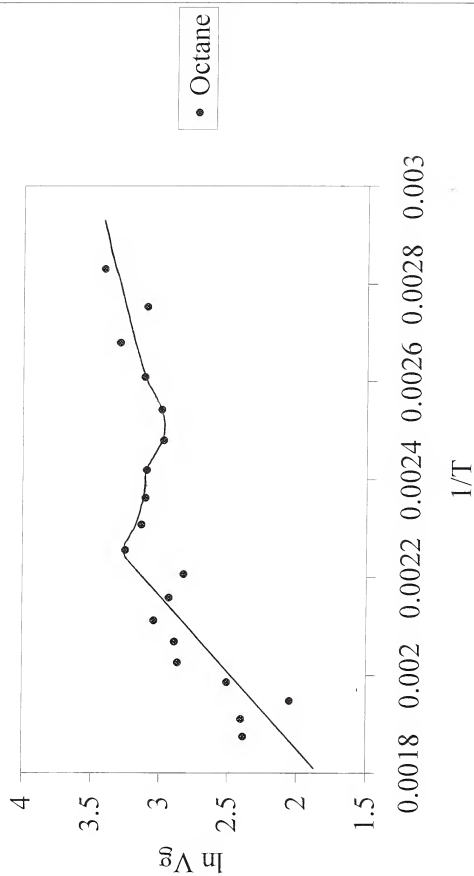


Figure C-45. Retention diagram for 75-25 Amylopectin-Polycaprolactone-Nonane.

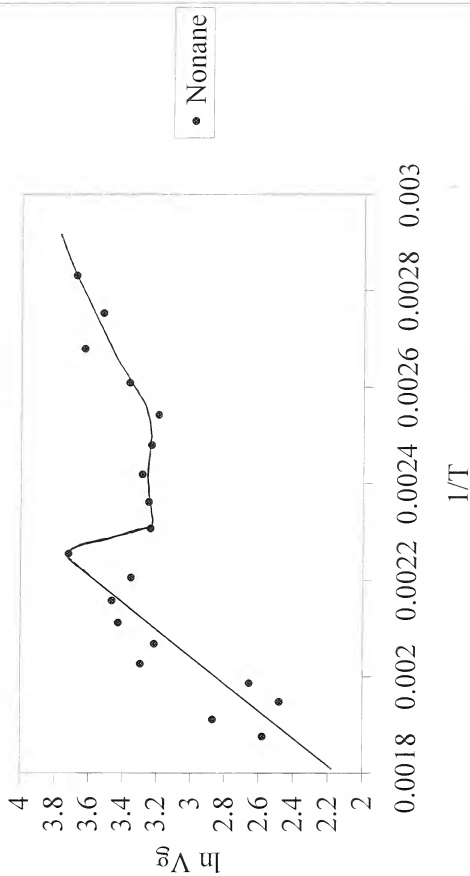


Figure C-46. Retention diagram for 75-25 Amylopectin-Polycaprolactone-Decane.

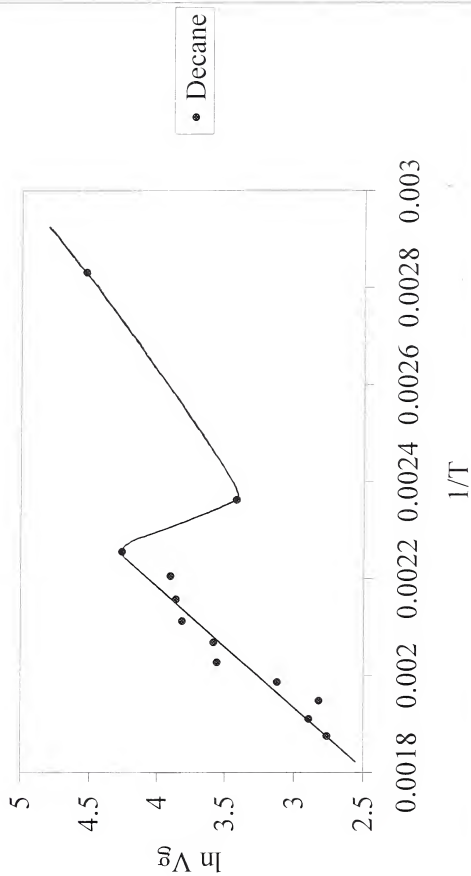


Figure C-47. Retention diagram for 75-25 Amylopectin-Polycaprolactone-Undecane.

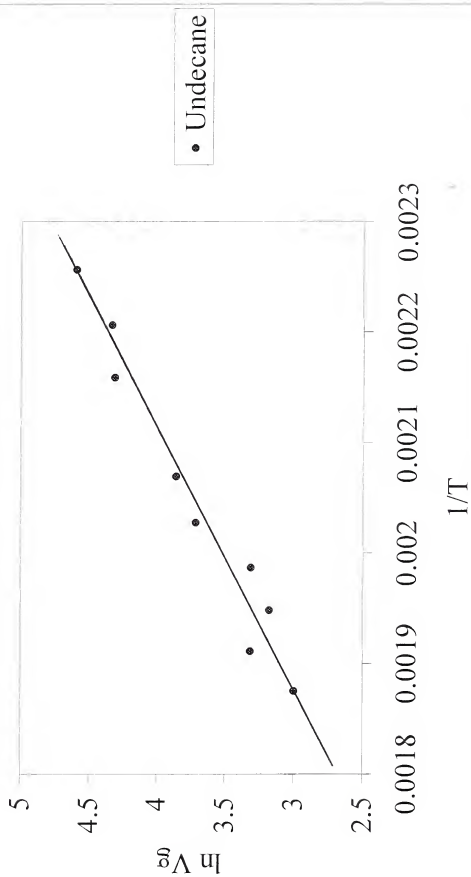


Figure C-48. Retention diagram for 75-25 Amylopectin-Polycaprolactone-Dodecane.

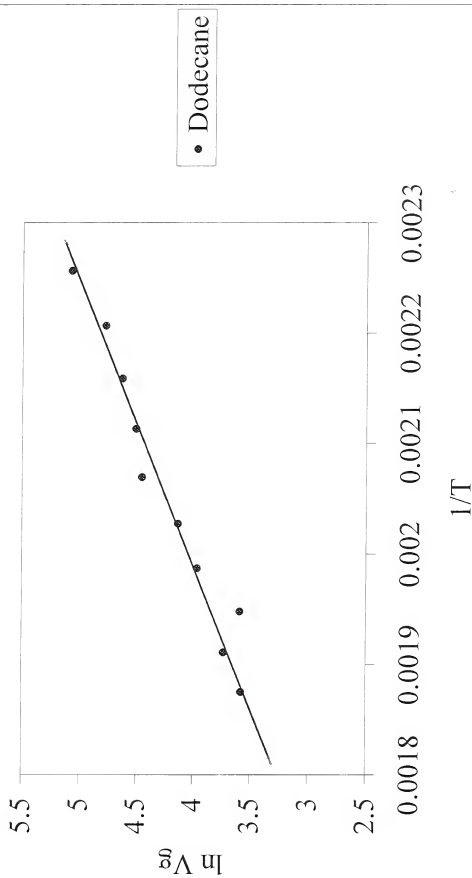


Figure C-49. Retention diagram for 75-25 Amylopectin-Polycaprolactone-MethylAcetate.

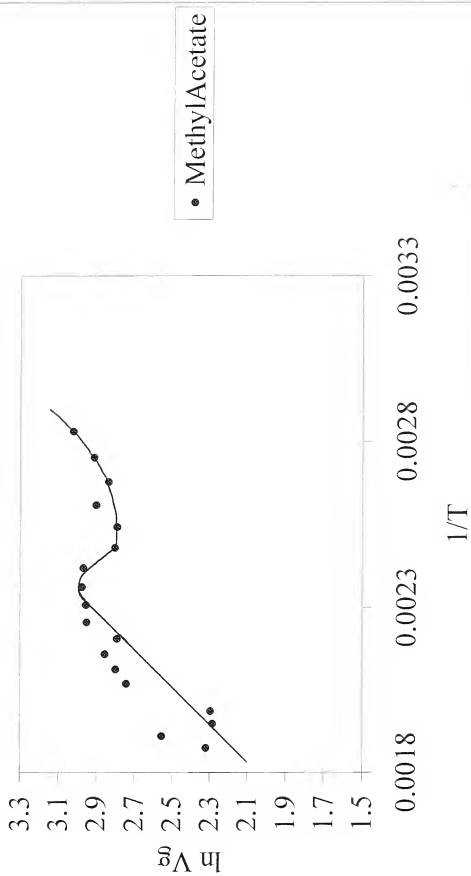


Figure C-50. Retention diagram for 75-25 Amylopectin-Polycaprolactone-EthylAcetate.

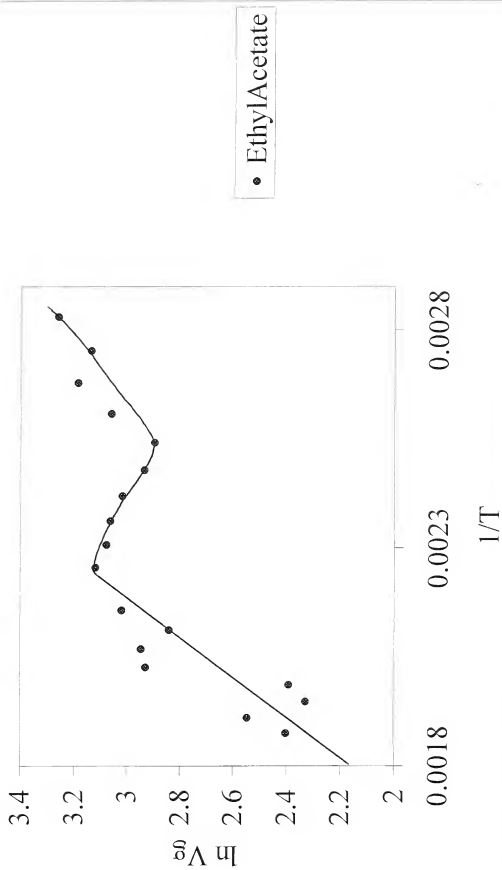


Figure C-51. Retention diagram for 75-25 Amylopectin-Polycaprolactone-PropylAcetate.

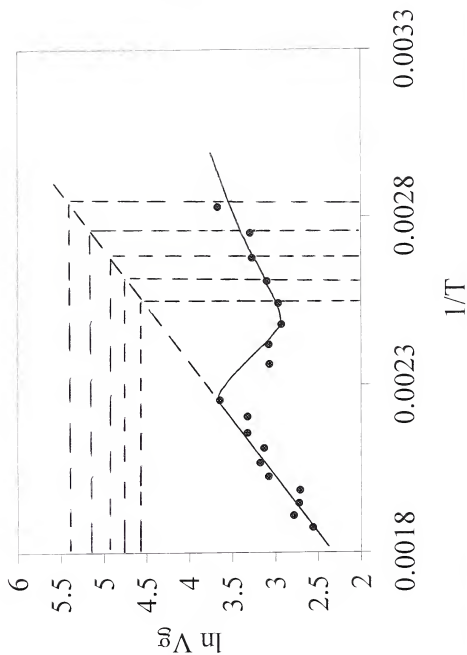


Figure C-52. Retention diagram for 75-25 Amylopectin-Polycaprolactone-ButylAcetate.

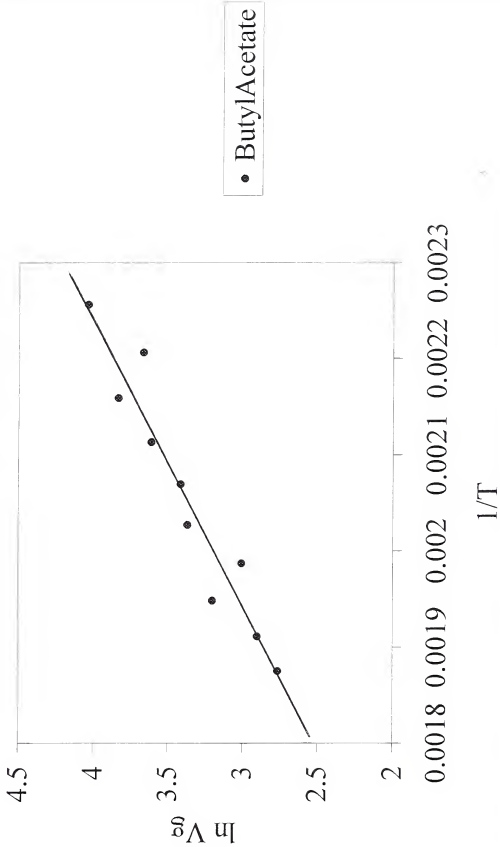


Figure C-53. Retention diagram for 50-50 Amylopectin-Poly(DL-lactide-co-glycolide)-Heptane.

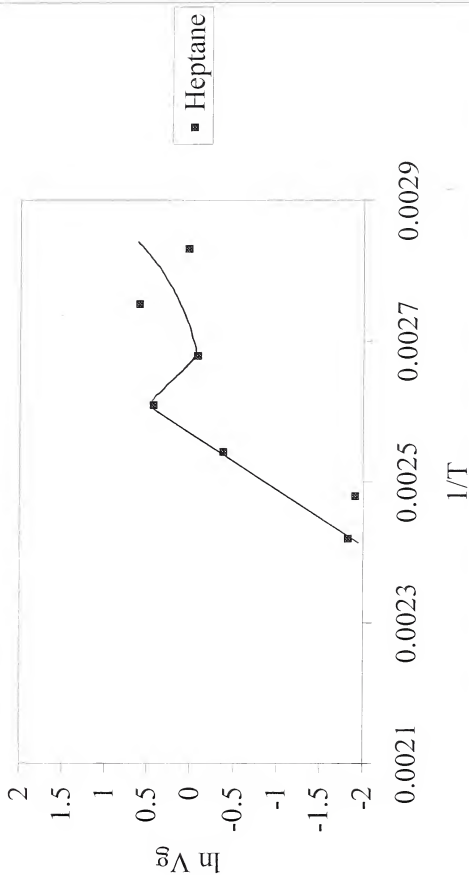


Figure C-54. Retention diagram for 50-50 Amylopectin-Poly(DL-lactide-co-glycolide)-Octane.

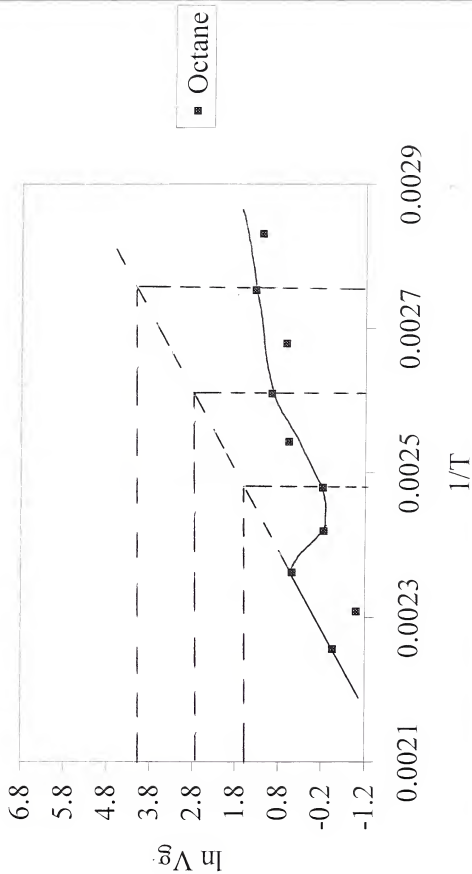


Figure C-55. Retention diagram for 50-50 Amylopectin-Poly(DL-lactide-co-glycolide)-Nonane.

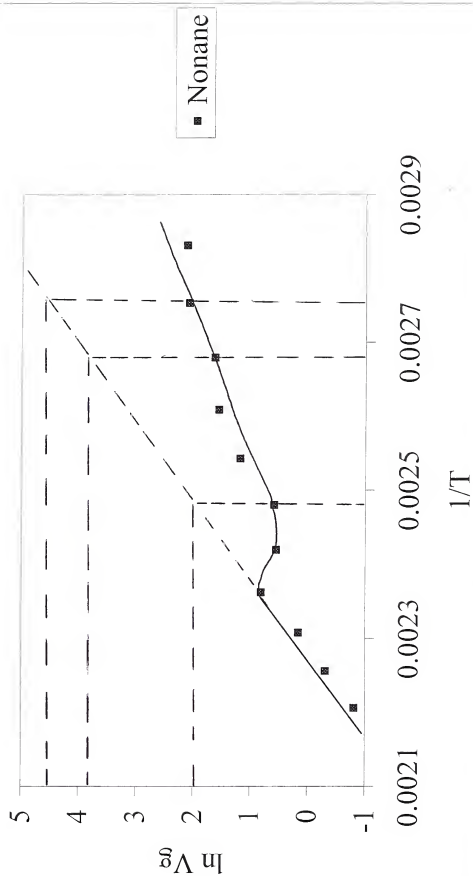


Figure C-56. Retention diagram for 50-50 Amylopectin-Poly(DL-lactide-co-glycolide)-Decane.

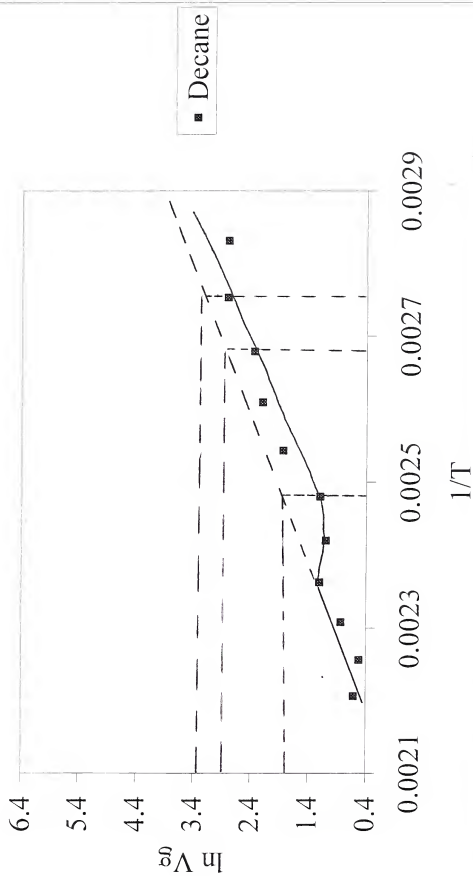


Figure C-57. Retention diagram for 50-50 Amylopectin-Poly(DL-lactide-co-glycolide)-Undecane.

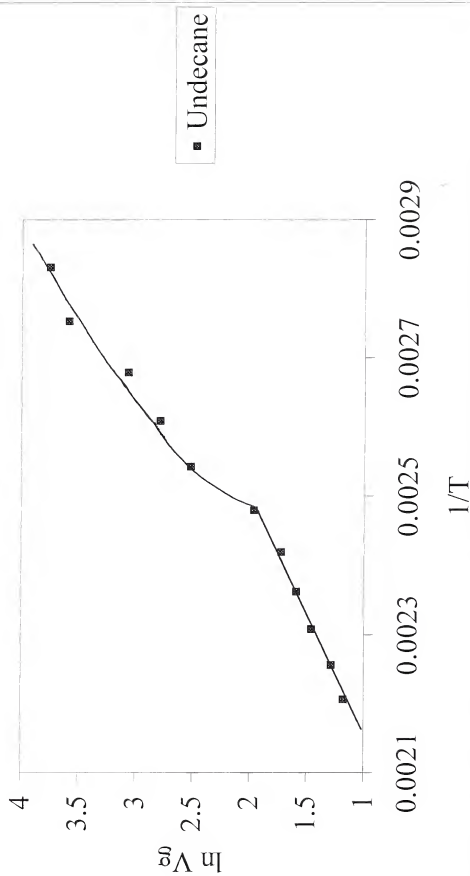


Figure C-58. Retention diagram for 50-50 Amylopectin-Poly(DL-lactide-co-glycolide)-Dodecane.

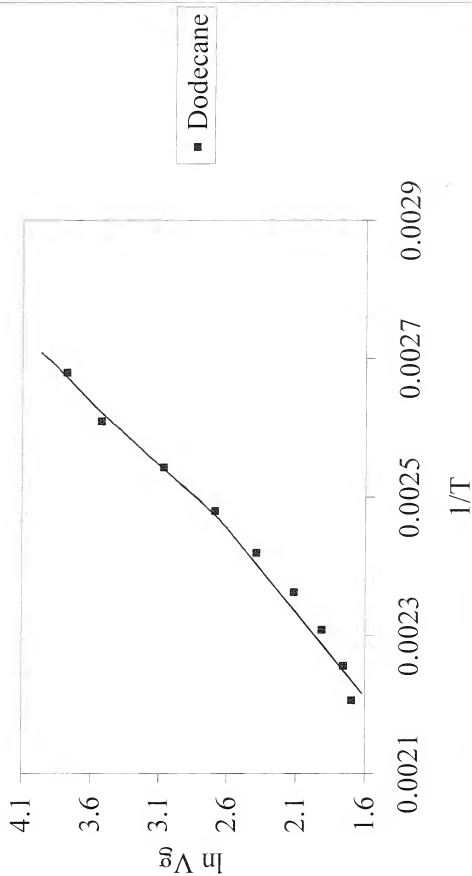


Figure C-59. Retention diagram for 50-50 Amylopectin-Poly(DL-lactide-co-glycolide)-MethylAcetate.

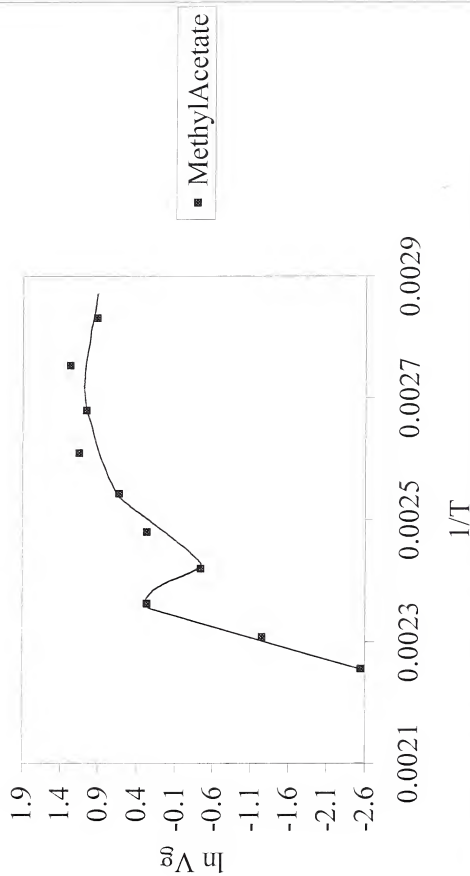


Figure C-60. Retention diagram for 50-50 Amylopectin-Poly(DL-lactide-co-glycolide)-EthylAcetate.

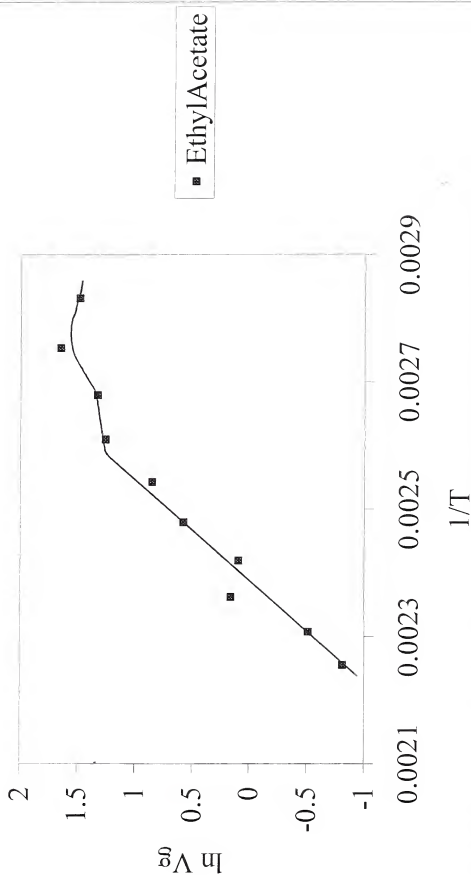


Figure C-61. Retention diagram for 50-50 Amylopectin-Poly(DL-lactide-co-glycolide)-PropylAcetate.

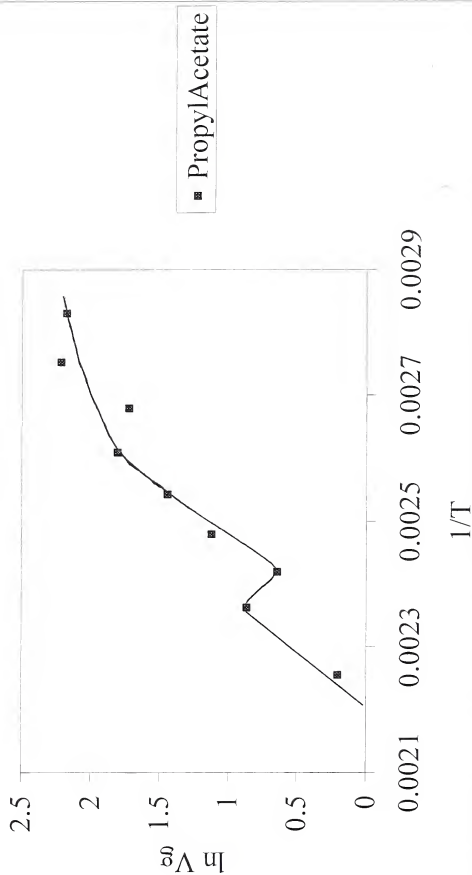


Figure C-62. Retention diagram for 50-50 Amylopectin-Poly(DL-lactide-co-glycolide)-ButylAcetate.

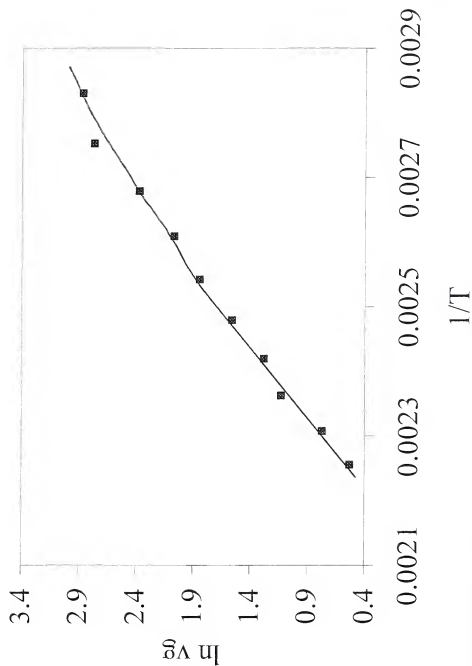


Figure C-63. Retention diagram for 50-50 Amylopectin-Poly(3-hydroxybutyric acid)-Heptane.

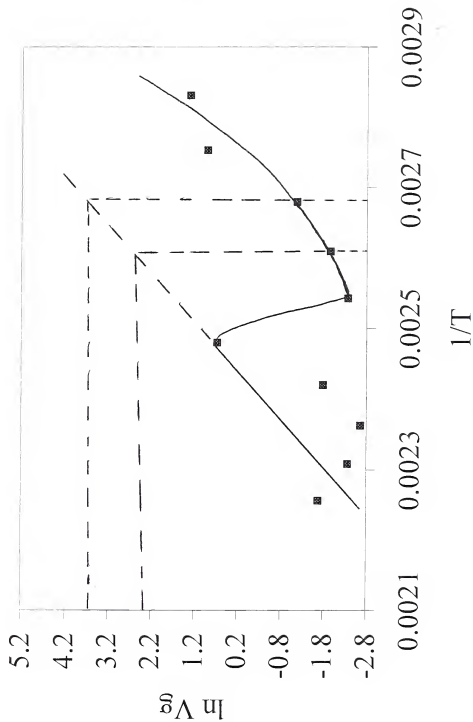


Figure C-64. Retention diagram for 50-50 Amylopectin-Poly(3-hydroxybutyric acid)-Octane.

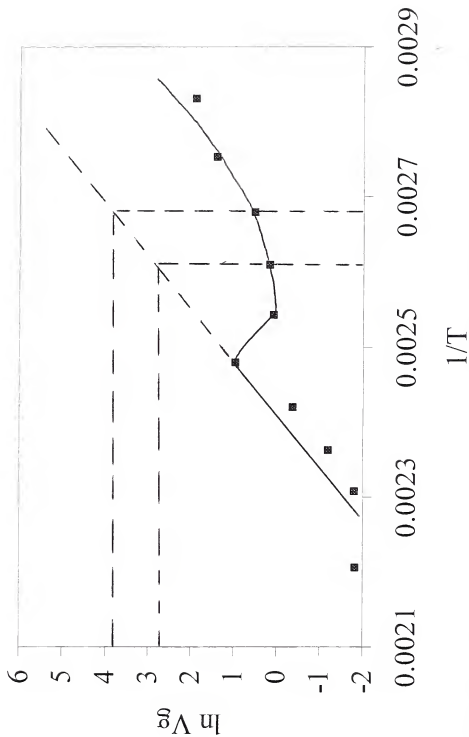


Figure C-65. Retention diagram for 50-50 Amylopectin-Poly(3-hydroxybutyric acid)-Nonane.

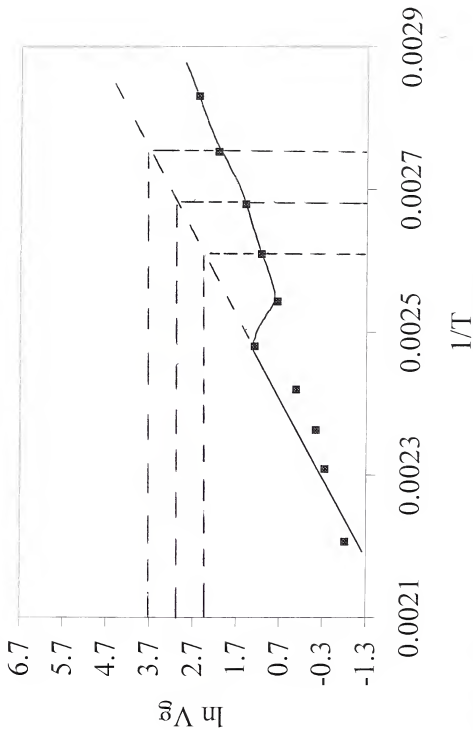


Figure C-66. Retention diagram for 50-50 Amylopectin-Poly(3-hydroxybutyric acid)-Decane.

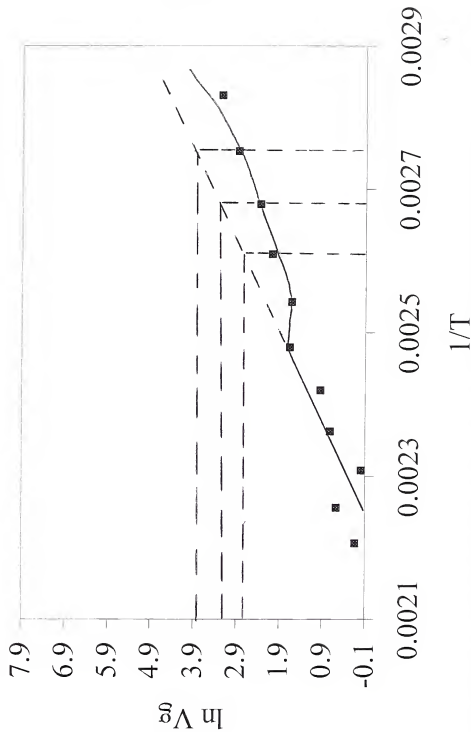


Figure C-67. Retention diagram for 50-50 Amylopectin-Poly(3-hydroxybutyric acid)-Undecane.

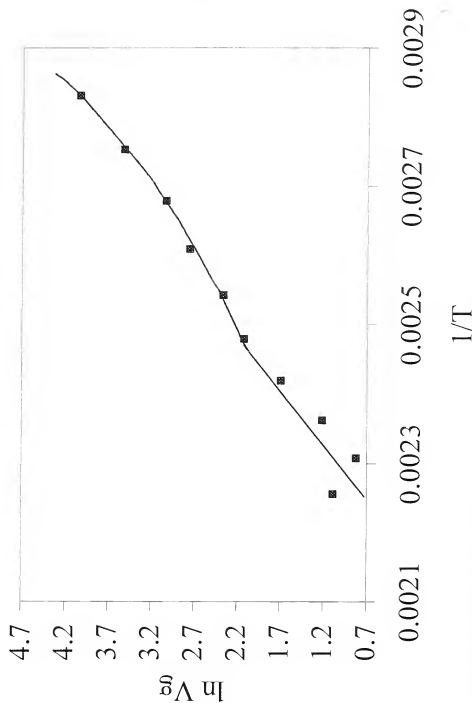


Figure C-68. Retention diagram for 50-50 Amylopectin-Poly(3-hydroxybutyric acid)-Dodecane.

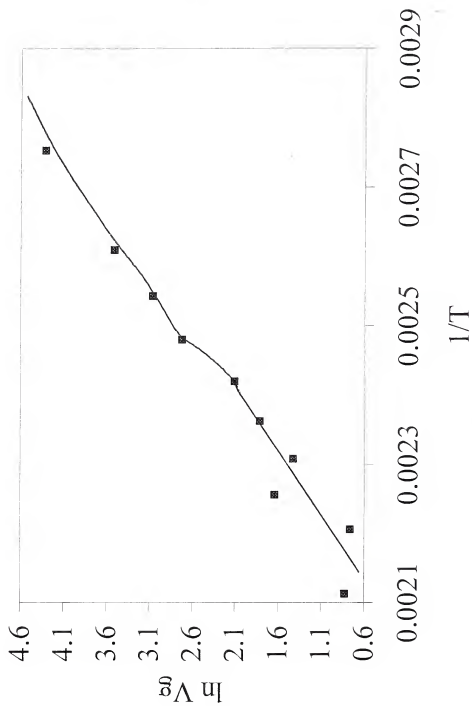


Figure C-69. Retention diagram for 50-50 Amylopectin-Poly(3-hydroxybutyric acid)-MethylAcetate.

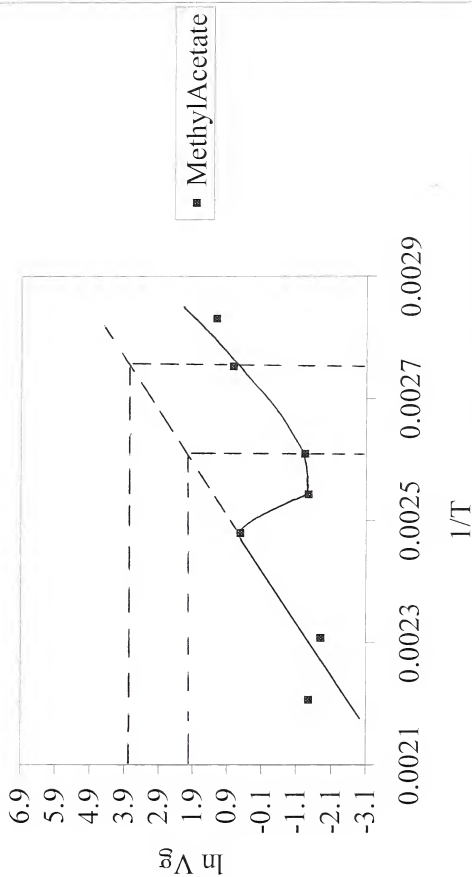


Figure C-70. Retention diagram for 50-50 Amylopectin-Poly(3-hydroxybutyric acid)-EthylAcetate.

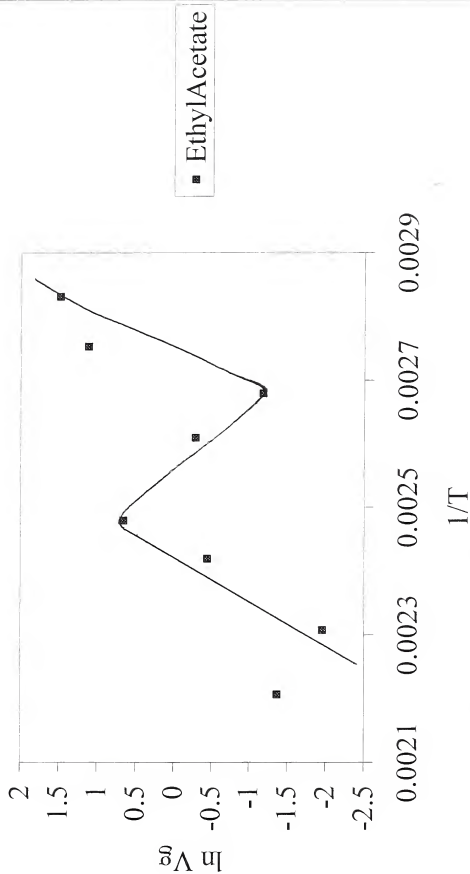


Figure C-71. Retention diagram for 50-50 Amylopectin-Poly(3-hydroxybutyric acid)-PropylAcetate.

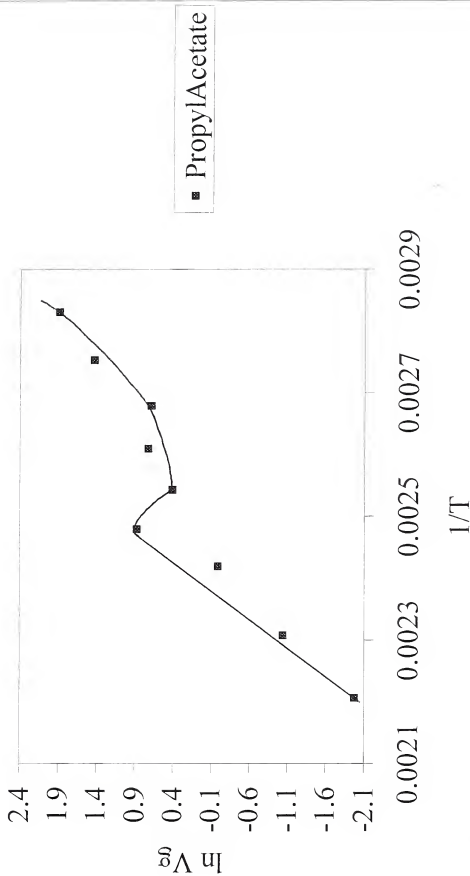


Figure C-72. Retention diagram for 50-50 Amylopectin-Poly(3-hydroxybutyric acid)-ButyIAcetate.

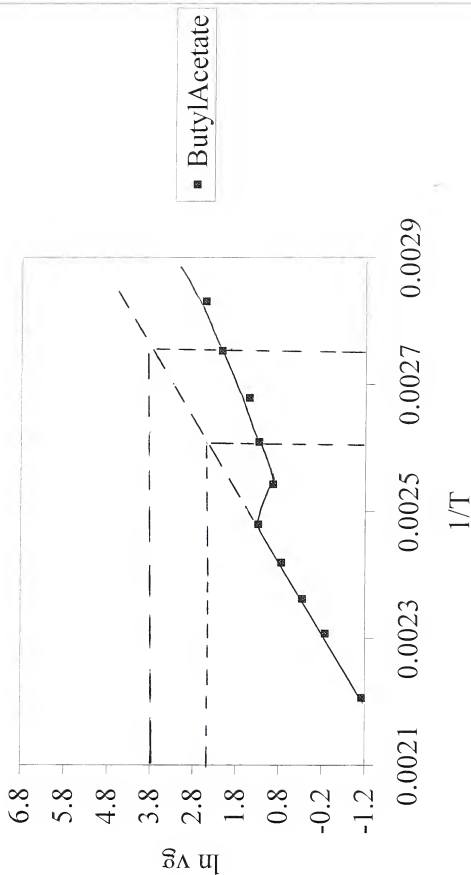


Figure C-73. Retention diagram for 50-50 Amylopectin-Poly(3-hydroxybutyric acid)-Butanol.

